On the Impact of Excited State Antiaromaticity Relief in a Fundamental Benzene Photoreaction Leading to Substituted Bicyclo[3.1.0]hexenes

Tomáš Slanina,[1,2] Rabia Ayub,[1,‡] Josene Toldo,[1,‡] Johan Sundell,[3] Wangchuk Rabten,[1] Marco Nicaso,[1] Igor Alabugin,[4] Ignacio Fdez. Galván,[5] Arvind K. Gupta,[1] Roland Lindh,[5,6] Andreas Orthaber,[1] Richard J. Lewis,[7] Gunnar Grönberg,[7] Joakim Bergman[3,]* and Henrik Ottosson[1,]*

[1] Department of Chemistry – Ångström Laboratory, Uppsala University, SE-751 20, Uppsala, Sweden. [2] Institute of Organic Chemistry and Biochemistry of the Czech Academy of Sciences, Flemingovo náměstí 2, 16610 Prague 6, Czech Republic [3] Medicinal Chemistry, Research and Early Development Cardiovascular, Renal and Metabolism, BioPharmaceuticals R&D, AstraZeneca, Gothenburg, Sweden. [4] Department of Chemistry and Biochemistry, Florida State University, Tallahassee, FL 32306-4390, USA, [5] Department of Chemistry – BMC, Uppsala University, 751 23, Uppsala, Sweden, [6] Uppsala Center for Computational Chemistry – UC_3, Uppsala University, 751 23, Uppsala Sweden, [7] Medicinal Chemistry, Research and Early Development Respiratory, Inflammation and Autoimmune, BioPharmaceutical R&D, AstraZeneca Gothenburg, Sweden.

[‡] These authors contributed equally.

Table of contents

1. Materials and Methods

1.1 General information

All reagents and solvents were purchased from TCI, Acros Organics (Thermofisher) and Sigma Aldrich (Merck) and were used as received. HPLC grade solvents were used for irradiation experiments and technical grade solvents were used for column chromatography and other reactions. Silica-precoated aluminium sheets containing fluorescent indicator from Sigma Aldrich were used for TLC. Visualization was done with UV light (254 and 365 nm) or with cerium molybdate (Hanessian's) stain. NMR spectra were recorded on a JEOL (400YH magnet) Resonance 400 MHz spectrometer. Chemical shifts δ are reported in ppm and coupling constants J in Hz. ^1H NMR and ^{13}C NMR chemical shifts are referenced to the residual protic solvent signal. The values used therefore were: $CDCl_3$ ^1H 7.26 ppm, ^{13}C 77.16 ppm. Deuterated solvents were used for sample preparation directly without purification. Chemical shifts (*δ*) are reported on a ppm scale. The following abbreviations (or combinations thereof) were used to describe multiplicities: s = singlet, d = doublet, t = triplet, q = quartet, m = multiplet, br = broad. Coupling constants (*J*) are reported in Hertz (Hz). Mass spectrometry was performed on a GCT Premier Mass TOF spectrometer coupled with gas chromatograph.

UV/vis spectra and fluorescence spectra were measured in a 1.0 cm quartz fluorescence cuvette.

Degassed samples were measured in 1.0 cm quartz fluorescence with a screw cap with a PTFE septum. The solutions were degassed by bubbling with argon by a glass capillary (metal needles were omitted as they partially dissolved in highly acidic solutions contaminating the sample with ferric ions acting as optical filter).

1.2 Bulk irradiation

A typical photochemical reaction was accomplished in a Rayonet® reactor equipped with 16 UV lamps RPR-2437Å. The light intensity in the irradiated area was approximately 1.65×10^{16} photons s^{-1} cm^{-3}. The samples were irradiated in quartz tubes (15 or 60 mL) equipped with a stirring bar and covered with a rubber septum which was sealed by parafilm and covered in aluminium foil which were degassed by bubbling by argon if needed. The irradiation chamber was cooled by a fan to temperature of ~35°C.

1.3 Irradiation in tubing reactors

The samples were irradiated in FEP (fluorinated ethylene propylene) tubing which is transparent for 254 nm light. The tubing was wound around a light source (254 nm lamp) and was either irradiated in a flow regime (pumped by gravity when the flow was adjusted by a valve between the reservoir and the tubing coil) or was loaded in the tube and irradiated without the flow.

2. Optimization and control experiments

2.1 Control experiments

The photoreaction has been tested by a series of control experiments confirming that all components are needed for the efficient product formation. Photorearrangement of TMS-benzene in methanol catalysed by DCA has been chosen as a model reaction. The results are summarized in Table S1. It was concluded that degassing does not significantly influence the course of the reaction (entries 1 and 2), light of a proper wavelength (entries 3 and 5) is needed for the reaction and that acid catalyses the reaction (entry 4). The reaction in neat substrate with added methanol as nucleophilic reagent yielded traces of product (entry 6).

Table S1: Control experiments of a model rearrangement reaction

Entry	TMS benzene [µmol]	DCA [µmol]	Irradiation[a] [h]	MeOH [mL]	Degassed	Yield[b] [%]
1	832	15	2	12	yes[c]	30
2	832	15	2	12	no	28
3	832	15	0[d]	12	no	0
4	832	0	2	12	no	7
5	832	15	2[e]	12	no	0
6	83200	15	2	1	no	2

[a] Irradiated by 254 nm light. [b] NMR yield of the reaction mixture of the test run, not complete conversion. [c] Degassed by bubbling with argon for 10 min. [d] Stirred in dark for 2 hours. [e] Irradiated by 365 nm light.

2.2 Optimization experiments TMS-benzene

The strength and amount of the acid which was found to catalyse the reaction was optimized in a series of experiments. Photorearrangement of TMS-benzene in methanol has been chosen for the optimization. The results are shown in Table S2. Strong acids catalyse the reaction but lead to the formation of by-products (entry 1), weak acids do not catalyse the reaction as efficiently (entry 3). Dichloroacetic acid (DCA) was found to has optimal strength which catalyses the reaction but does not lead to by-products (polymers etc.). The optimal acid loading was found to be approx. 2 mol% (entries 4 – 9). The reaction in a flow apparatus was found to be more efficient (less secondary photoproducts, entry 10).

Table S2: Optimization of a model rearrangement reaction.[a]

Entry	Acid	x_{acid} [%]	Reaction type[b]	Yield[c] [%]
1	H_3PO_4	1.8	batch	3
2	HCl	1.8	batch	18
3	AcOH	1.8	batch	7
4	DCA	1.8	batch	28
5	DCA	4	batch	27
6	DCA	9	batch	25
7	DCA	18	batch	9
8	DCA	40	batch	1
9	DCA	90	batch	0
10	DCA	1.8	flow	45

[a] Typical reaction conditions: TMS benzene (832 µmol), MeOH (12 mL), non-degassed, irradiated for 2 h at 254 nm. [b] batch = quartz test tube with stir bar, flow = FEP tubing reactor. [c] NMR yield, not complete conversion.

2.3 Reactivity scope

The photorearrangement reaction has been tested on a series of aromatic compounds (Scheme S1). As it was known that the reaction does not tolerate many functional groups, substrates with simple and "inert" functional groups were tested. As the reaction generates often mixtures of tens of different isomers, the reaction output is only briefly commented in Table S3 and only few examples have been chosen for further optimization, separation and synthetic modifications.

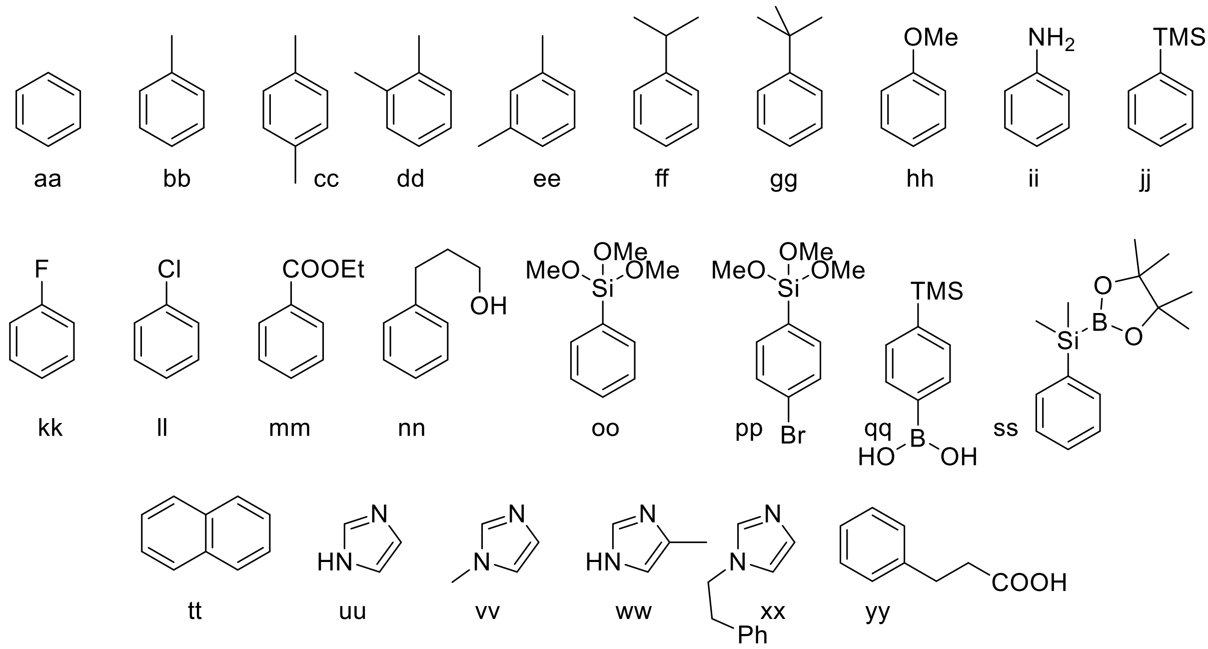

Scheme S1: Structures of substrates for the model photoreaction.

Table S3: Tested substrates, reaction conditions and output of the studied photoreaction.

Entry	Substrate	Conditions[a]	Output
1	aa	MeOH/DCA	Mixture of ~bicyclic adducts, competing polymerization and decomposition, products decompose on the column
2	aa	H_2O/HOAc	Hydroxy adduct **1a** (69%), clean reaction, formation of insoluble precipitate at high (>~60%) conversions
3	aa	H_2O/HOAc/MeCN[b]	Analogous to entry 2, complicated separation of the product by extraction
4	aa	H_2O/HCl	Hydroxy adduct **1a** (32%), competing decomposition of the product, formation of insoluble precipitate at high (>~40%) conversions

	aa	MeOH	Mixture of >5 bicyclic products, competing polymerization and degradation
5	aa	HOAc[c]	Acetate adduct **1b** (25%), mixture of ~3 minor by-products
6	bb	MeOH/DCA	Mixture of >5 products
7	bb	H_2O/HOAc	Immiscible with the solvent, no conversion
8	cc	MeOH/DCA	Mixture of >5 products
9	cc	H_2O/HOAc	Immiscible with the solvent, no conversion
10	dd	MeOH/DCA	Mixture of >5 products
11	dd	H_2O/HOAc	Immiscible with the solvent, no conversion
12	ee	MeOH/DCA	Mixture of >5 products
13	ee	H_2O/HOAc	Immiscible with the solvent, no conversion
14	ff	MeOH/DCA	Mixture of ~4 bicyclic products
15	gg	MeOH/DCA	Methoxy adduct **1c** (52%), 3 minor by-products
16	hh	MeOH/DCA	No reaction
17	ii	MeOH/DCA	decomposition
18	jj	MeOH/DCA	Methoxy adduct **1d** (75%), 2 minor bicyclic by-products
19	jj	MeOH/HCl	Methoxy adduct **1d** (48%), 2 minor bicyclic by-products, competing decomposition
20	jj	MeOH/HOAc	Methoxy adduct **1d** (11%), 2 minor bicyclic by-products
21	jj	MeOH	Methoxy adduct **1d** (9%), 2 minor bicyclic by-products
22	kk	MeOH/DCA	Mixture of >5 products
23	ll	MeOH/DCA	Mixture of >5 products
24	mm	H_2O/HOAc	No reaction
25	nn	MeOH/DCA	Mixture of ~4 bicyclic products
26	nn	MeCN/HCl	No reaction
27	oo	MeOH/DCA	Mixture of ~4 bicyclic products
28	pp	MeOH/DCA	Decomposition
29	qq	MeOH/DCA	Decomposition
30	ss	MeOH/DCA	Mixture of ~4 bicyclic products
31	tt	MeOH/HCl	No reaction
32	uu	MeOH/HCl	No reaction

33	vv	MeOH/HCl	No reaction
34	ww	MeOH/HCl	No reaction
35	xx	MeOH/HCl	Mixture of >5 bicyclic products
36	yy	MeOH/HCl	No reaction

[a] Conditions description: substrate (832 µmol), solvent (12 mL), acid catalyst (if specified, 1.8 mol%). [b] 1.8 mol% of HOAc, H_2O/MeCN 1:1 (v/v, 12 mL). [c] Neat acetic acid.

2.4 Reactivity of phenyl silanes

The relative reactivity of four differently substituted phenyl silanes (Scheme S2) in photochemical addition of methanol catalysed by dichloroacetic acid (DCA) was compared.

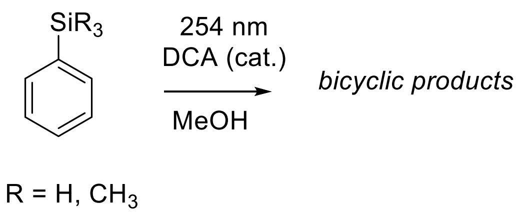

Scheme S2: Photochemical rearrangement of silyl-substituted benzenes

The relative rates determined from the ^{1}H NMR of the crude reaction mixtures together with Hammett's σ values for the respective substituents are shown in Table S4.

Table S4: Relative rates and Hammett's σ constants of differently substituted phenyl silanes.

#	R_1	R_2	R_3	k_{rel}[a]	σ_m[b]	σ_p[b]	$\log(k_{rel})$	$\log(k/k_0)$[c]
1	H	H	H	3.8	0.05	0.1	0.584	0.292

2	CH_3	H	H	17.8	*0.03*[d]	*0.07*[d]	1.250	0.625
3	CH_3	CH_3	H	36.0	0.01	0.04	1.557	0.778
4	CH_3	CH_3	CH_3	100	-0.04	-0.07	2.000	1.000

[a] Relative rate calculated from ^{1}H NMR of parallel reaction. [b] Taken from ref.[1] [c] Logarithm of the ratio of relative rates of the reaction, k_0 is the rate of reaction for TMS benzene. [d] Linearly interpolated value from the constants known for compounds in the entry 1 and 3.

Figure S1 shows a correlation between relative reactivity and Hammett's σ constants (m and p). The data show linear correlation of these data.

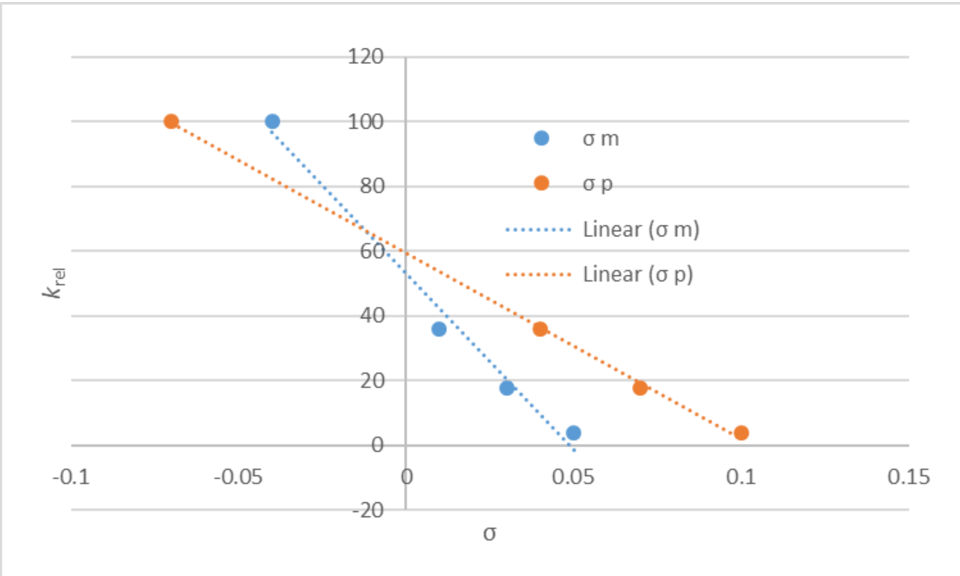

Figure S1: Correlation between relative reactivity (k_{rel}) and Hammett's σ constants.

The LFER analysis of these data (TMS-benzene photorearrangement taken as k_0) is shown in Figure S2. The fit has slightly negative slope with faster reaction with more electron donating (= more negative) σ constant, however, it is not linear as other factors (e. g. steric effects, hyperconjugation) might play role.

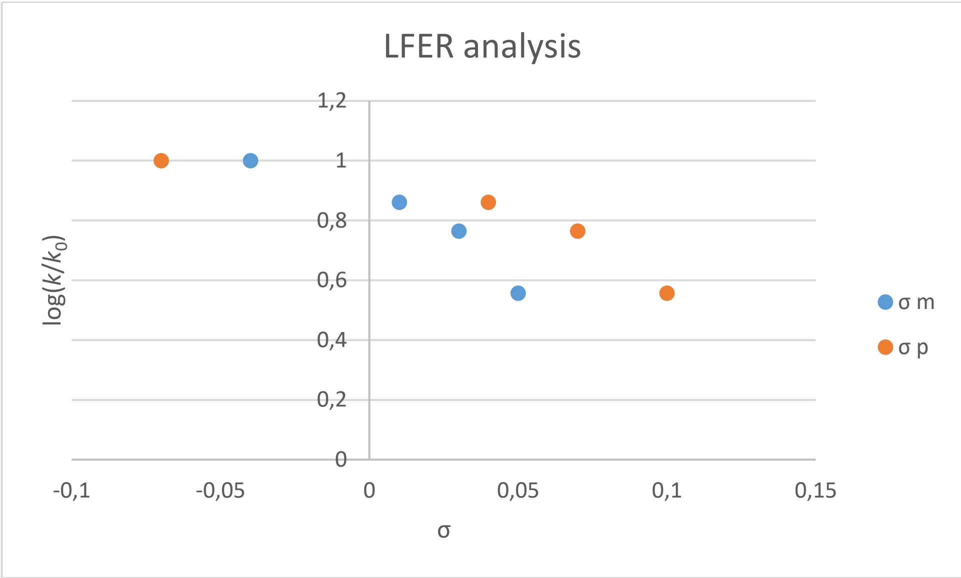

Figure S2: LFER analysis of the photorearrangement of differently substituted phenylsilanes.

3. Synthesis of the products

3.1 Product purity and separation

The irradiation of arenes leads to complex mixtures of regio- and stereoisomers (often more than 20 different isomers) that interconvert between each other thermally and photochemically (vide infra). They also decompose to undefined polymeric products based on polymerization of fulvene. Since the physical properties of all these small, non-polar, volatile and non-absorbing molecules are very similar, it was often impossible to separate products with purity higher than 70 – 80%. Neither chromatographic techniques (HPLC of column) nor fraction distillation sometimes helped to significantly increase the purity of the final product. However, the products after derivatization (such as the compound **7**) were stable and could be isolated in high final purity. The chemical yields are isolated yields with correction on the product purity calculated based on NMR unless stated elsewhere.

3.2 (±)-((1*S*,4*S*,5*S*,6*R*)-4-methoxybicyclo[3.1.0]hex-2-en-6-yl)trimethylsilane (±)-**1d**

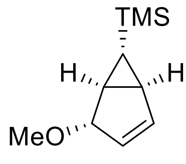

(±)-**1d**

Solution of phenyl trimethylsilane (1.2 mL, 6.97 mmol, 1 eq.) and dichloroacetic acid (10.3 µL, 0.125 mmol, 0.018 eq.) in methanol (100 mL) was irradiated in a quartz tube equipped with a stir bar by 254 nm light in a Rayonet reactor equipped with a cooling fan (reaction temperature ~35 °C) for 8 hours. The reaction mixture turned slightly yellow and the solvent was carefully evaporated under reduced pressure. The crude product (1.131 g, 89%, dark brown oil) was purified by column chromatography in Et_2O in *n*-pentane (2 – 4 %, v/v, R_f = 0.2 – 0.4, the TLC was analysed by Hanessian's stain) to give the title compound as colourless liquid of characteristic smell (953 mg, 75%).

^{1}H NMR (400 MHz, Chloroform-*d*) δ (ppm) 6.37 (d, J = 5.5 Hz, 1H, *a*), 5.52 (pseudo dt, J = 5.5, 1.5 Hz, 1H, *b*), 4.19 (pseudo t, J = 2.2 Hz, 1H, *c*), 3.38 (s, 3H, *d*), 1.83 – 1.77 (m, 1H, *e*), 1.74 (pseudo td, J = 5.5, 1.1 Hz, 1H, *f*), -0.03 (s, 9H, *g*), -0.67 (dd, J = 5.5, 4.4 Hz, 1H, *h*).

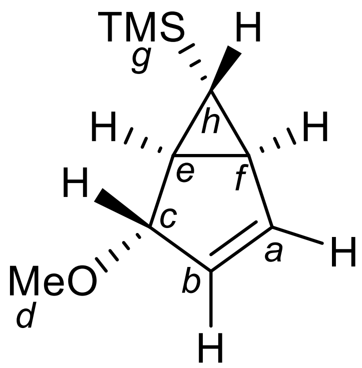

^{13}C NMR (101 MHz, Chloroform-*d*) δ (ppm) 142.71 (CH, *a*), 126.90 (CH, *b*), 86.22 (CH, *c*), 54.80 (OMe, *d*), 26.53 (CH, *f*), 26.40 (CH, *e*), 25.23 (CH, *h*), -2.20 (CH, *g*).

HRMS: $C_{10}H_{18}OSi$: calculated 182.1127, found 182.1129 (rel. error 1.1 ppm).

Assignment of the relative configuration on the stereocentres:

As the molecule is synthetized in one step from a planar substituted benzene, the topology and relative configuration of the carbon atoms on the scaffold could not be determined from the chemical history of the compound (i.e. from relative geometry of the starting material). A detailed analysis of the COSY spectra (Figure S5) resulted into following conclusions:

- TMS group must be attached to a secondary carbon atom (multiplet at –0.68 ppm)
- OMe group must be attached at secondary carbon (multiplet at 4.18 ppm)
- Structure contains only CH signals (no CH_2 signals present)

All these considerations limit the possible product structure to following stereoisomers (Figure S3):

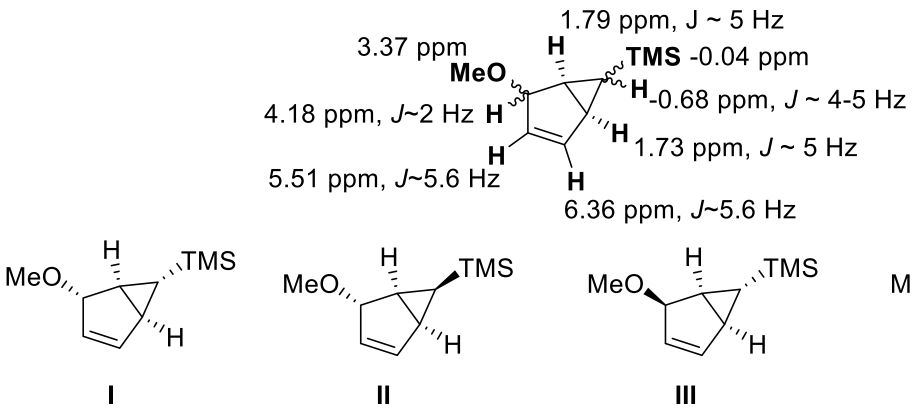

Figure S3: Assignment of the ^{1}H NMR signals and possible structures of photoproducts.

Coupling constant analysis according to the Karplus equation led to the following findings:

- Coupling constants are generally lower than 7-8 typical for antiperiplanar and synperiplanar conformation
- The structure is puckered and the protons at 1.73 and 1.79 ppm must be *cis* to each other
- All other pairs of protons are *trans* to each other

This suggests the structure **I** as the formed product (Figure 4):

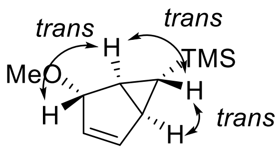

I

Figure S4: Absolute stereochemistry of the major photoproduct

The absolute assignment is in accordance with computational prediction (for details see the computational part). We have further experimentally proven the relative geometry by selective 1D NOE experiment (Figure S5). The selective excitation of the signal at 4.19 ppm (proton *c*) leads to the transfer of magnetization through space to proton *h* (Figure S5, middle, signal 1) and to the neighbouring proton *b* (Figure S5, middle, signal 2). The selective excitation of the signal at -0.67 ppm (proton *h*) leads to the transfer of magnetization to the neighbouring TMS group - protons *g* (Figure S5, bottom, signal 3) and through space to proton *c* (Figure S5, bottom, signal 4).

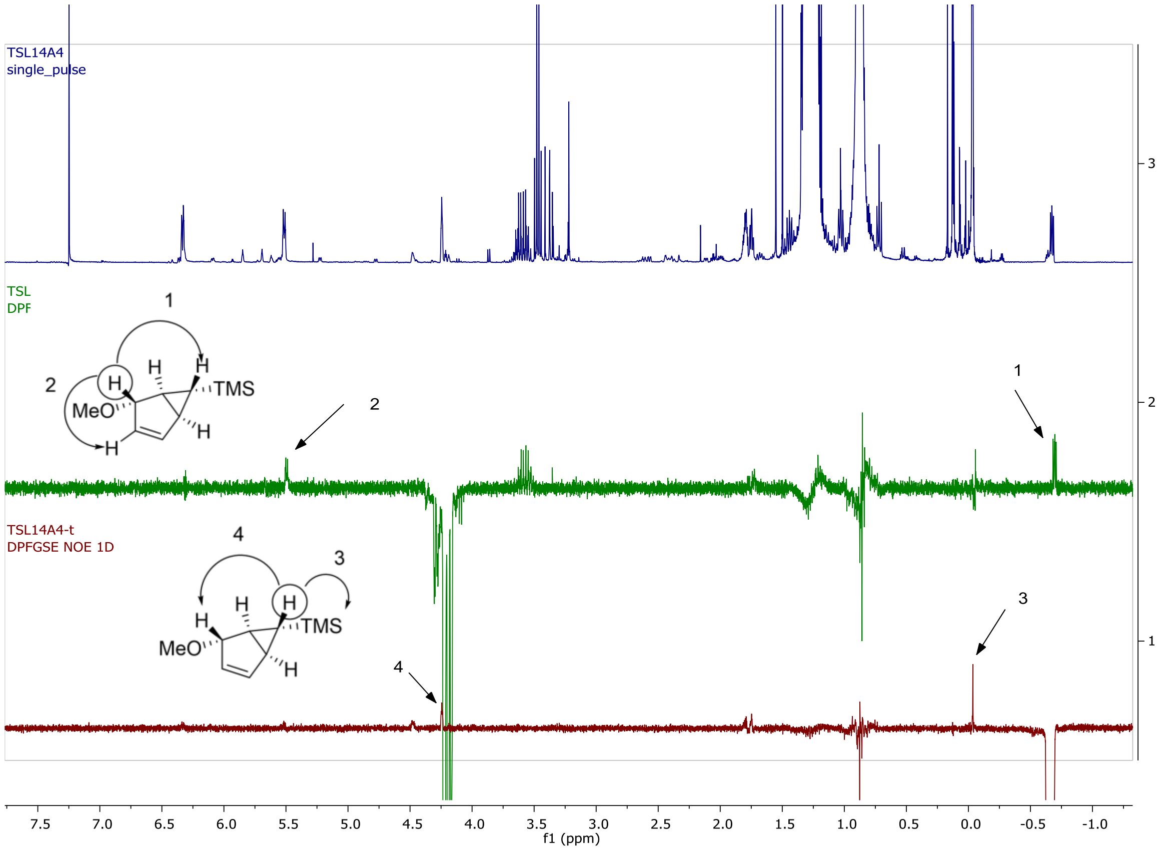

Figure S5: 1D NOE analysis of the stereochemistry of the derivative **1d**. ^{1}H NMR spectrum of the crude irradiated mixture after exhaustive irradiation (top), ^{1}H NOE spectrum with selective excitation at 4.19 ppm (middle) and at -0.67 ppm (bottom). The positive signals showing the transfer of magnetization are highlighted by arrows.

3.3 (±)-((1*R*,2*R*,5*S*)-2-methoxybicyclo[3.1.0]hex-3-en-1-yl)trimethylsilane (±)-**1e**

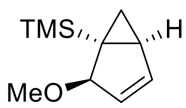

(±)-**1e**

The compound **1e** was identified as a by-product in the synthesis of (±)-**1d.** The product could not be isolated by column as it decomposed on silica. It also decomposed in exhaustive irradiation (vide infra). The maximum yield at ~90% conversion was 40% (NMR), colourless oil with characteristic smell. The structure was determined by careful analysis of its mixture with **1d**.

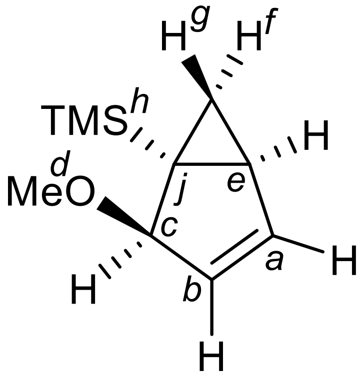

^{1}H NMR (400 MHz, Chloroform-*d*) δ (ppm) 6.19 (ddd, J = 5.5, 1.1, 0.6 Hz, 1H, *a*), 5.53 – 5.50 (m, 1H, *b*), 4.40 (s, 1H, *c*), 3.30 (s, 3H, *d*), 1.83 – 1.77 (m, 1H, *e*), 1.76 – 1.68 (m, 1H, *f*), 0.97 (ddd, J = 7.9, 3.5, 0.3 Hz, 1H, *g*), 0.02 (s, 9H, *h*).

^{13}C NMR (101 MHz, Chloroform-*d*) δ (ppm) 143.82 (CH, *a*), 127.22 (CH, *b*), 85.69 (CH, *c*), 53.77 (OMe, *d*), 27.17 (CH, *e*), 26.39 (CH_2, *f*/*g*), 22.83 (C, *j*), -2.29 (TMS, *h*).

HRMS: $C_{10}H_{18}OSi$: calculated 182.1127, found 182.1129 (rel. error 1.1 ppm).

Assignment of the relative configuration on the stereocentres:

The structure of the by-product **1e** has been elucidated based on NMR studies of the irradiated mixture of **1d**, **1e**, unknown isomeric product and TMS benzene. The structure determination based on ^{1}H NMR and 2D experiments could reliably determine all signals except the relative configuration on the carbon bearing the methoxy group (Figure S6).

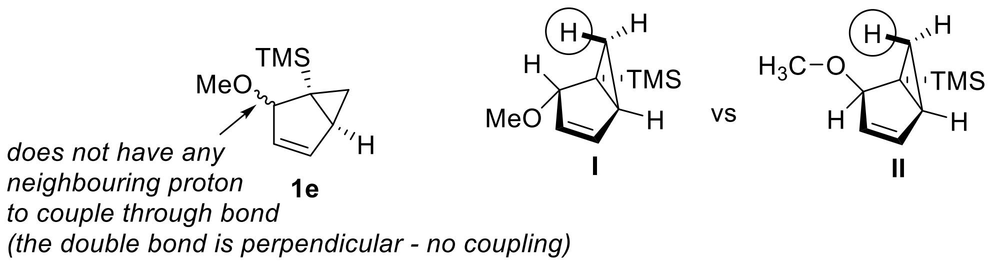

Figure S6: Structure of **1e** determined by NMR (1H, COSY).

The computational prediction of the 1H NMR spectrum of both structures depicted in Figure 3 (vide infra) provided the clarification of the structure. The most characteristic signal was from the proton directing *endo* to the bicyclic structure (Figure S6 emphasised by the ring). This signal has been shifted downfield in comparison to the molecule **1d** by 1.7 ppm! This huge effect cannot be caused only by the absence of the TMS group in the close proximity (this absence would cause the difference only of about ~0.7 ppm according to the computations). The shift is caused by the transannular interaction (intramolecular hydrogen bond, bond length only 2.7Å according to the computations) with the methoxy group which weakens the C–H bond and shifts its NMR signal upfield (Figure S7). We managed to observe also the isomer with the MeO group pointing to the opposite side (*exo*) as one of the minor by-products.

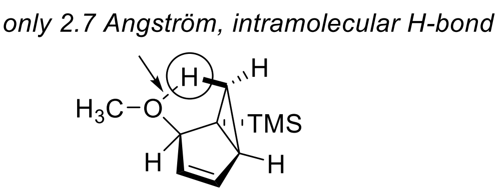

1e

Figure S7: Final determined structure of the molecule **1e**.

The absolute assignment has been further experimentally proven the relative geometry by selective 1D NOE experiment (Figure S8). The selective excitation of the signal at 4.40 ppm (proton *c*) leads to the transfer of magnetization to the neighbouring proton *b* (Figure S8, middle, signal 1) and through space to proton *e* (Figure S8, middle, signal 2). No transfer of the magnetization to the proton *g* has been observed which confirms that *c* and *g* are located at the oposite faces of the molecule. The selective excitation of the signal at 0.96 ppm (proton *g*) leads to the transfer of magnetization to the neighbouring proton *f* (Figure S8, bottom, signal 3). Again, no transfer of the magnetization to the proton *c* has been observed.

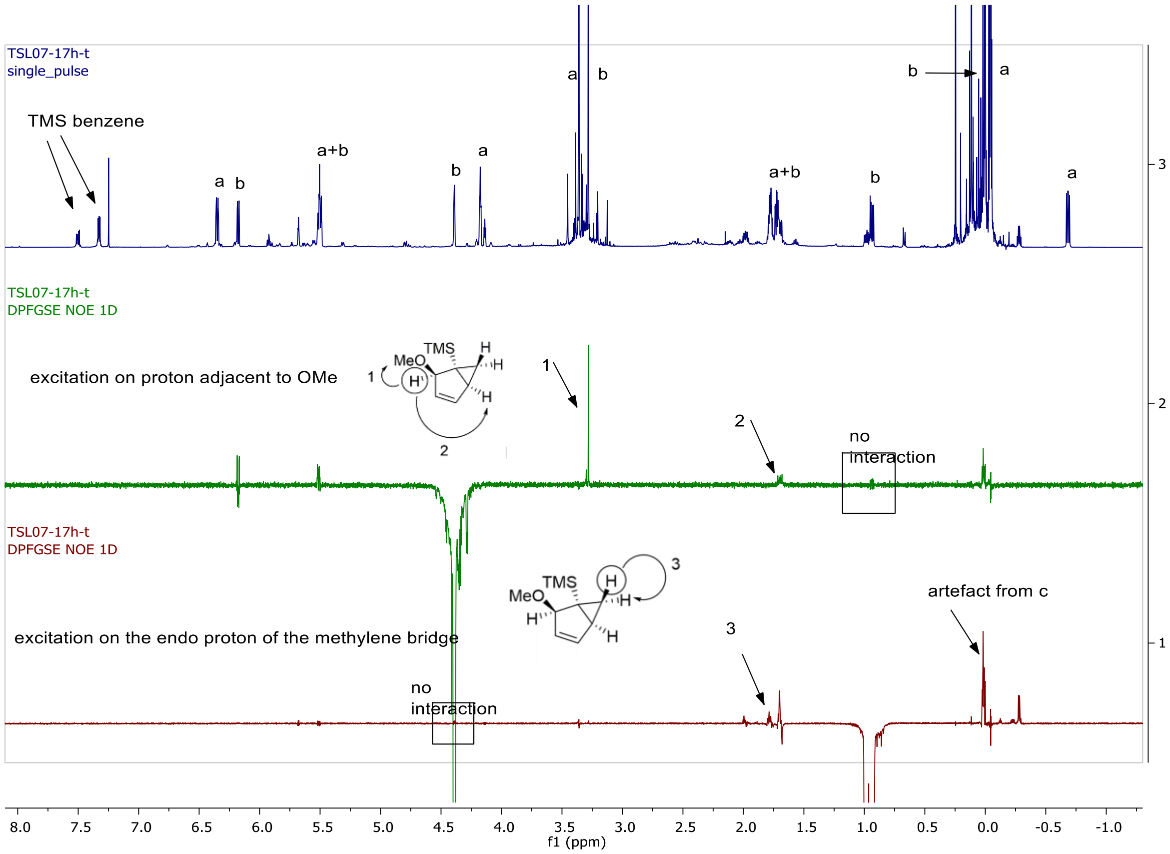

Figure S8: NOE analysis of the stereochemistry of the derivative **1e**. ^{1}H NMR spectrum of the crude irradiated mixture after exhaustive irradiation (top; signals of two isomers: a: **1d**, b: **1e**), ^{1}H NOE spectrum with selective excitation at 4.40 ppm (middle) and at 0.96 ppm (bottom). The positive signals showing the transfer of magnetization are highlighted by arrows, the expected missing interactions are highlighted by black squares.

3.4 (±)-(1*R*,4*S*,5*S*)-1-(tert-butyl)-4-methoxybicyclo[3.1.0]hex-2-ene, (±)-**1c**

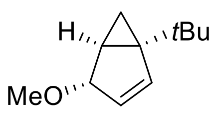

(±)-**1c**

Solution of *tert*-butyl benzene (0.537 mL, 3.49 mmol, 1 eq.) and dichloroacetic acid (5.2 µL, 0.0625 mmol, 0.018 eq.) in methanol (50 mL) was irradiated in a quartz tube equipped with a stir bar by 254 nm light in a Rayonet reactor equipped with a cooling fan (reaction temperature ~35 °C) for 6 hours. The reaction mixture turned slightly yellow and the solvent was carefully evaporated under reduced pressure. The crude product (0.54 g, 93%, dark yellow oil) contained a mixture of three main products which is consistent to the literature.[2] The mixture was purified by column chromatography in Et_2O in *n*-pentane (2 – 10 %, v/v, R_f = 0.3 – 0.6, the TLC was analysed by Hanessian's stain) to give the title compound as colourless liquid of characteristic smell (301 mg, 52%). The compound has been previously described in the literature.[2]

^{1}H NMR (400 MHz, Chloroform-*d*) δ (ppm) 6.24 (d, *J* = 5.6 Hz, 1H, *a*), 5.43 (dt, *J* = 5.6, 1.9 Hz, 1H, *b*), 4.12 (s, 1H, *c*), 3.32 (s, 3H, *d*), 1.66 (dd, *J* = 8.5, 4.2 Hz, 1H, *e*), 0.99 (t, *J* = 2.1 Hz, 1H, *f*), 0.90 (s, 9H, *g*), -0.13 (t, *J* = 4.1 Hz, 1H, *h*).

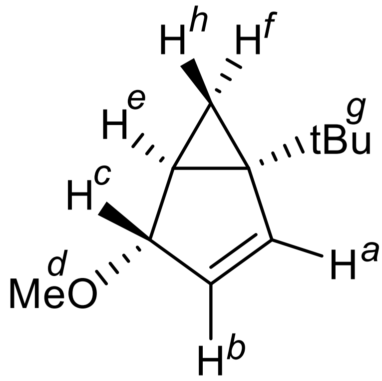

Assignment of the relative configuration on the stereocentres:

The major photoproduct of the rearrangement of the *tert*-butyl benzene has ^{1}H NMR spectrum (Figure S55) similar to the products TMS-benzene rearrangement (Figures S44 and S49). Based on COSY experiments (Figure S11), its structure has been assigned as with *t*Bu-group at the bridging atom and MeO in *exo* position (Figure S9).

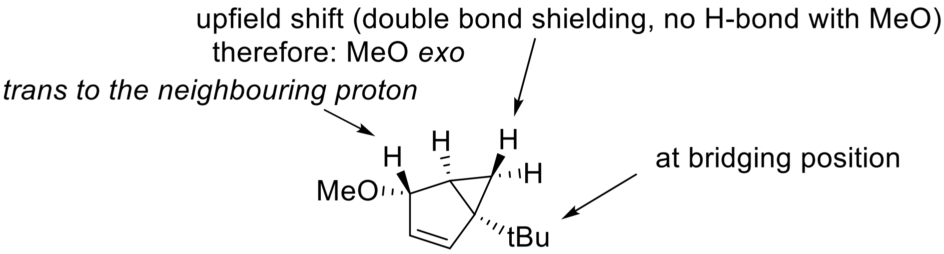

Figure S9: Assignment of the constitution of the product **1c** based on ^{1}H NMR and COSY.

To confirm the structure, we have calculated sum of squared residuals calculated by subtraction of measured NMR shifts from the predicted shifts by computation for total 12 possible products (Figure S10). The assignment is shown in the Table S5.

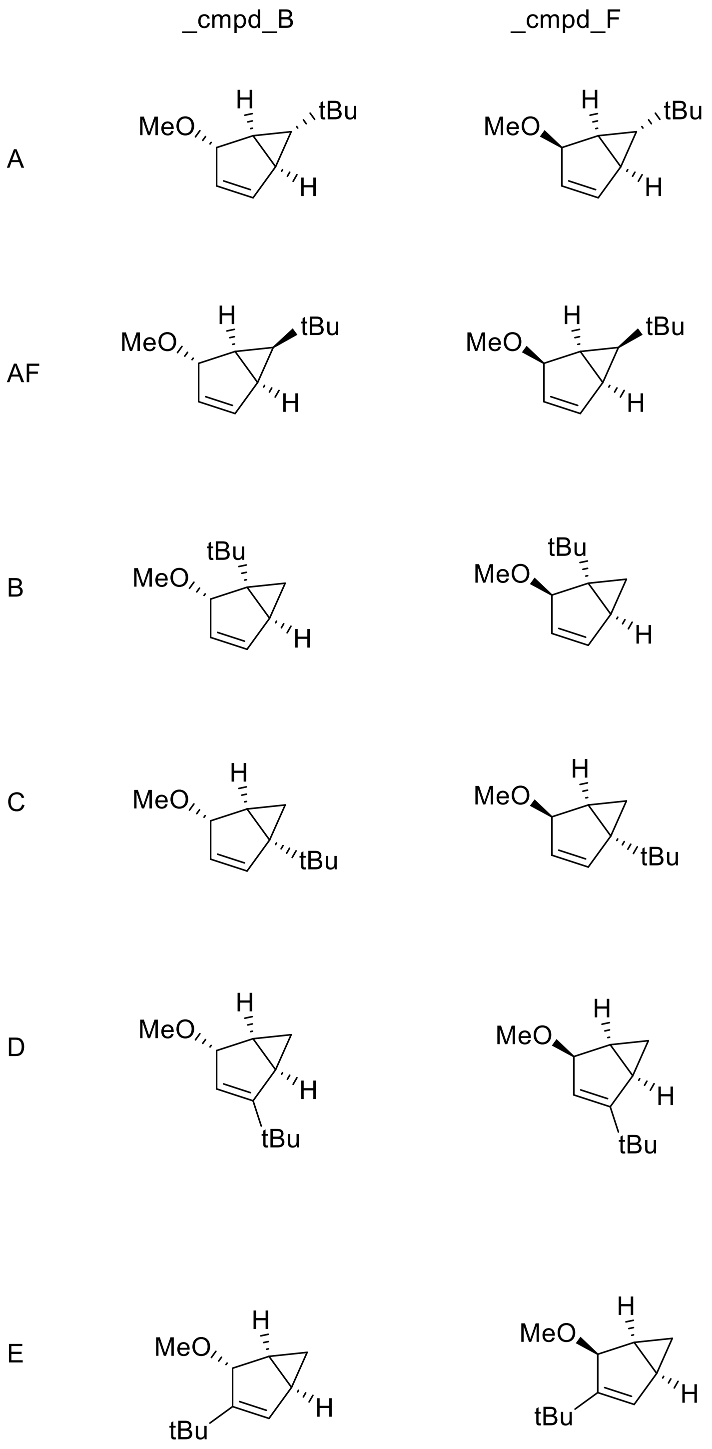

Figure S10: Possible rearrangement product of tert-Bu-benzene in methanol

Table 5: ^{1}H NMR signals (in ppm) measured and predicted for the possible structures.[a]

exp	6.24	5.43	4.12	3.32	1.66	0.99	0.9	-0.13
A_cmpd_B	6.4025	5.7368	4.137	n.d.[b]	1.82295	1.82295	n.d.	0.1118
A_cmpd_F	6.2387	5.4975	4.9876	n.d.	1.8015	1.4573	n.d.	0.9272
AF_cmpd_B	6.3689	6.2189	4.3604	n.d.	2.0942	1.8557	n.d.	1.041
AF_cmpd_F	5.9789	5.639	5.0372	n.d.	2.1656	1.5383	n.d.	0.7302
B_cmpd_B	6.6075	6.0575	4.2217	n.d.	1.7016	1.3034	n.d.	-0.153
B_cmpd_F	6.4669	5.9744	4.7200	n.d.	1.5221	0.9443	n.d.	0.7435
C_cmpd_B	6.6497	6.0503	4.1047	n.d.	1.7126	1.0861	n.d.	-0.088
C_cmpd_F	6.4468	5.8701	4.8227	n.d.	1.5413	0.7818	n.d.	0.6679
D_cmpd_B	0.9349	5.6215	4.1326	n.d.	1.8269	1.744	n.d.	-0.135
D_cmpd_F	0.5745	5.0295	4.8564	n.d.	1.804	1.5482	n.d.	0.5745
E_cmpd_B	6.0589	0.8412	4.2564	n.d.	1.7536	1.7536	n.d.	-0.125
E_cmpd_F	5.9128	0.5487	4.9486	n.d.	1.7467	1.5356	n.d.	0.5487

[a] Computational details about used methods are shown in the computational part below. [b] n.d. = not determined (not relevant for the structural determination, the NMR shifts do not differ between studied isomers)

The best fit corresponds to the structures A_cmpd_B, B_cmpd_B and C_cmpd_B. The COSY analysis excludes the possibility of A_cmpd_B because the tert-butyl group must be located on the bridging atom.

1D NOE experiments (Figure S11) show weak transfer of magnetisation from the *tert*-butyl group to the methoxy group (and vice versa) which indicates that they are far from each other but *cis* to each other. Moreover, a strong transfer of magnetisation was observed from the *tert*-butyl group to the proton of double bond at 6.23 ppm (Figure S11, signal 5, bottom).

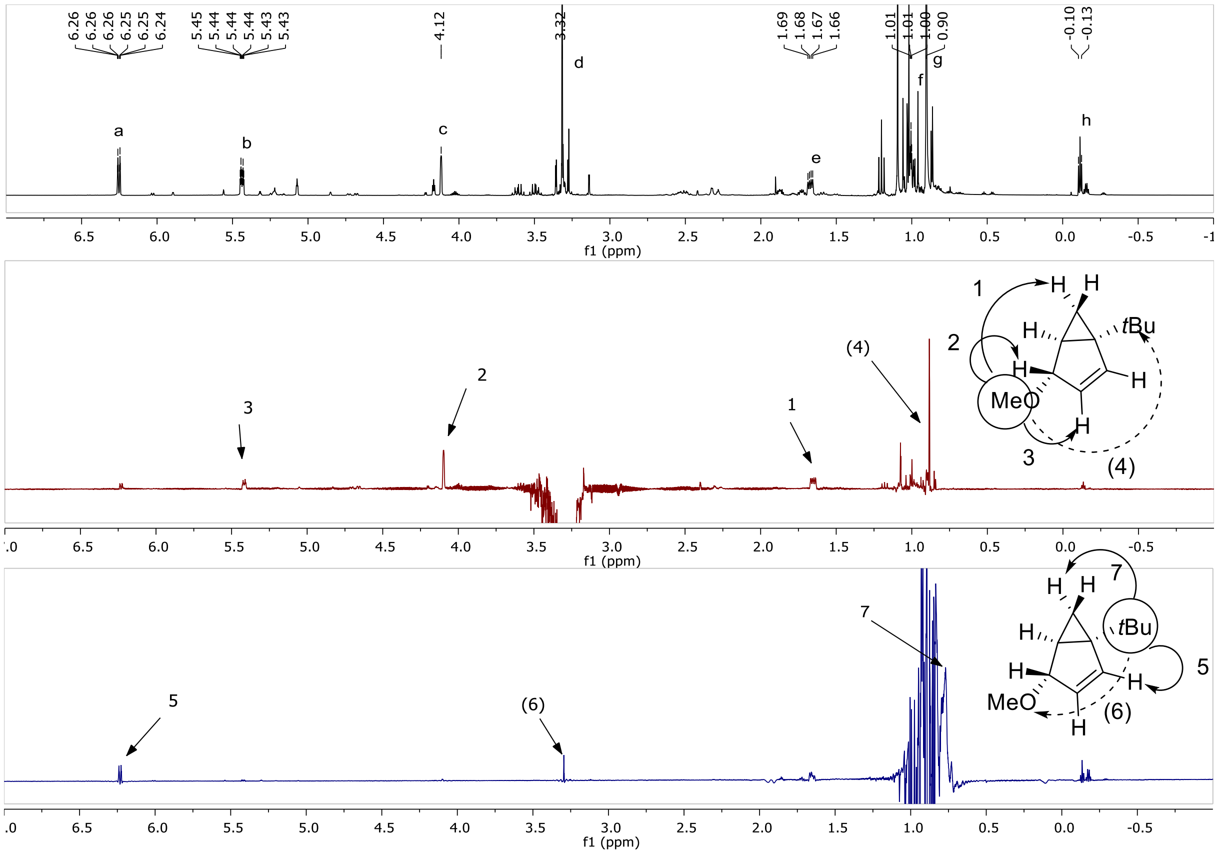

Figure S11: NOE analysis of the stereochemistry of the derivative **1c**. [1]H NMR spectrum of **1c** (top), [1]H NOE spectrum with selective excitation at 3.30 ppm (middle) and at 0.98 ppm (bottom). The positive signals showing the transfer of magnetization are highlighted by arrows and numbered. Weak interactions have numbers in brackets.

All spectral measurements suggest the structure **C_cmpd_B** as the correct one (Figure S12). This also corresponds to the calculated predictions and mechanistic considerations where the bulky *tert*-butyl group should facilitate the addition of the solvent at the opposite side in the cation (Figure S12, right side).

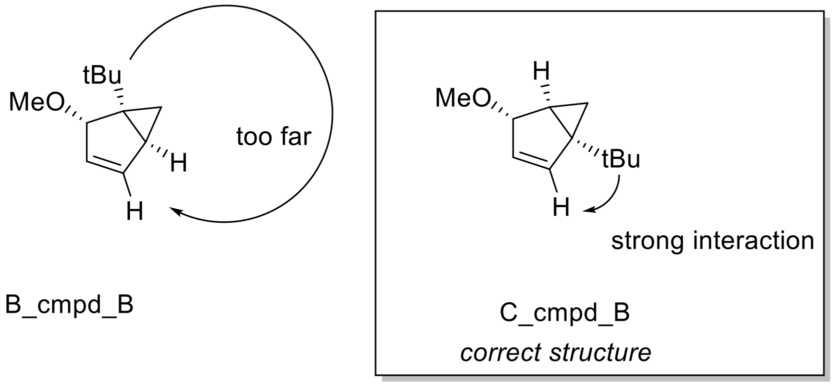

Figure S12: Structural elucidation of the product of the rearrangement of *tert*-butylbenzene in methanol.

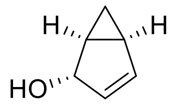

(±)-**1a**

3.5 (±)-(1*S*,2*S*,5*S*)-bicyclo[3.1.0]hex-3-en-2-ol, (±)-**1a**

A solution of benzene (111 µL, 1.421 mmol, 1 eq.) in water (18 mL) and acetic acid (1.5 mg, 26 µmol, 0.018 eq.) was loaded into a tube reactor and irradiated for 15 h by 254 nm light in a flow reactor. A white turbid precipitate was created in the tubing gradually over the course of the reaction. The reaction mixture was extracted by diethyl ether (2 × 10 mL), the organic phase was dried over $MgSO_4$ and the solvent was carefully removed under reduced pressure to give colorless oil (94 mg, 69%). The compound has been previously described in the literature.[3,4] The relative configuration on the stereocentres has been determined by ^{1}H and COSY NMR analysis and corresponds to the previous reports.[3,4]

^{1}H NMR (500 MHz, Chloroform-*d*) δ (ppm) 6.22 (dd, J = 5.4, 1.7 Hz, 1H, *a*), 5.52 (d, J = 5.4 Hz, 1H, *b*), 4.41 (s, 1H, *c*), 1.97 – 1.82 (m, 1H, *d*), 1.74 (dt, J = 8.1, 4.8 Hz, 1H, *e*), 0.96 (td, J = 8.0, 3.9 Hz, 1H, *f*), -0.11 (q, J = 3.9 Hz, 1H, *g*).

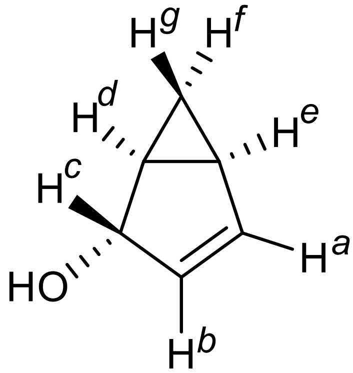

3.6 (±)-(1*S*,2*S*,5*S*)-bicyclo[3.1.0]hex-3-en-2-yl acetate, (±)-**1b**

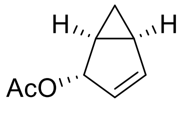

(±)-**1b**

Solution of benzene (74 µL, 0.83 mmol, 1 eq.) in glacial acetic acid (12 mL) was irradiated in a quartz tube equipped with a stir bar by 254 nm light in a Rayonet reactor equipped with a cooling fan (reaction temperature ~35 °C) for 6 hours. The reaction mixture was diluted with distilled water (150 mL) and neutralized with sodium bicarbonate (30 mL, saturated aq., carefully added) and extracted to diethyl ether (3 × 30 mL). The combined organic extracts were dried by $MgSO_4$ and evaporated under reduced to give the title compound as colourless liquid of characteristic smell (52 mg, yield recalculated on the purity: 45%).The compound was obtained in a mixture of other inseparable isomers (~20%) that interconverted between each other thermally and photochemically. The compound has been previously described in the literature. The relative configuration on the stereocentres has been determined by ^{1}H and COSY NMR analysis and corresponds to the previous reports.[3]

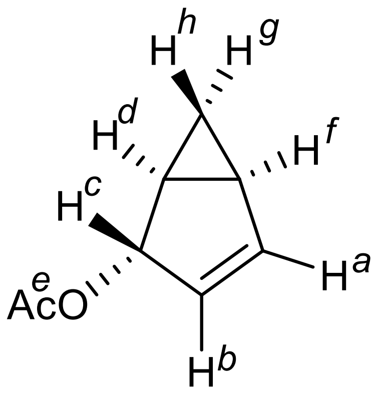

^{1}H NMR (400 MHz, Chloroform-*d*) δ (ppm) 6.34 (dd, *J* = 4.4, 1.2 Hz, 1H, *a*), 5.49 (d, *J* = 5.6 Hz, 1H, *b*), 3.99 (t, *J* = 6.5 Hz, 1H, *c*), 2.68 – 2.55 (m, 1H, *d*), 1.96 (s, 3H, *e*), 1.80 (t, *J* = 8.8 Hz, 1H, *f*), 1.03 (t, *J* = 7.2 Hz, 1H, *g*), 0.04 – 0.02 (m, 1H, *h*).

3.7 (±)-(1*S*,2*S*,5*S*)-bicyclo[3.1.0]hex-3-en-2-yl (*tert*-butoxycarbonyl)-L-phenylalaninate, (±)-**7**

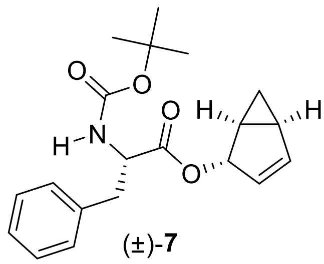

(±)-**7**

N-Boc-L-Phenylalanine (377 mg, 1.4231 mmol, 2.0 eq.), 4-dimethylaminopyridine (DMAP, 43 mg, 0.3557 mmol, 0.5 eq.) and (±)-**5a** (68 mg, 0.7115 mmol, 1.0 eq.) were mixed in a Schlenk flask under nitrogen atmosphere. Anhydrous THF (2 mL) was added to dissolve the acid followed by addition of anhydrous DCM (5 mL) and the resultant suspension was stirred for 4 min at 0 °C. A solution of dicyclohexylcarbodiimide (DCC, 293 mg, 1.4231 mmol, 2 eq.) in anhydrous DCM (5 mL) was added slowly and the reaction mixture was stirred for 18h at room temperature. The reaction mixture turned light yellow over the course of the reaction. The precipitate was filtered out and the organic solvent was removed under reduced pressure and the crude product was purified by column chromatography (Et_2O:pentane = 1:2 to 1:0, R_f = 0.2 to 0.8) to give the title compound as a colorless oil which upon standing in the freezer gave off-white solid with a characteristic smell (204 mg, 84 %). Isolated as a mixture of diastereomers.

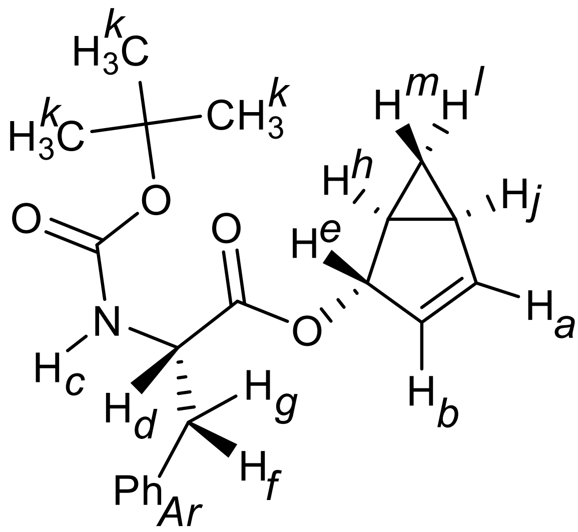

^{1}H NMR (400 MHz, Chloroform-*d*) *δ* (ppm) 7.32 – 7.21 (m, 3H, *Ar*), 7.19 – 7.12 (m, 2H, *Ar*), 6.40 – 6.34 (m, 1H, *a*), 5.49-5.41 (m, 2H, *b* and *e*), 5.07 – 4.96 (m, 1H, *f*), 4.63 – 4.51 (m, 1H, *g*), 3.22-3.01 (*m*, 2H, *c* and *d*), 2.04-1.96 (*m*, 1H, *h*), 1.84-1.66 (*m*, 1H, *j*), 1.42 (*s*, 9H, *k*), 1.09-1.00 (m, 1H, *l*), 0.10-0.02 (*m*, , 1H, *m*).

NMR (101 MHz, Chloroform-*d*) *δ* (ppm) 171.49 (*C*OOR), 155.22 (N*C*(O)OR), 142.96 (CH, *a*), 136.23 (C_{Ar}), 129.64 (C_{Ar}H), 128.58 (C_{Ar}H), 127.05 (C_{Ar}H), 125.95 (CH, *b*), 80.51 (C, *t*-Bu), 79.89 (CH, *e*), 54.62 (CH, *d*), 38.46 (CH_2, *g*/*f*), 28.41 (CH_3, *k*), 23.04 (CH_2. *m*/*l*), 22.26 (CH, *j*), 21.77 (CH, *h*).

HRMS (QTOF MS ESI+): calculated for $C_{20}H_{26}NO_4^+$ [M+H$^+$] 344.1856, found 344.1867, Δm = 3.1 ppm.

3.8 Chiral separation

Enantiomers of **7** (total amount 60 mg, injected amount 12 mg per run, *c* = 30 mg/mL) were separated by supercritical fluid chromatography (SFC) with a chiral column (Chiralpak ID) in supercritical 2-propanol/CO_2 (1/1, 120 bar, flow 70 mL/min) at 30°C. The isomers **7-RRR** and **7-SSS** were obtained in amount and purity 25 mg (ee = 98.8 %) and 26 mg (ee = 96.9 %), respectively. The purity of separated enantiomers is shown in Figures S13 and S14.

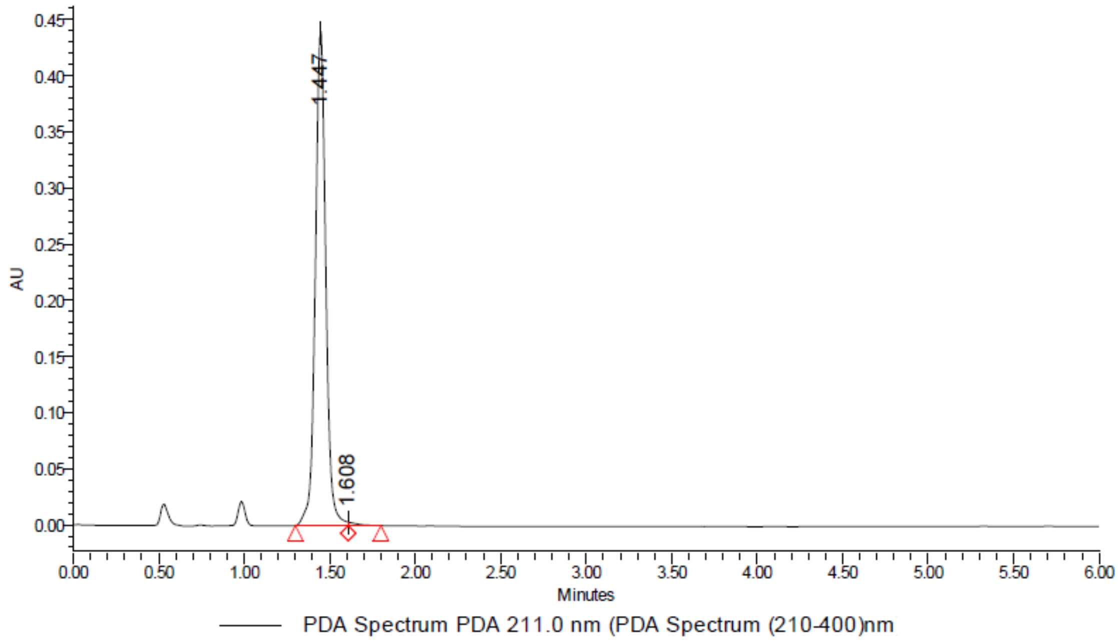

	Retention Time	Area	% Area	K'	N	USP Resolution
1	1.447	1879749	99.41	0.000	2859.1	
2	1.608	11240	0.59	0.111		

ee = 98.8

Figure S13: SFC chromatogram of **7-RRR**.

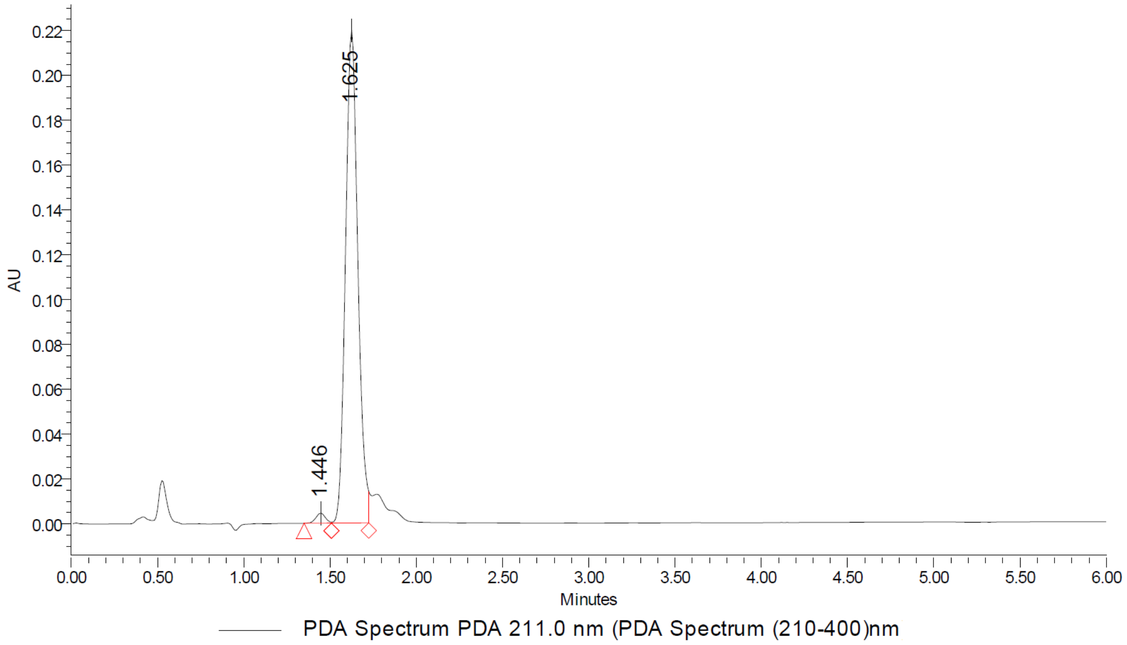

	Retention Time	Area	% Area	k'	N	USP Resolution
1	1.446	17122	1.54	0.000	3202.8	
2	1.625	1092889	98.46	0.123	2417.7	1.490

ee = 96.9

Figure S14: SFC chromatogram of **7-SSS**.

3.9 Structural NMR characterization of the isolated diastereomers

The separated diastereomers were analyzed by detailed NMR-2D analysis (COSY, HMBC, NOE). The samples were measured in $CDCl_3$ with 600 MHz NMR spectrometer. The structures of diastereomers for the means of structural determination were numbered according to the Figure S15.

Numbering:

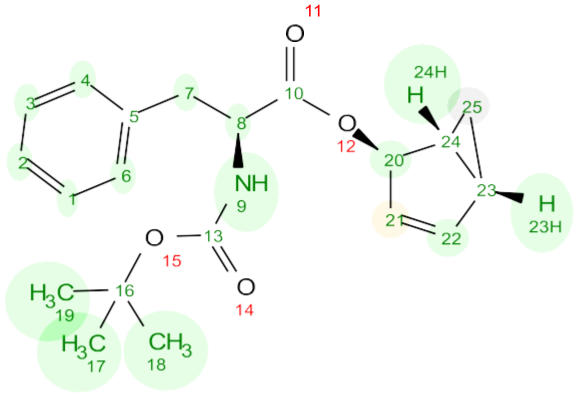

Figure S15: numbering of the derivative **7.**

Results:

Spectra of both samples are fully assigned and agree with proposed structures. The spectra from show very small shift differences both for ^{1}H and ^{13}C, as to be expected from two diastereomers. The NOESY spectra show some differences between the two substances and NOSY data to the 3D- structures obtained by MonteCarlo molecular mechanics searches used for VCD determination. NMR NOESY correlations fit the structures obtained from VCD experiments (see below).

In NOESY expansions below (Figures S16 – S23) it is observed that the phenyl ring CH(4/6) in **7-SSS** are in contact with CH(21). In **7-RRR** on the other hand CH(4/6) have correlations to CH(24) and not CH(21). (The same correlations are obtained for CH(7) but these are even more weak.)

NOE data can be fitted to the low energy structures obtained in VIDA to suggest the structures below:

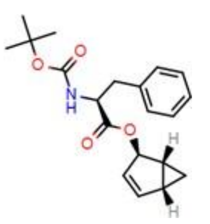

7-RRR

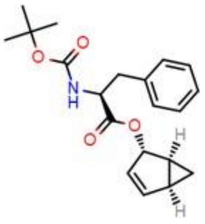

7-SSS

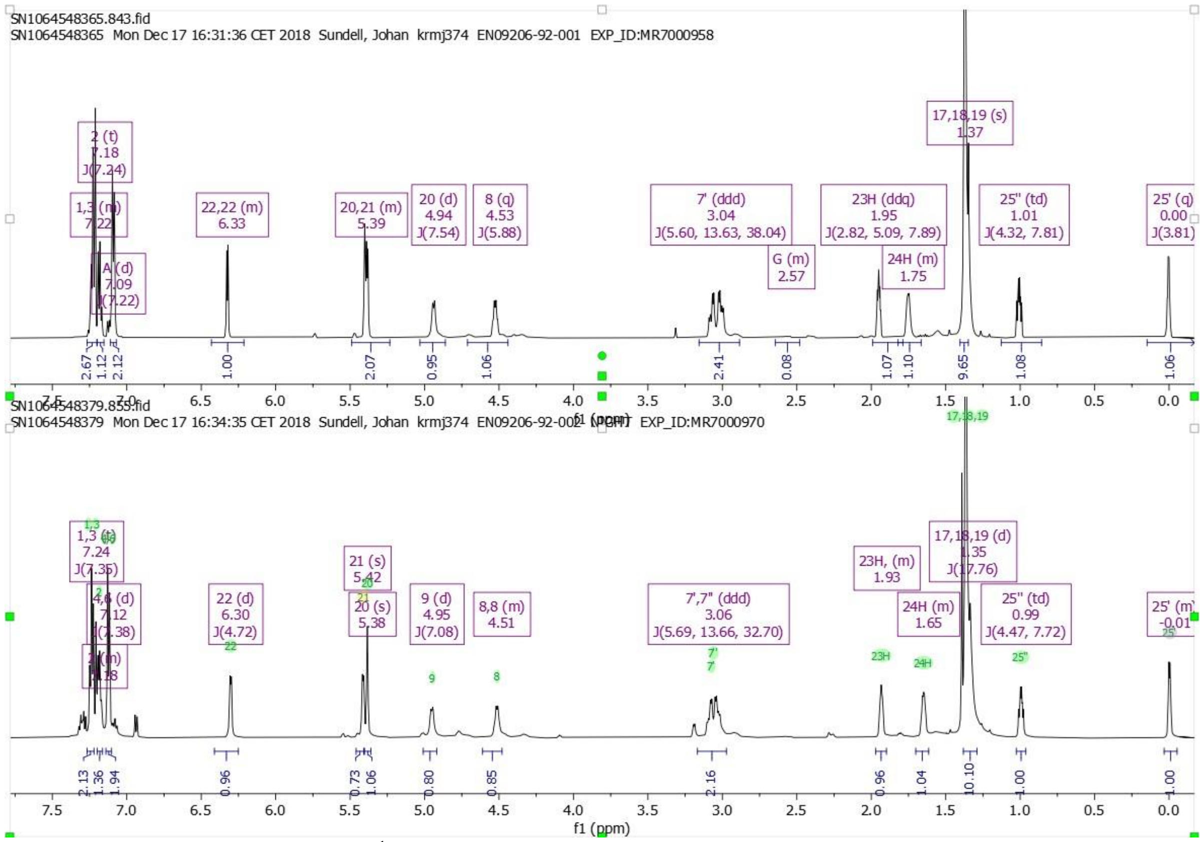

Figure S16: Comparision of ^{1}H spectra.

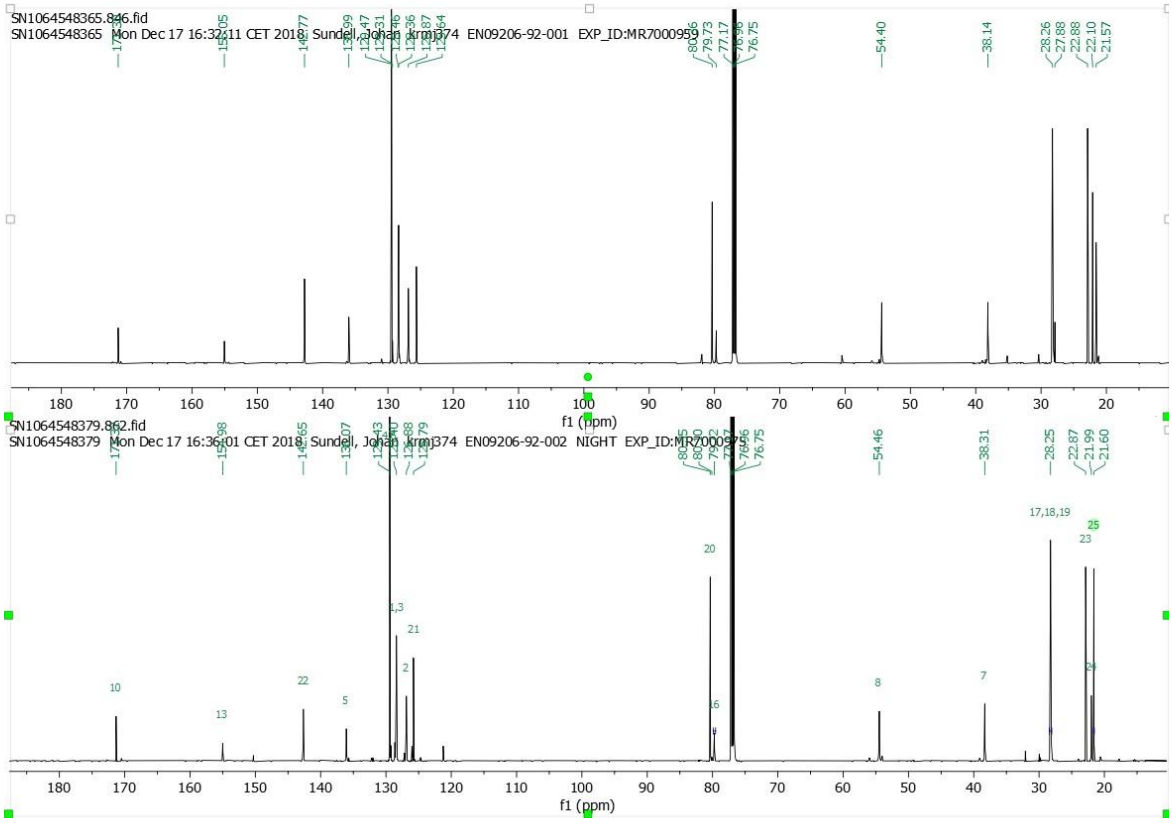

Figure S17: Comparision of ^{13}C spectra.

Indicating NOE correlations for **7-RRR.**

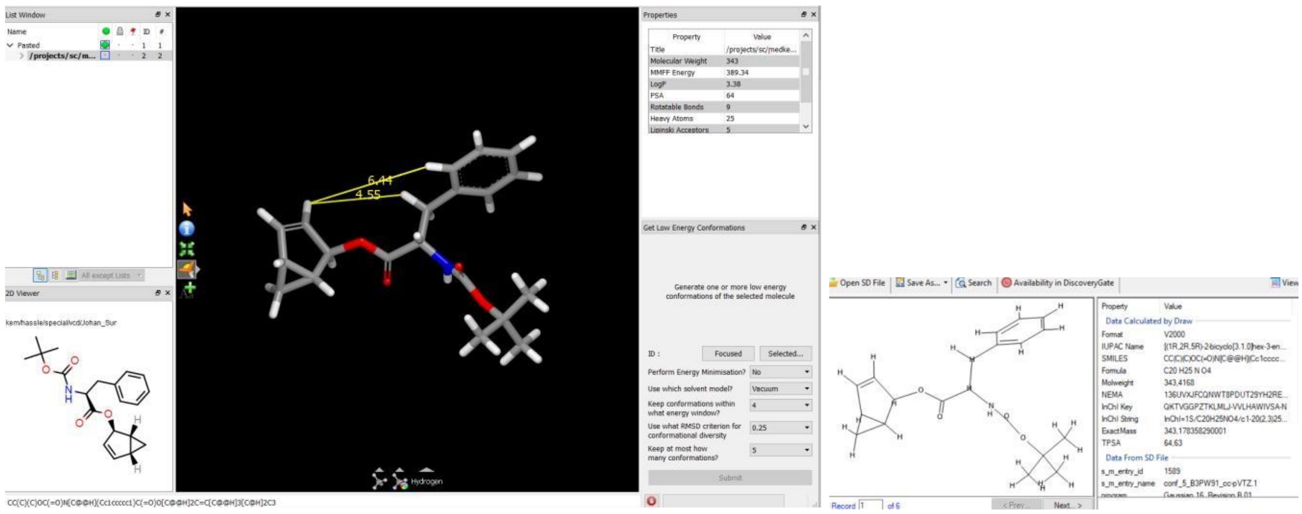

Figure S18: 3D representation low energy conformer of **7-RRR.**

Showing NOE correlations from **7-SSS.**

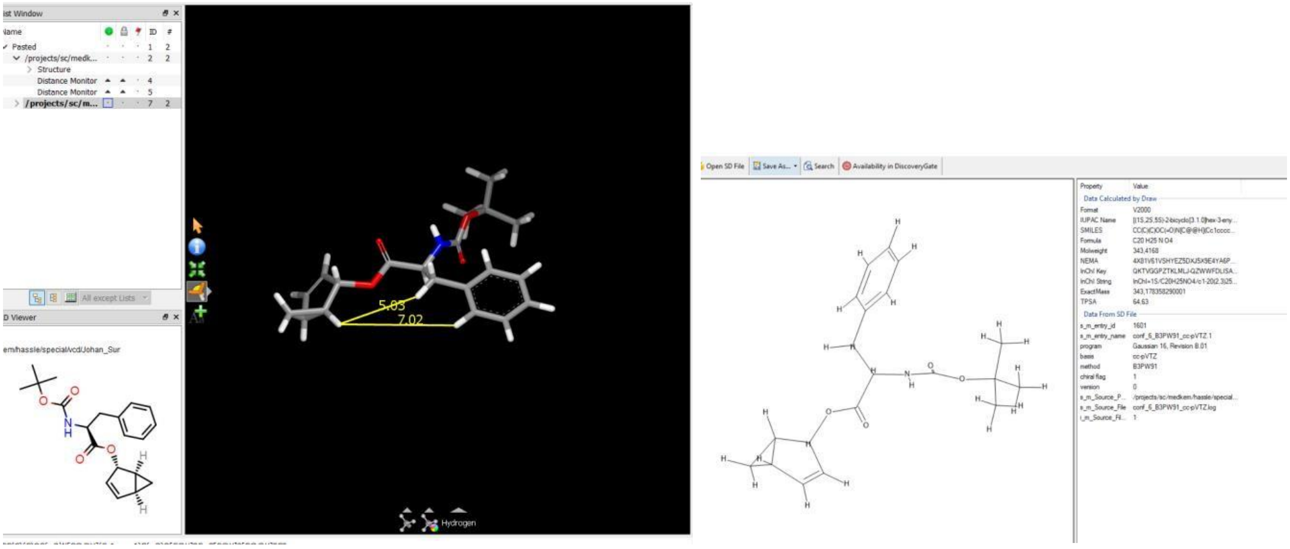

Figure S19: 3D representation low energy conformer of structure **7-SSS**.

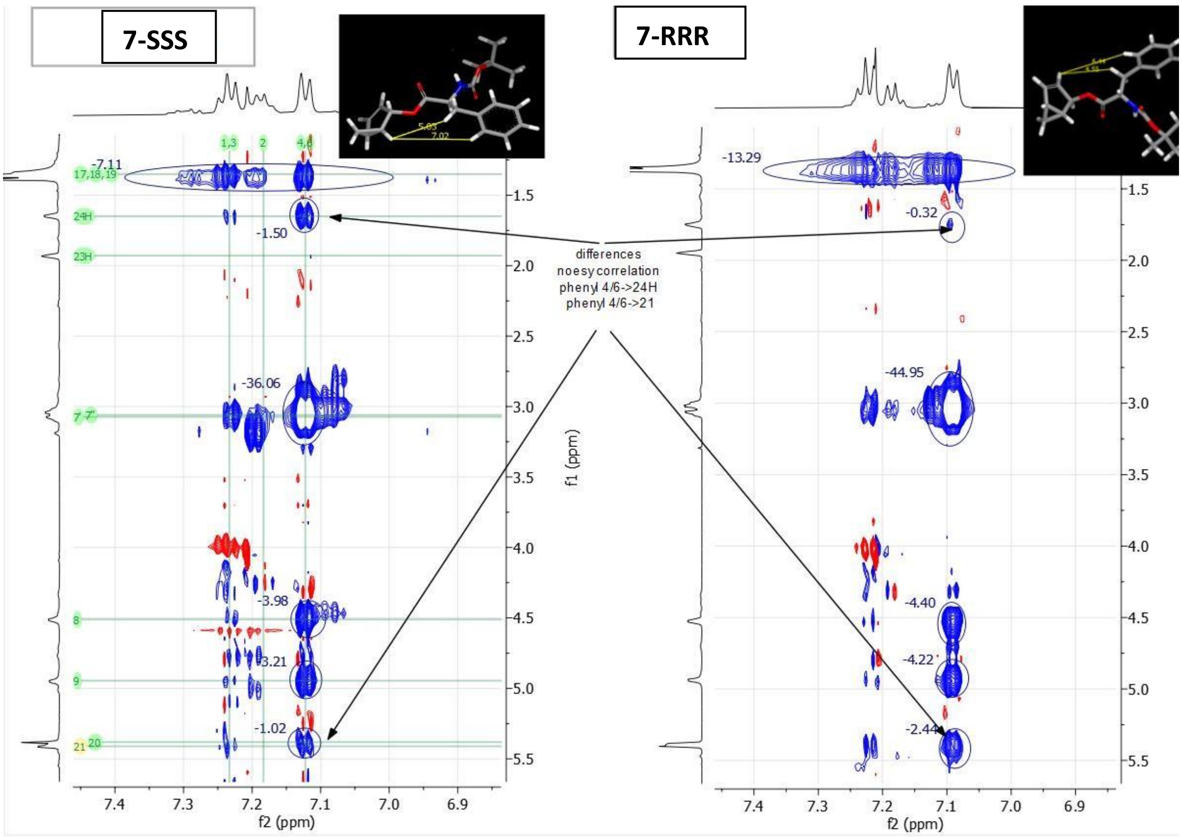

Figure S20: NOESY comparison. CH4/6

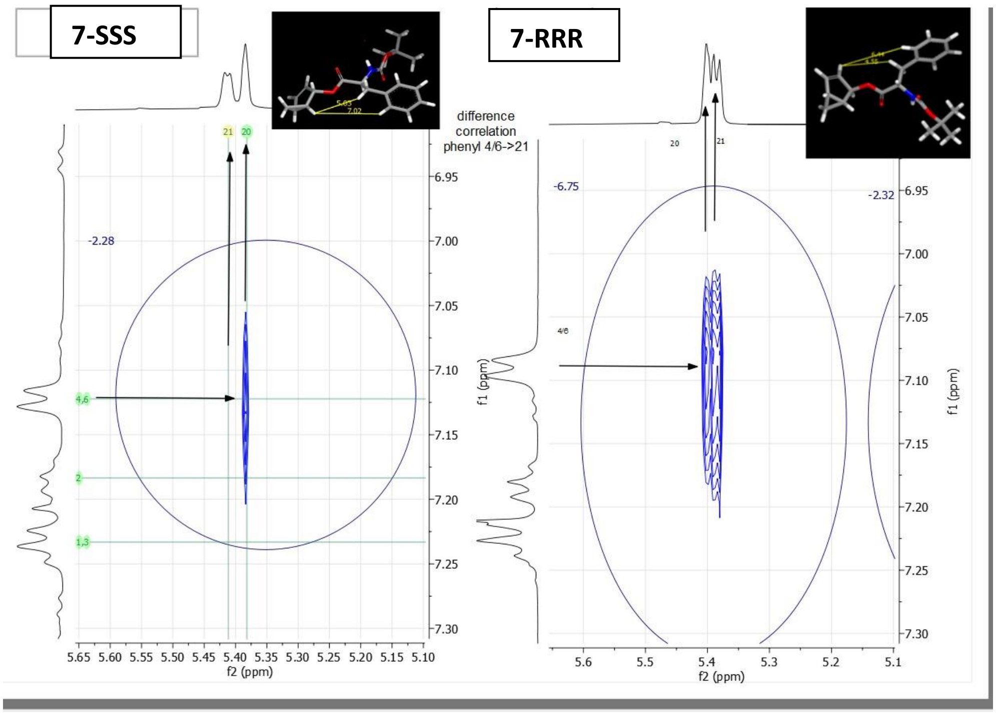

Figure S21: NOESY comparison expansion CH(21).

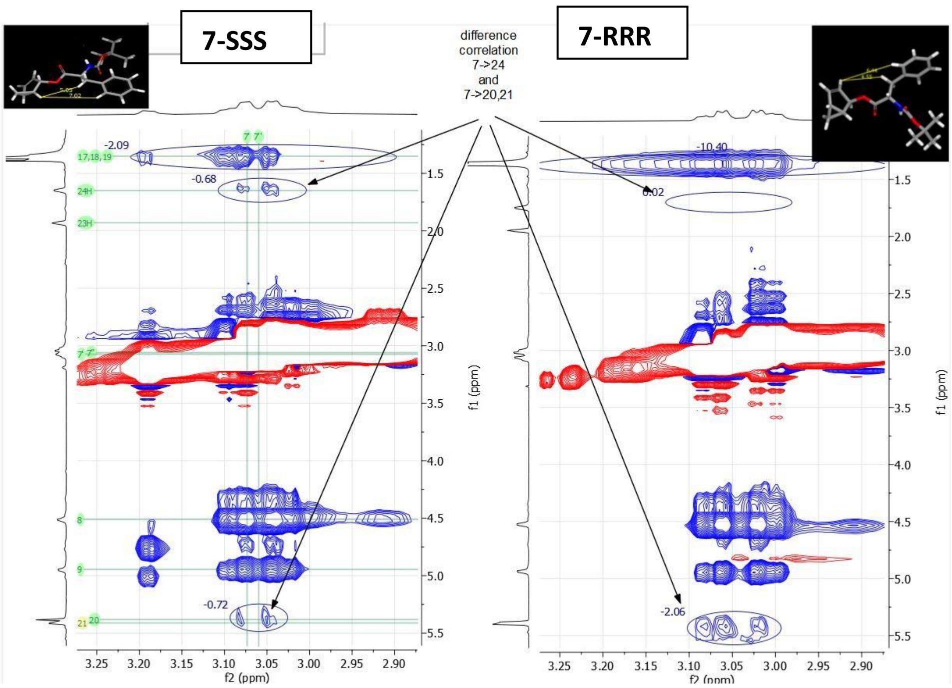

Figure S22: NOESY comparison expansion CH(7).

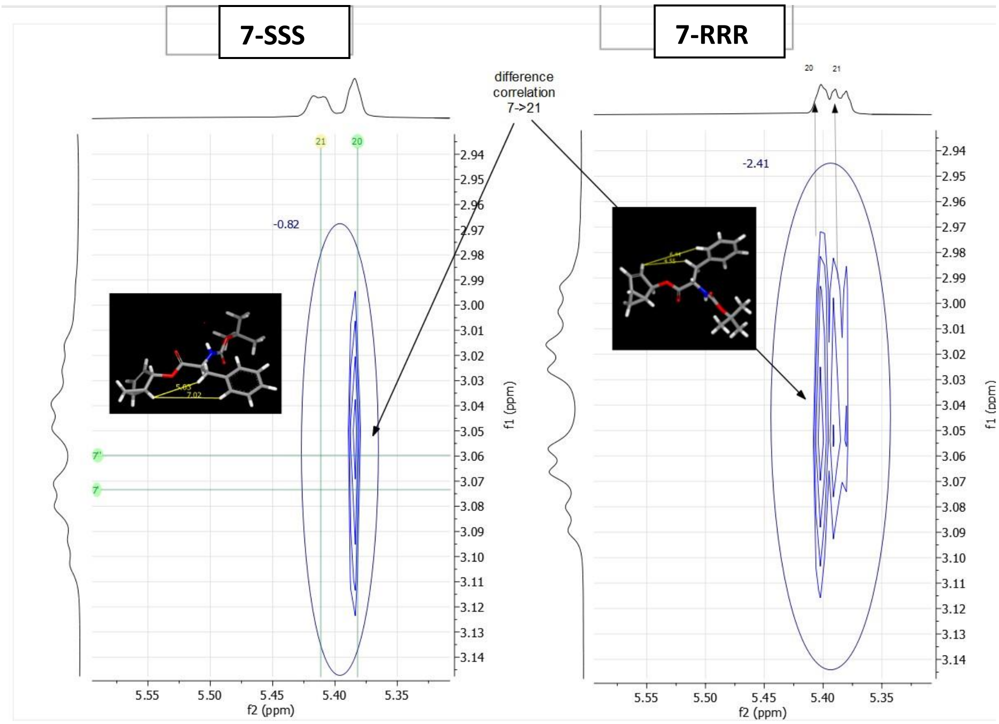

Figure S23: NOESY comparison expansion CH(21)->CH(7).

Table S6: List of NMR signals and key NOE correlations of diastereomers **7-RRR** and **7-SSS**.

7-SSS

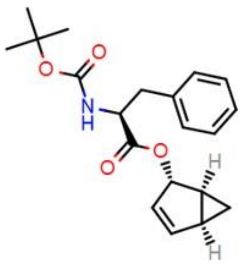

7-RRR

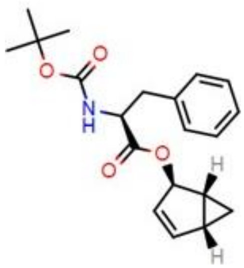

Atom	Shift	NOE
1 C	128.41	
H	7.23	
2 C	126.87	
H	7.23	
3 C	128.41	
H	7.23	

Atom	Shift	NOE
1 C	128.38	
H	7.23	
2 C	126.86	
H	7.18	
3 C	128.38	
H	7.23	

4 C	129.47		**4 C**	129.40	
H	7.09	4/6->24	**H**	7.12	4/6->21
5 C	135.99		**5 C**	136.26	
6 C	129.47		**6 C**	129.40	
H	7.09		**H**	7.12	
7 C	38.14		**7 C**	38.40	
H'	3.06	7->24	**H'**	3.07	7->21
H''			**H''**	3.06	
8 C	54.40		**8 C**	54.48	
H	4.53		**H**	4.51	
9 N			**9 N**		
H	4.95		**H**	4.95	
10 C	171.30		**10 C**	171.41	
11 O			**11 O**		
12 O			**12 O**		
13 C	155.05		**13 C**	155.09	
14 O			**14 O**		
15 O			**15 O**		
16 C	79.73		**16 C**	79.72	
17 C	28.26		**17 C**	28.25	
H3	1.37		**H3**	1.35	
18 C	28.26		**18 C**	28.25	
H3	1.37		**H3**	1.35	
19 C	28.26		**19 C**	28.25	
H3	1.37		**H3**	1.35	
20 C	80.36		**20 C**	80.33	
H	5.40		**H**	5.38	
21 C	125.64		**21 C**	125.74	
H	5.39		**H**	5.41	
22 C	142.77		**22 C**	142.63	
H	6.34		**H**	6.30	
23 C	22.88		**23 C**	22.87	
23H H	1.95		**23H H**	1.93	
24 C	22.10		**24 C**	21.99	
24H H	1.75		**24H H**	1.65	
25 C	21.57		**25 C**	21.60	
H'	0.00		**H'**	-0.01	
H''	1.01		**H''**	0.99	

3.10 Vibrational circular dichroism analysis

Experimental: 9.6 mg of **7-RRR** was dissolved in 150 µl $CDCl_3$ and 7.2 mg **7-SSS** in 113 µl $CDCl_3$. The solutions were transferred to 0.100 mm BaF_2 cells and VCD spectra acquired for six hours in a Biotools ChiralIR2X instrument. Resolution was 4 cm^{-1}. A VCD spectrum of a sample of $CDCl_3$ in the same cell was also acquired.

Computational Spectral Simulations: A Monte Carlo molecular mechanics search for low energy geometries was conducted for both diastereoisomers. *MacroModel* within the *Maestro* graphical interface (Schrödinger Inc.) was used to generate 135 (**7-RRR**) and 125 (**7-SSS**) starting coordinates for conformers within 5 kcal/mole of the lowest energy conformer. These conformers were initially minimized at B3LYP/6-31G(d) level in *Gaussian16*.[5] The energies of these conformations were examined, and all conformations greater than 2 kcal above the minimum and all duplicate conformations were discarded. This left 22 (**7-RRR**) and 19 (**7-SSS**) conformers which were used as starting point for further density functional theory (DFT) minimizations within *Gaussian16* at the B3PW91/cc-pVTZ level.

Optimized structures, harmonic vibrational frequencies/intensities, VCD rotational strengths, and free energies at STP (including zero-point energies) were determined at B3PW91/cc-pVTZ level of theory. For the **7-RRR** diastereoisomer, six conformations were found contributing to the solution conformation at a level greater than 10%. For the **7-SSS** diastereoisomer, four conformations were found contributing to the solution conformation at a level greater than 10%.

For both diastereoisomers, an in-house program was used to generate Boltzmann-weighted IR and VCD spectra from the selected conformations and fit Lorentzian line shapes (12 cm^{-1} line width) to the computed spectra thereby allowing direct comparisons between simulated and experimental spectra.

Fit between calculated and experimental IR spectra:

There is a good fit between calculated (red and green) and experimental (blue and pink) IR spectra for both diastereoisomers, shown below in Figure S24. The IR spectrum of the $CDCl_3$ blank was subtracted from the spectra below. Note that the two experimental IR spectra are essentially identical, and the two calculated spectra show only small differences.

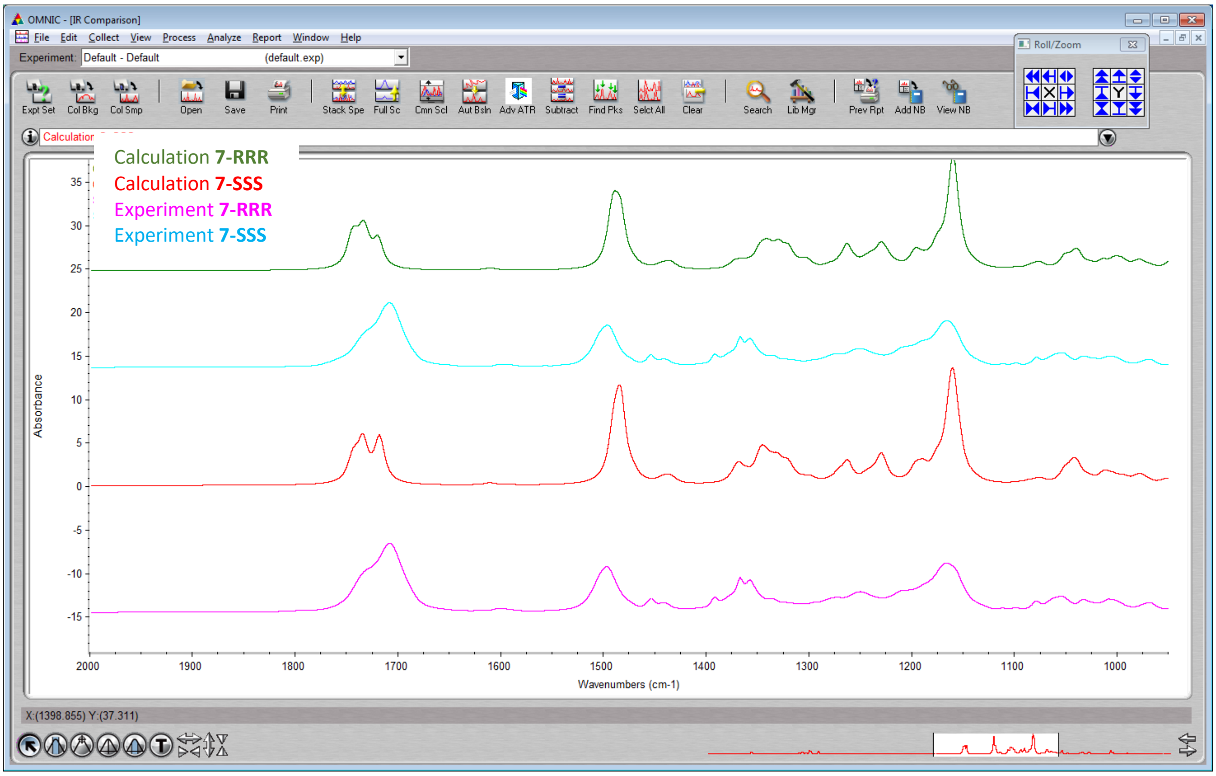

Figure S24: Calculated and experimental IR signature for **7**.

Fit between calculated and experimental VCD spectra:

The experimental spectrum for the $CDCl_3$ blank was subtracted from both experimental spectra. These two experimental spectra are shown in Figure S25 in red and dark green (below). The two calculated spectra are shown in purple (**7-RRR**) and light green (**7-SSS**).

First to note is that the spectra are complicated, and that there are many similarities between the calculated spectra for the two diastereosiomers and both experimental spectra. Therefore, the analysis described here concentrates on the differences between the spectra of the diastereoisomers.

The IR spectra were used to assign bands in the VCD spectrum. The experimental wavenumber, calculated wavenumber (according to the assignment) and sign observed are recorded in the Table S7 below. This shows a clear match between measured and calculated signs for the **7-RRR** diastereoisomer.

Table S7: List of important calculated and experimental VCD signatures for **7-RRR**.

Experimental wavenumber (cm^{-1})	Calculated wavenumber for matching peak (cm^{-1})	Measured signs in experimental VCD spectrum	Calculated signs for **7-RRR** diastereoisomer
1590	1610	-	-
1440	1440	+	+
1295	1295	+	+
1260	1260	+	+
1110	1095	+	+
1050	1040	+	+
1000	1000	+	+
970	980	+	+

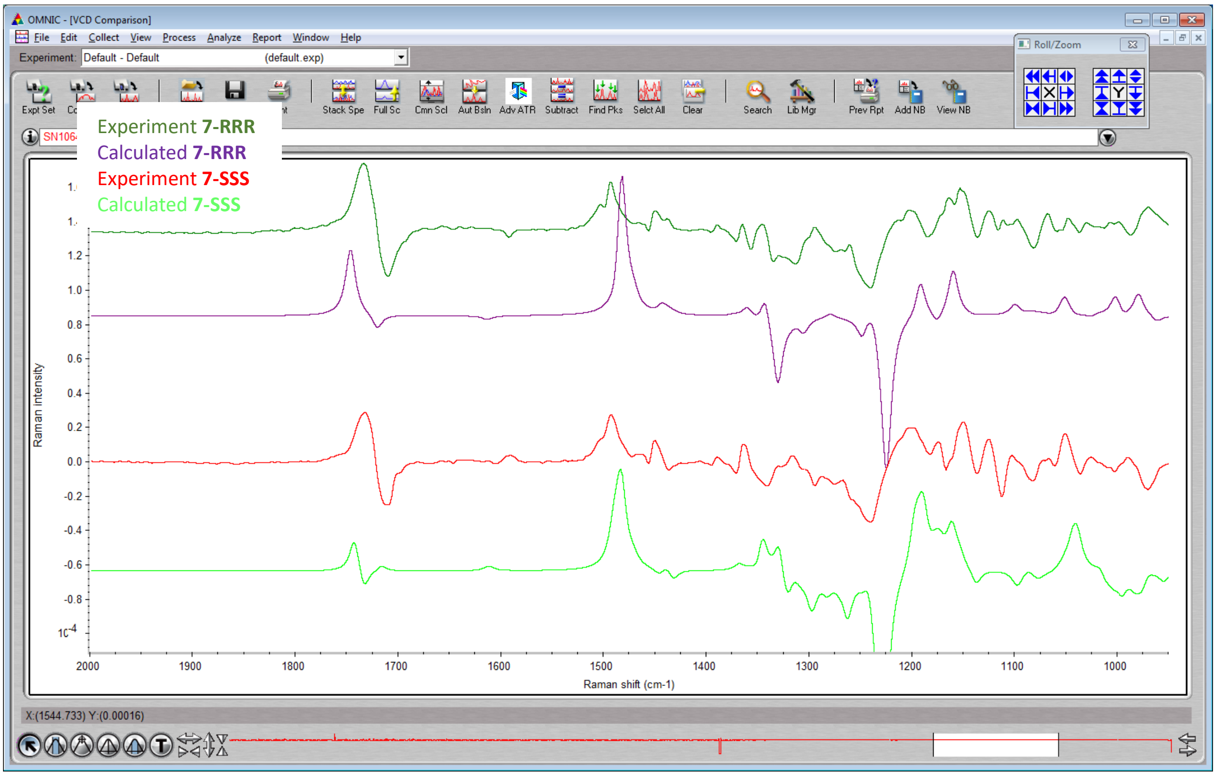

Figure S25: Experimental and calculated VCD spectra of **7**.

A difference spectrum was also calculated for the two experimental and two calculated spectra. In the Figure S26 below, the difference in the experimental spectra is shown in blue (**7-RRR** – **7-SSS**), and the calculated spectra in red (**7-SSS** – **7-RRR**) and purple (**7-RRR** –**7-SSS**). The good match between blue and purple spectra confirms the assignment of experimental spectra and calculated data for the **7-RRR** diastereomer.

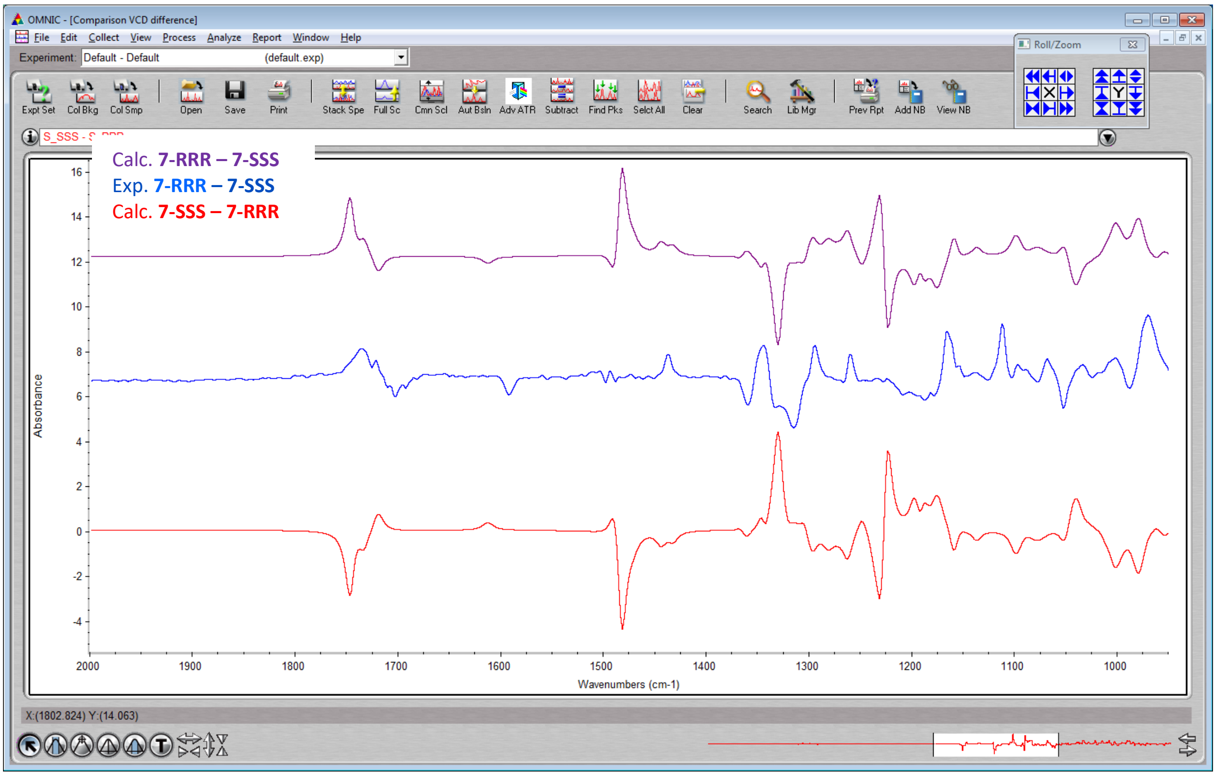

Figure S26: Experimental and calculated difference VCD spectra of **7**.

3.11 X-ray crystallography analysis

X-ray Crystallography

Single crystal of **7** crystalized as a mixture of diastereomers **7-RRR** and **7-SSS** has been collected on a Bruker D8 APEX-II equipped with a CCD camera using Mo Kα radiation (λ = 0.71073 Å). Crystal was mounted on a fibre loop and fixated using Fomblin oil. The data was collected at 150(2) K. Data reduction was performed with SAINT.[1] Absorption corrections for the area detector were performed using SADABS.[2] The structure was solved by direct methods and refined by least squares methods on F2 using the SHELX and the OLEX2 suit of programs.[3] Non-hydrogen atoms were refined anisotropically. Few of the carbon atoms have been restricted using SADI and RIGU constraints. Hydrogen atoms were constrained in geometrical positions to their parent atoms. Crystal was partially twinned and therefore twin matrix applied which is generated by Olex2 program. Further details can be found in the cif file.

(1) Bruker, Bruker AXS Inc., Madison, Wisconsin, USA, 2007.

(2) Bruker, Bruker AXS Inc., Madison, Wisconsin, USA, 2001.

(3) (a) G. Sheldrick, Acta Crystallogr., Sect. A: Found. Crystallogr. 2008, A64, 112-122; (b) O. V. Dolomanov, L. J. Bourhis, R. J. Gildea, J. A. K. Howard, H. Puschmann, J. Appl. Crystallogr. 2009, 42, 339-341.

Table S8: Crystal data and structure refinement for **7**.

Identification code	ag_ag_515_0m_a	
Empirical formula	C20 H25 N O4	
Formula weight	343.41	
Temperature	150 K	
Wavelength	0.71073 Ĺ	
Crystal system	Monoclinic	
Space group	P 1 21 1	
Unit cell dimensions	a = 5.1902(10) Ĺ	α= 90°.
	b = 37.256(7) Ĺ	β= 90.248(4)°.
	c = 9.5140(18) Ĺ	γ = 90°.
Volume	1839.7(6) Ĺ^3	
Z	4	
Density (calculated)	1.240 Mg/m^3	
Absorption coefficient	0.086 mm^{-1}	
F(000)	736	
Crystal size	0.2 x 0.1 x 0.07 mm^3	
Theta range for data collection	1.640 to 24.995°.	
Index ranges	-6<=h<=6, -44<=k<=44, -11<=l<=11	
Reflections collected	32095	
Independent reflections	6452 [R(int) = 0.0928]	
Completeness to theta = 24.995°	99.9 %	
Absorption correction	Semi-empirical from equivalents	
Max. and min. transmission	0.7457 and 0.6717	
Refinement method	Full-matrix least-squares on F^2	
Data / restraints / parameters	6452 / 47 / 459	
Goodness-of-fit on F^2	1.045	
Final R indices [I>2sigma(I)]	R1 = 0.0673, wR2 = 0.1633	
R indices (all data)	R1 = 0.1016, wR2 = 0.1846	
Absolute structure parameter	0.3(7)	

Extinction coefficient	0.017(3)
Largest diff. peak and hole	0.456 and -0.263 e.Ĺ$^{-3}$

Table S9: Atomic coordinates (x 10^4) and equivalent isotropic displacement parameters (Ĺ^{2}x 10^3) for **7**. U(eq) is defined as one third of the trace of the orthogonalized U^{ij} tensor.

	x	y	z	U(eq)
O(7)	13047(8)	3746(1)	3345(4)	35(1)
O(1)	4494(7)	6287(1)	7513(4)	37(1)
O(8)	10232(7)	3748(1)	1492(4)	35(1)
O(2)	1797(8)	6285(1)	9390(4)	36(1)
N(1)	6158(9)	6272(2)	9632(5)	31(1)
N(2)	8732(9)	3764(2)	3623(5)	30(1)
O(6)	5453(12)	3922(2)	6724(6)	63(2)
C(5)	3945(11)	6283(2)	8877(6)	29(1)
O(3)	7874(13)	5694(1)	10872(6)	65(2)
O(5)	7240(13)	4318(2)	5272(7)	74(2)
C(25)	10853(11)	3749(2)	2868(6)	29(1)
O(4)	8949(14)	5980(2)	12797(7)	80(2)
C(28)	9472(13)	3042(2)	4997(7)	36(2)
C(1)	2458(12)	6296(2)	6426(6)	35(2)
C(14)	7836(14)	5974(2)	11712(8)	39(2)
C(6)	6250(12)	6279(2)	11147(6)	30(1)
C(22)	12224(12)	3721(2)	393(6)	34(2)
C(8)	5589(12)	6953(2)	11290(7)	34(2)
C(7)	7290(14)	6636(2)	11682(8)	38(2)
C(9)	6025(15)	7138(2)	10050(8)	45(2)
C(34)	6974(14)	3990(2)	5825(7)	38(2)
C(26)	8700(12)	3715(2)	5120(6)	32(1)
C(27)	7783(13)	3344(2)	5553(8)	39(2)
C(29)	11556(13)	2919(2)	5791(8)	46(2)
C(4)	947(15)	6640(2)	6555(9)	46(2)
C(2)	791(14)	5963(2)	6532(8)	45(2)
C(23)	13962(13)	4044(2)	442(8)	41(2)
C(12)	2057(16)	7345(2)	11753(10)	57(2)
C(30)	13085(15)	2640(2)	5314(12)	64(3)
C(33)	9020(15)	2887(2)	3715(8)	45(2)
C(13)	3599(13)	7055(2)	12127(8)	45(2)
C(21)	13660(16)	3370(2)	551(9)	51(2)

C(31)	12583(17)	2485(2)	4053(12)	62(2)
C(32)	10584(16)	2608(2)	3226(10)	54(2)
C(11)	2517(18)	7524(2)	10528(11)	64(3)
C(3)	3983(14)	6293(3)	5082(7)	57(2)
C(10)	4498(18)	7425(2)	9684(11)	64(2)
C(24)	10600(14)	3720(3)	-941(7)	59(2)
C(17)	10670(30)	4963(3)	9627(13)	92(4)
C(15)	9610(20)	5397(2)	11264(12)	83(4)
C(18)	8730(30)	4806(3)	10529(19)	106(5)
C(16)	11380(30)	5286(4)	10127(18)	118(5)
C(19)	8120(30)	5076(3)	11501(19)	134(6)
C(20)	9580(40)	4733(4)	11910(20)	153(7)
C(3AA)	6260(20)	5211(2)	5328(10)	67(2)
C(0AA)	5810(30)	4612(4)	6130(20)	167(8)
C(4AA)	7190(40)	4913(4)	6335(17)	142(6)
C(5AA)	6130(30)	5208(5)	6864(14)	120(4)
C(2AA)	4330(40)	5031(6)	4651(15)	200(11)
C(1AA)	4020(40)	4678(5)	5236(18)	153(7)

Table S10: Bond lengths [Ĺ] and angles [°] for **7**.

O(7)-C(25)	1.224(7)
O(1)-C(5)	1.329(7)
O(1)-C(1)	1.476(7)
O(8)-C(25)	1.347(7)
O(8)-C(22)	1.478(7)
O(2)-C(5)	1.219(7)
N(1)-H(1)	0.8800
N(1)-C(5)	1.353(8)
N(1)-C(6)	1.442(8)
N(2)-H(2)	0.8800
N(2)-C(25)	1.319(8)
N(2)-C(26)	1.435(8)
O(6)-C(34)	1.194(8)
O(3)-C(14)	1.312(9)
O(3)-C(15)	1.474(10)
O(5)-C(34)	1.336(9)
O(5)-C(0AA)	1.559(16)
O(4)-C(14)	1.181(8)
C(28)-C(27)	1.521(10)
C(28)-C(29)	1.395(10)
C(28)-C(33)	1.369(10)
C(1)-C(4)	1.506(10)
C(1)-C(2)	1.517(10)
C(1)-C(3)	1.507(10)
C(14)-C(6)	1.504(9)
C(6)-H(6)	1.0000
C(6)-C(7)	1.520(9)
C(22)-C(23)	1.503(10)
C(22)-C(21)	1.514(10)
C(22)-C(24)	1.520(9)
C(8)-C(7)	1.520(10)
C(8)-C(9)	1.385(10)
C(8)-C(13)	1.361(10)
C(7)-H(7A)	0.9900
C(7)-H(7B)	0.9900
C(9)-H(9)	0.9500

C(9)-C(10)	1.377(11)
C(34)-C(26)	1.520(10)
C(26)-H(26)	1.0000
C(26)-C(27)	1.519(9)
C(27)-H(27A)	0.9900
C(27)-H(27B)	0.9900
C(29)-H(29)	0.9500
C(29)-C(30)	1.384(13)
C(4)-H(4A)	0.9800
C(4)-H(4B)	0.9800
C(4)-H(4C)	0.9800
C(2)-H(2A)	0.9800
C(2)-H(2B)	0.9800
C(2)-H(2C)	0.9800
C(23)-H(23A)	0.9800
C(23)-H(23B)	0.9800
C(23)-H(23C)	0.9800
C(12)-H(12)	0.9500
C(12)-C(13)	1.390(12)
C(12)-C(11)	1.363(13)
C(30)-H(30)	0.9500
C(30)-C(31)	1.357(14)
C(33)-H(33)	0.9500
C(33)-C(32)	1.401(10)
C(13)-H(13)	0.9500
C(21)-H(21A)	0.9800
C(21)-H(21B)	0.9800
C(21)-H(21C)	0.9800
C(31)-H(31)	0.9500
C(31)-C(32)	1.378(12)
C(32)-H(32)	0.9500
C(11)-H(11)	0.9500
C(11)-C(10)	1.358(14)
C(3)-H(3A)	0.9800
C(3)-H(3B)	0.9800
C(3)-H(3C)	0.9800
C(10)-H(10)	0.9500

C(24)-H(24A)	0.9800
C(24)-H(24B)	0.9800
C(24)-H(24C)	0.9800
C(17)-H(17)	0.9500
C(17)-C(18)	1.449(19)
C(17)-C(16)	1.346(19)
C(15)-H(15)	1.0000
C(15)-C(16)	1.482(19)
C(15)-C(19)	1.439(17)
C(18)-H(18)	1.0000
C(18)-C(19)	1.40(2)
C(18)-C(20)	1.41(2)
C(16)-H(16)	0.9500
C(19)-H(19)	1.0000
C(19)-C(20)	1.534(17)
C(20)-H(20A)	0.9900
C(20)-H(20B)	0.9900
C(3AA)-H(3AA)	1.0000
C(3AA)-C(4AA)	1.540(18)
C(3AA)-C(5AA)	1.463(15)
C(3AA)-C(2AA)	1.361(16)
C(0AA)-H(0AA)	1.0000
C(0AA)-C(4AA)	1.344(18)
C(0AA)-C(1AA)	1.280(19)
C(4AA)-H(4AA)	1.0000
C(4AA)-C(5AA)	1.328(19)
C(5AA)-H(5AA)	0.9900
C(5AA)-H(5AB)	0.9900
C(2AA)-H(2AA)	0.9500
C(2AA)-C(1AA)	1.437(19)
C(1AA)-H(1AA)	0.9500
C(5)-O(1)-C(1)	121.9(5)
C(25)-O(8)-C(22)	121.5(4)
C(5)-N(1)-H(1)	118.2
C(5)-N(1)-C(6)	123.7(5)
C(6)-N(1)-H(1)	118.2
C(25)-N(2)-H(2)	118.4

C(25)-N(2)-C(26)	123.2(5)
C(26)-N(2)-H(2)	118.4
O(1)-C(5)-N(1)	109.5(5)
O(2)-C(5)-O(1)	126.2(5)
O(2)-C(5)-N(1)	124.3(6)
C(14)-O(3)-C(15)	117.0(6)
C(34)-O(5)-C(0AA)	112.7(7)
O(7)-C(25)-O(8)	125.4(5)
O(7)-C(25)-N(2)	125.2(5)
N(2)-C(25)-O(8)	109.4(5)
C(29)-C(28)-C(27)	120.1(7)
C(33)-C(28)-C(27)	121.7(6)
C(33)-C(28)-C(29)	118.2(7)
O(1)-C(1)-C(4)	109.6(5)
O(1)-C(1)-C(2)	109.9(5)
O(1)-C(1)-C(3)	102.6(5)
C(4)-C(1)-C(2)	113.1(6)
C(4)-C(1)-C(3)	110.5(6)
C(3)-C(1)-C(2)	110.6(6)
O(3)-C(14)-C(6)	113.1(6)
O(4)-C(14)-O(3)	122.6(7)
O(4)-C(14)-C(6)	124.2(7)
N(1)-C(6)-C(14)	111.0(5)
N(1)-C(6)-H(6)	108.0
N(1)-C(6)-C(7)	111.2(5)
C(14)-C(6)-H(6)	108.0
C(14)-C(6)-C(7)	110.4(5)
C(7)-C(6)-H(6)	108.0
O(8)-C(22)-C(23)	110.2(5)
O(8)-C(22)-C(21)	109.6(5)
O(8)-C(22)-C(24)	101.8(5)
C(23)-C(22)-C(21)	113.2(5)
C(23)-C(22)-C(24)	111.0(6)
C(21)-C(22)-C(24)	110.5(6)
C(9)-C(8)-C(7)	119.9(6)
C(13)-C(8)-C(7)	121.0(6)
C(13)-C(8)-C(9)	119.2(7)

C(6)-C(7)-H(7A)	109.0
C(6)-C(7)-H(7B)	109.0
C(8)-C(7)-C(6)	113.1(5)
C(8)-C(7)-H(7A)	109.0
C(8)-C(7)-H(7B)	109.0
H(7A)-C(7)-H(7B)	107.8
C(8)-C(9)-H(9)	119.8
C(10)-C(9)-C(8)	120.4(8)
C(10)-C(9)-H(9)	119.8
O(6)-C(34)-O(5)	123.1(7)
O(6)-C(34)-C(26)	124.5(7)
O(5)-C(34)-C(26)	112.4(6)
N(2)-C(26)-C(34)	111.2(5)
N(2)-C(26)-H(26)	108.2
N(2)-C(26)-C(27)	112.9(5)
C(34)-C(26)-H(26)	108.2
C(27)-C(26)-C(34)	108.0(6)
C(27)-C(26)-H(26)	108.2
C(28)-C(27)-H(27A)	108.9
C(28)-C(27)-H(27B)	108.9
C(26)-C(27)-C(28)	113.3(6)
C(26)-C(27)-H(27A)	108.9
C(26)-C(27)-H(27B)	108.9
H(27A)-C(27)-H(27B)	107.7
C(28)-C(29)-H(29)	119.5
C(30)-C(29)-C(28)	120.9(8)
C(30)-C(29)-H(29)	119.5
C(1)-C(4)-H(4A)	109.5
C(1)-C(4)-H(4B)	109.5
C(1)-C(4)-H(4C)	109.5
H(4A)-C(4)-H(4B)	109.5
H(4A)-C(4)-H(4C)	109.5
H(4B)-C(4)-H(4C)	109.5
C(1)-C(2)-H(2A)	109.5
C(1)-C(2)-H(2B)	109.5
C(1)-C(2)-H(2C)	109.5
H(2A)-C(2)-H(2B)	109.5

H(2A)-C(2)-H(2C)	109.5
H(2B)-C(2)-H(2C)	109.5
C(22)-C(23)-H(23A)	109.5
C(22)-C(23)-H(23B)	109.5
C(22)-C(23)-H(23C)	109.5
H(23A)-C(23)-H(23B)	109.5
H(23A)-C(23)-H(23C)	109.5
H(23B)-C(23)-H(23C)	109.5
C(13)-C(12)-H(12)	120.1
C(11)-C(12)-H(12)	120.1
C(11)-C(12)-C(13)	119.7(8)
C(29)-C(30)-H(30)	119.9
C(31)-C(30)-C(29)	120.1(8)
C(31)-C(30)-H(30)	119.9
C(28)-C(33)-H(33)	119.6
C(28)-C(33)-C(32)	120.8(7)
C(32)-C(33)-H(33)	119.6
C(8)-C(13)-C(12)	120.3(8)
C(8)-C(13)-H(13)	119.9
C(12)-C(13)-H(13)	119.9
C(22)-C(21)-H(21A)	109.5
C(22)-C(21)-H(21B)	109.5
C(22)-C(21)-H(21C)	109.5
H(21A)-C(21)-H(21B)	109.5
H(21A)-C(21)-H(21C)	109.5
H(21B)-C(21)-H(21C)	109.5
C(30)-C(31)-H(31)	119.9
C(30)-C(31)-C(32)	120.3(8)
C(32)-C(31)-H(31)	119.9
C(33)-C(32)-H(32)	120.2
C(31)-C(32)-C(33)	119.6(8)
C(31)-C(32)-H(32)	120.2
C(12)-C(11)-H(11)	119.7
C(10)-C(11)-C(12)	120.6(8)
C(10)-C(11)-H(11)	119.7
C(1)-C(3)-H(3A)	109.5
C(1)-C(3)-H(3B)	109.5

C(1)-C(3)-H(3C)	109.5
H(3A)-C(3)-H(3B)	109.5
H(3A)-C(3)-H(3C)	109.5
H(3B)-C(3)-H(3C)	109.5
C(9)-C(10)-H(10)	120.1
C(11)-C(10)-C(9)	119.8(9)
C(11)-C(10)-H(10)	120.1
C(22)-C(24)-H(24A)	109.5
C(22)-C(24)-H(24B)	109.5
C(22)-C(24)-H(24C)	109.5
H(24A)-C(24)-H(24B)	109.5
H(24A)-C(24)-H(24C)	109.5
H(24B)-C(24)-H(24C)	109.5
C(18)-C(17)-H(17)	125.0
C(16)-C(17)-H(17)	125.0
C(16)-C(17)-C(18)	110.0(12)
O(3)-C(15)-H(15)	110.1
O(3)-C(15)-C(16)	113.9(10)
C(16)-C(15)-H(15)	110.1
C(19)-C(15)-O(3)	109.8(10)
C(19)-C(15)-H(15)	110.1
C(19)-C(15)-C(16)	102.6(10)
C(17)-C(18)-H(18)	119.7
C(19)-C(18)-C(17)	105.1(10)
C(19)-C(18)-H(18)	119.7
C(19)-C(18)-C(20)	66.1(11)
C(20)-C(18)-C(17)	114.3(13)
C(20)-C(18)-H(18)	119.7
C(17)-C(16)-C(15)	109.6(11)
C(17)-C(16)-H(16)	125.2
C(15)-C(16)-H(16)	125.2
C(15)-C(19)-H(19)	118.4
C(15)-C(19)-C(20)	117.9(14)
C(18)-C(19)-C(15)	111.7(13)
C(18)-C(19)-H(19)	118.4
C(18)-C(19)-C(20)	57.2(9)
C(20)-C(19)-H(19)	118.4

C(18)-C(20)-C(19)	56.7(10)
C(18)-C(20)-H(20A)	118.1
C(18)-C(20)-H(20B)	118.1
C(19)-C(20)-H(20A)	118.1
C(19)-C(20)-H(20B)	118.1
H(20A)-C(20)-H(20B)	115.3
C(4AA)-C(3AA)-H(3AA)	121.8
C(5AA)-C(3AA)-H(3AA)	121.8
C(5AA)-C(3AA)-C(4AA)	52.4(8)
C(2AA)-C(3AA)-H(3AA)	121.8
C(2AA)-C(3AA)-C(4AA)	99.6(12)
C(2AA)-C(3AA)-C(5AA)	115.7(12)
O(5)-C(0AA)-H(0AA)	111.9
C(4AA)-C(0AA)-O(5)	114.1(12)
C(4AA)-C(0AA)-H(0AA)	111.9
C(1AA)-C(0AA)-O(5)	97.6(17)
C(1AA)-C(0AA)-H(0AA)	111.9
C(1AA)-C(0AA)-C(4AA)	108.5(14)
C(3AA)-C(4AA)-H(4AA)	117.0
C(0AA)-C(4AA)-C(3AA)	110.3(13)
C(0AA)-C(4AA)-H(4AA)	117.0
C(5AA)-C(4AA)-C(3AA)	60.8(8)
C(5AA)-C(4AA)-C(0AA)	122(2)
C(5AA)-C(4AA)-H(4AA)	117.0
C(3AA)-C(5AA)-H(5AA)	117.0
C(3AA)-C(5AA)-H(5AB)	117.0
C(4AA)-C(5AA)-C(3AA)	66.8(11)
C(4AA)-C(5AA)-H(5AA)	117.0
C(4AA)-C(5AA)-H(5AB)	117.0
H(5AA)-C(5AA)-H(5AB)	114.1
C(3AA)-C(2AA)-H(2AA)	124.8
C(3AA)-C(2AA)-C(1AA)	110.5(14)
C(1AA)-C(2AA)-H(2AA)	124.8
C(0AA)-C(1AA)-C(2AA)	110.6(15)
C(0AA)-C(1AA)-H(1AA)	124.7
C(2AA)-C(1AA)-H(1AA)	124.7

Symmetry transformations used to generate equivalent atoms:

Table S11: Anisotropic displacement parameters (Ĺ^{2}x 10^3) for **7**. The anisotropic displacement factor exponent takes the form: $-2\pi^2[h^2 a^{*2}U^{11} + ... + 2 h k a^* b^* U^{12}]$

	U^{11}	U^{22}	U^{33}	U^{23}	U^{13}	U^{12}
O(7)	21(2)	51(3)	33(2)	7(2)	-3(2)	-5(2)
O(1)	22(2)	60(3)	28(2)	2(2)	-5(2)	6(2)
O(8)	21(2)	59(3)	27(2)	-1(2)	4(2)	1(2)
O(2)	19(2)	46(3)	44(3)	-2(2)	2(2)	0(2)
N(1)	21(2)	42(3)	29(3)	0(2)	3(2)	2(3)
N(2)	21(2)	44(3)	24(3)	3(2)	-2(2)	2(3)
O(6)	68(4)	67(4)	53(3)	1(3)	35(3)	5(3)
C(5)	27(3)	26(3)	34(4)	4(3)	-4(3)	-1(3)
O(3)	99(5)	29(3)	68(4)	-4(2)	-41(3)	15(3)
O(5)	82(4)	39(3)	102(5)	2(3)	61(4)	6(3)
C(25)	20(3)	35(3)	32(3)	4(3)	0(3)	-2(3)
O(4)	106(5)	75(4)	57(4)	-15(3)	-44(4)	35(4)
C(28)	32(4)	35(4)	42(4)	8(3)	0(3)	-11(3)
C(1)	25(3)	50(4)	31(3)	2(3)	-11(3)	2(3)
C(14)	38(4)	39(4)	40(4)	6(3)	-6(3)	-3(3)
C(6)	29(3)	34(3)	27(3)	-4(3)	1(2)	-1(3)
C(22)	26(3)	51(4)	24(3)	-3(3)	10(2)	-5(3)
C(8)	28(3)	39(4)	36(4)	-8(3)	-1(3)	-6(3)
C(7)	35(4)	44(4)	36(4)	-4(3)	-5(3)	-7(3)
C(9)	42(4)	40(4)	53(5)	5(3)	-4(4)	-1(3)
C(34)	35(4)	44(4)	35(4)	-3(3)	6(3)	-6(3)
C(26)	26(3)	42(4)	27(3)	4(3)	-5(2)	1(3)
C(27)	30(4)	45(4)	41(4)	-4(3)	4(3)	-12(3)
C(29)	32(4)	49(4)	57(5)	22(4)	-11(3)	-10(4)
C(4)	42(4)	43(4)	54(5)	2(4)	-13(4)	5(4)
C(2)	36(4)	42(4)	56(5)	-10(4)	-9(3)	-2(3)
C(23)	31(4)	44(4)	48(5)	6(3)	9(3)	2(3)
C(12)	39(4)	48(5)	85(7)	-32(5)	1(4)	1(4)
C(30)	32(4)	56(5)	105(8)	46(5)	-4(4)	-3(4)
C(33)	45(4)	38(4)	51(5)	1(3)	-2(4)	0(3)
C(13)	34(4)	45(4)	55(5)	-14(3)	-2(3)	-2(3)
C(21)	52(5)	41(4)	59(5)	-13(4)	17(4)	-6(4)

C(31)	45(5)	39(4)	102(8)	5(5)	1(5)	5(4)
C(32)	55(5)	34(4)	72(6)	-6(4)	7(4)	0(4)
C(11)	52(6)	38(5)	101(8)	0(5)	-19(5)	2(4)
C(3)	36(4)	106(7)	28(4)	8(5)	-5(3)	6(5)
C(10)	57(6)	45(5)	91(7)	16(4)	-7(5)	1(4)
C(24)	40(4)	111(7)	27(4)	-9(4)	6(3)	-7(5)
C(17)	119(10)	77(8)	81(8)	-1(6)	-24(7)	35(8)
C(15)	120(9)	30(4)	98(8)	0(4)	-66(7)	22(5)
C(18)	76(8)	57(7)	186(15)	-10(9)	-4(9)	-23(6)
C(16)	84(9)	103(11)	167(14)	50(10)	21(9)	-6(8)
C(19)	141(13)	47(7)	213(16)	47(8)	71(12)	48(8)
C(20)	191(18)	60(8)	208(19)	48(10)	23(15)	49(10)
C(3AA)	76(6)	46(5)	80(6)	-5(4)	12(5)	4(4)
C(0AA)	83(9)	90(9)	330(20)	103(12)	94(11)	3(7)
C(4AA)	192(17)	121(11)	113(11)	-12(8)	-55(11)	22(9)
C(5AA)	118(11)	146(12)	95(8)	14(8)	2(8)	-24(10)
C(2AA)	260(20)	268(19)	72(9)	58(11)	-77(12)	-177(17)
C(1AA)	176(15)	136(12)	146(13)	-92(10)	64(11)	-66(11)

Table S12: Hydrogen coordinates (x 10^4) and isotropic displacement parameters (Ĺ^{2}x 10 ^{3}) for **7**.

	x	y	z	U(eq)
H(1)	7623	6259	9173	37
H(2)	7263	3806	3189	36
H(6)	4451	6251	11503	36
H(7A)	7455	6625	12718	46
H(7B)	9032	6675	11291	46
H(9)	7386	7065	9448	54
H(26)	10495	3748	5483	38
H(27A)	6001	3309	5205	46
H(27B)	7745	3331	6592	46
H(29)	11932	3028	6672	55
H(4A)	-32	6637	7433	70
H(4B)	-244	6661	5757	70
H(4C)	2135	6844	6557	70
H(2A)	1893	5749	6558	67
H(2B)	-359	5950	5713	67
H(2C)	-238	5974	7392	67
H(23A)	12920	4263	393	61
H(23B)	15147	4037	-357	61
H(23C)	14951	4042	1321	61
H(12)	690	7418	12347	69
H(30)	14488	2558	5871	77
H(33)	7628	2970	3150	54
H(13)	3262	6927	12971	54
H(21A)	14848	3385	1351	76
H(21B)	14636	3321	-308	76
H(21C)	12425	3175	710	76
H(31)	13614	2290	3739	75
H(32)	10269	2504	2329	64
H(11)	1441	7719	10263	77
H(3A)	5010	6514	5019	85
H(3B)	2801	6280	4277	85

H(3C)	5131	6085	5074	85
H(10)	4830	7555	8844	77
H(24A)	9336	3525	-894	89
H(24B)	11717	3684	-1757	89
H(24C)	9699	3950	-1032	89
H(17)	11343	4853	8805	111
H(15)	10607	5460	12129	99
H(18)	7314	4658	10106	127
H(16)	12804	5423	9802	141
H(19)	6292	5102	11807	161
H(20A)	11451	4752	12110	184
H(20B)	8654	4548	12454	184
H(3AA)	7494	5368	4812	81
H(0AA)	5105	4516	7032	200
H(4AA)	9089	4885	6455	171
H(5AA)	7285	5375	7373	144
H(5AB)	4399	5183	7289	144
H(2AA)	3339	5126	3897	240
H(1AA)	2679	4517	4992	183

checkCIF/PLATON report

Structure factors have been supplied for datablock(s) ag_ag_515_0m_a

THIS REPORT IS FOR GUIDANCE ONLY. IF USED AS PART OF A REVIEW PROCEDURE FOR PUBLICATION, IT SHOULD NOT REPLACE THE EXPERTISE OF AN EXPERIENCED CRYSTALLOGRAPHIC REFEREE.

No syntax errors found. CIF dictionary Interpreting this report

Datablock: ag_ag_515_0m_a

```
Bond precision:  C-C = 0.0146 A          Wavelength=0.71073

Cell:           a=5.1902(10)     b=37.256(7)        c=9.5140(18)
                alpha=90         beta=90.248(4)     gamma=90
Temperature:    150 K

               Calculated                  Reported
Volume         1839.7(6)                   1839.7(6)
Space group    P 21                        P 1 21 1
Hall group     P 2yb                       P 2yb
Moiety formula C20 H25 N O4                C20 H25 N O4
Sum formula    C20 H25 N O4                C20 H25 N O4
Mr             343.41                      343.41
Dx,g cm-3      1.240                       1.240
Z              4                           4
Mu (mm-1)      0.086                       0.086
F000           736.0                       736.0
F000'          736.36
h,k,lmax       6,44,11                     6,44,11
Nref           6459[ 3284]                 6452
Tmin,Tmax      0.990,0.994                 0.672,0.746
Tmin'          0.983

Correction method= # Reported T Limits: Tmin=0.672 Tmax=0.746
AbsCorr = MULTI-SCAN

Data completeness= 1.96/1.00      Theta(max)= 24.995

R(reflections)= 0.0673( 4622)     wR2(reflections)= 0.1846( 6452)

S = 1.045                 Npar= 459
```

The following ALERTS were generated. Each ALERT has the format
test-name_ALERT_alert-type_alert-level.
Click on the hyperlinks for more details of the test.

Alert level B

```
PLAT035_ALERT_1_B _chemical_absolute_configuration Info  Not Given      Please Do !
PLAT220_ALERT_2_B Non-Solvent  Resd 2  C   Ueq(max)/Ueq(min) Range        6.9 Ratio
PLAT230_ALERT_2_B Hirshfeld Test Diff for    O5        --C0AA     .      11.5 s.u.
PLAT241_ALERT_2_B High   'MainMol' Ueq as Compared to Neighbors of       C2AA Check
PLAT242_ALERT_2_B Low    'MainMol' Ueq as Compared to Neighbors of       C3AA Check
PLAT340_ALERT_3_B Low Bond Precision on  C-C Bonds ...............    0.01461 Ang.
PLAT360_ALERT_2_B Short  C(sp3)-C(sp3) Bond  C4AA      - C5AA     .      1.33 Ang.
PLAT362_ALERT_2_B Short  C(sp3)-C(sp2) Bond  C0AA      - C1AA     .      1.28 Ang.
```

Alert level C

```
STRVA01_ALERT_4_C          Flack test results are meaningless.
           From the CIF: _refine_ls_abs_structure_Flack     0.300
           From the CIF: _refine_ls_abs_structure_Flack_su     0.700
PLAT089_ALERT_3_C Poor Data / Parameter Ratio (Zmax < 18) ........       7.15 Note
PLAT213_ALERT_2_C Atom C19              has ADP max/min Ratio .....       3.3 prolat
PLAT213_ALERT_2_C Atom C0AA             has ADP max/min Ratio .....       3.9 prolat
PLAT213_ALERT_2_C Atom C2AA             has ADP max/min Ratio .....       3.2 prolat
PLAT220_ALERT_2_C Non-Solvent  Resd 1  C   Ueq(max)/Ueq(min) Range        5.3 Ratio
PLAT222_ALERT_3_C Non-Solv.  Resd 1  H   Uiso(max)/Uiso(min) Range        5.1 Ratio
PLAT222_ALERT_3_C Non-Solv.  Resd 2  H   Uiso(max)/Uiso(min) Range        6.7 Ratio
PLAT234_ALERT_4_C Large Hirshfeld Difference C16       --C17      .      0.22 Ang.
PLAT234_ALERT_4_C Large Hirshfeld Difference C17       --C18      .      0.18 Ang.
PLAT234_ALERT_4_C Large Hirshfeld Difference C3AA      --C4AA     .      0.19 Ang.
PLAT234_ALERT_4_C Large Hirshfeld Difference C30       --C31      .      0.18 Ang.
PLAT241_ALERT_2_C High   'MainMol' Ueq as Compared to Neighbors of        C16 Check
PLAT241_ALERT_2_C High   'MainMol' Ueq as Compared to Neighbors of        C19 Check
PLAT241_ALERT_2_C High   'MainMol' Ueq as Compared to Neighbors of        C20 Check
PLAT241_ALERT_2_C High   'MainMol' Ueq as Compared to Neighbors of       C0AA Check
PLAT241_ALERT_2_C High   'MainMol' Ueq as Compared to Neighbors of       C4AA Check
PLAT242_ALERT_2_C Low    'MainMol' Ueq as Compared to Neighbors of        C14 Check
PLAT242_ALERT_2_C Low    'MainMol' Ueq as Compared to Neighbors of        C15 Check
PLAT242_ALERT_2_C Low    'MainMol' Ueq as Compared to Neighbors of        C17 Check
PLAT242_ALERT_2_C Low    'MainMol' Ueq as Compared to Neighbors of        C18 Check
PLAT242_ALERT_2_C Low    'MainMol' Ueq as Compared to Neighbors of         O5 Check
PLAT242_ALERT_2_C Low    'MainMol' Ueq as Compared to Neighbors of       C1AA Check
PLAT242_ALERT_2_C Low    'MainMol' Ueq as Compared to Neighbors of        C34 Check
PLAT360_ALERT_2_C Short  C(sp3)-C(sp3) Bond  C18       - C19      .      1.40 Ang.
PLAT360_ALERT_2_C Short  C(sp3)-C(sp3) Bond  C18       - C20      .      1.41 Ang.
PLAT360_ALERT_2_C Short  C(sp3)-C(sp3) Bond  C0AA      - C4AA     .      1.34 Ang.
PLAT362_ALERT_2_C Short  C(sp3)-C(sp2) Bond  C3AA      - C2AA     .      1.37 Ang.
PLAT911_ALERT_3_C Missing FCF Refl Between Thmin & STh/L=    0.595          3 Report
```

Alert level G

```
PLAT002_ALERT_2_G Number of Distance or Angle Restraints on AtSite          7 Note
PLAT003_ALERT_2_G Number of Uiso or Uij Restrained non-H Atoms ...          6 Report
PLAT007_ALERT_5_G Number of Unrefined Donor-H Atoms ..............          2 Report
PLAT032_ALERT_4_G Std. Uncertainty on Flack Parameter Value High .      0.700 Report
PLAT172_ALERT_4_G The CIF-Embedded .res File Contains DFIX Records          2 Report
PLAT176_ALERT_4_G The CIF-Embedded .res File Contains SADI Records          2 Report
PLAT187_ALERT_4_G The CIF-Embedded .res File Contains RIGU Records          1 Report
PLAT720_ALERT_4_G Number of Unusual/Non-Standard Labels ..........         13 Note
PLAT791_ALERT_4_G Model has Chirality at C3AA         (Chiral SPGR)         R Verify
PLAT791_ALERT_4_G Model has Chirality at C0AA         (Chiral SPGR)         R Verify
PLAT791_ALERT_4_G Model has Chirality at C4AA         (Chiral SPGR)         R Verify
PLAT791_ALERT_4_G Model has Chirality at C6           (Chiral SPGR)         R Verify
PLAT791_ALERT_4_G Model has Chirality at C15          (Chiral SPGR)         R Verify
PLAT791_ALERT_4_G Model has Chirality at C18          (Chiral SPGR)         R Verify
PLAT791_ALERT_4_G Model has Chirality at C19          (Chiral SPGR)         R Verify
```

```
PLAT791_ALERT_4_G Model has Chirality at C26          (Chiral SPGR)          R Verify
PLAT860_ALERT_3_G Number of Least-Squares Restraints ............           47 Note
PLAT870_ALERT_4_G ALERTS Related to Twinning Effects Suppressed ..           ! Info
PLAT910_ALERT_3_G Missing # of FCF Reflection(s) Below Theta(Min).           1 Note
PLAT916_ALERT_2_G Hooft y and Flack x Parameter Values Differ by .        0.15 Check
PLAT992_ALERT_5_G Repd & Actual _reflns_number_gt Values Differ by           1 Check
```

```
 0 ALERT level A = Most likely a serious problem - resolve or explain
 8 ALERT level B = A potentially serious problem, consider carefully
29 ALERT level C = Check. Ensure it is not caused by an omission or oversight
21 ALERT level G = General information/check it is not something unexpected

 1 ALERT type 1 CIF construction/syntax error, inconsistent or missing data
29 ALERT type 2 Indicator that the structure model may be wrong or deficient
 7 ALERT type 3 Indicator that the structure quality may be low
19 ALERT type 4 Improvement, methodology, query or suggestion
 2 ALERT type 5 Informative message, check
```

It is advisable to attempt to resolve as many as possible of the alerts in all categories. Often the minor alerts point to easily fixed oversights, errors and omissions in your CIF or refinement strategy, so attention to these fine details can be worthwhile. In order to resolve some of the more serious problems it may be necessary to carry out additional measurements or structure refinements. However, the purpose of your study may justify the reported deviations and the more serious of these should normally be commented upon in the discussion or experimental section of a paper or in the "special_details" fields of the CIF. checkCIF was carefully designed to identify outliers and unusual parameters, but every test has its limitations and alerts that are not important in a particular case may appear. Conversely, the absence of alerts does not guarantee there are no aspects of the results needing attention. It is up to the individual to critically assess their own results and, if necessary, seek expert advice.

Publication of your CIF in IUCr journals

A basic structural check has been run on your CIF. These basic checks will be run on all CIFs submitted for publication in IUCr journals (*Acta Crystallographica*, *Journal of Applied Crystallography*, *Journal of Synchrotron Radiation*); however, if you intend to submit to *Acta Crystallographica Section C* or *E* or *IUCrData*, you should make sure that full publication checks are run on the final version of your CIF prior to submission.

Publication of your CIF in other journals

Please refer to the *Notes for Authors* of the relevant journal for any special instructions relating to CIF submission.

PLATON version of 07/08/2019; check.def file version of 30/07/2019

Figure S27: Single crystal structure of **7**.

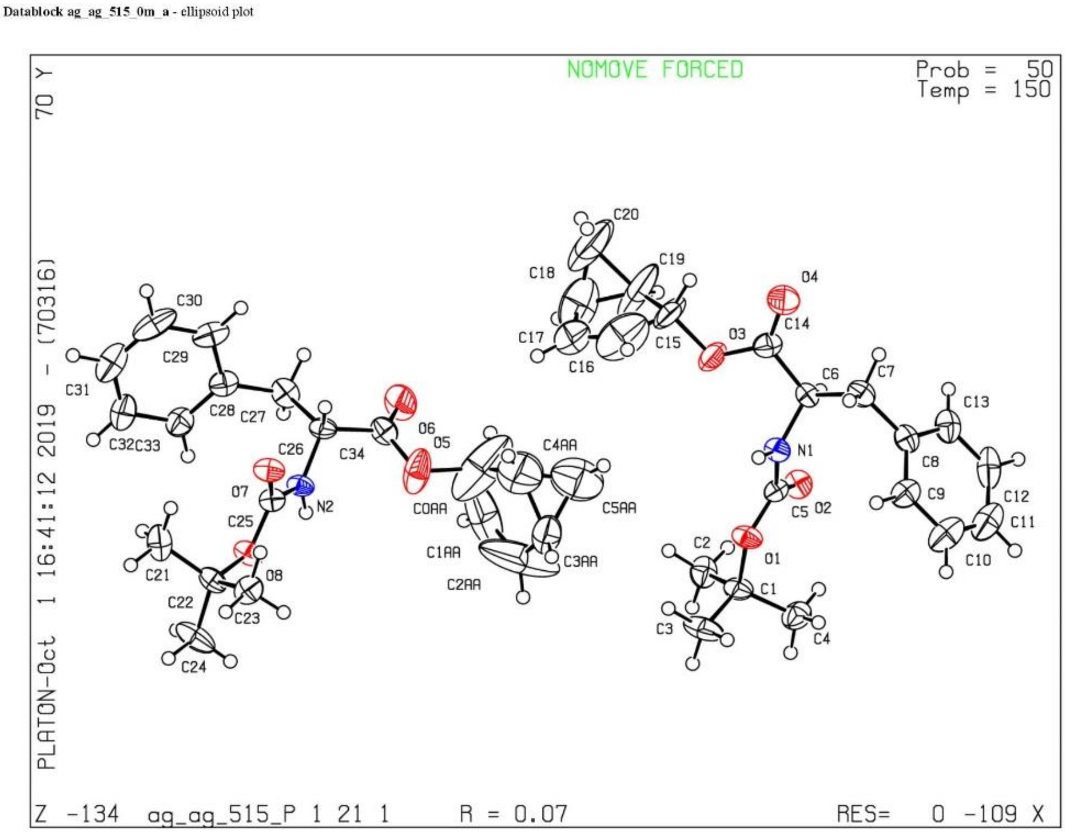

4. Reactivity of prepared bicyclic structures

4.1 Epimerization study (photoequilibration)

It has been found that the bicyclic products photoequilibrate during the irradiation at 254 nm. Despite the fact that they do not absorb the light, the photoequilibration occurs by sensitization by triplet benzene which has been described in the literature.[6] Kinetic experiments sampling the reaction mixture of TMS benzene rearrangement in MeOH catalysed by DCA (standard conditions) have revealed that there are different families of photoproducts (Figure S28). The initial photoproducts (a) rapidly interconvert into secondary photoproducts which either accumulate in the system (b, the most stable products) or are further interconverted into other isomers (c). The change in product distribution has been also observed in the dark where some less-stable products epimerized and/or decomposed thermally. This has been described previously.[4]

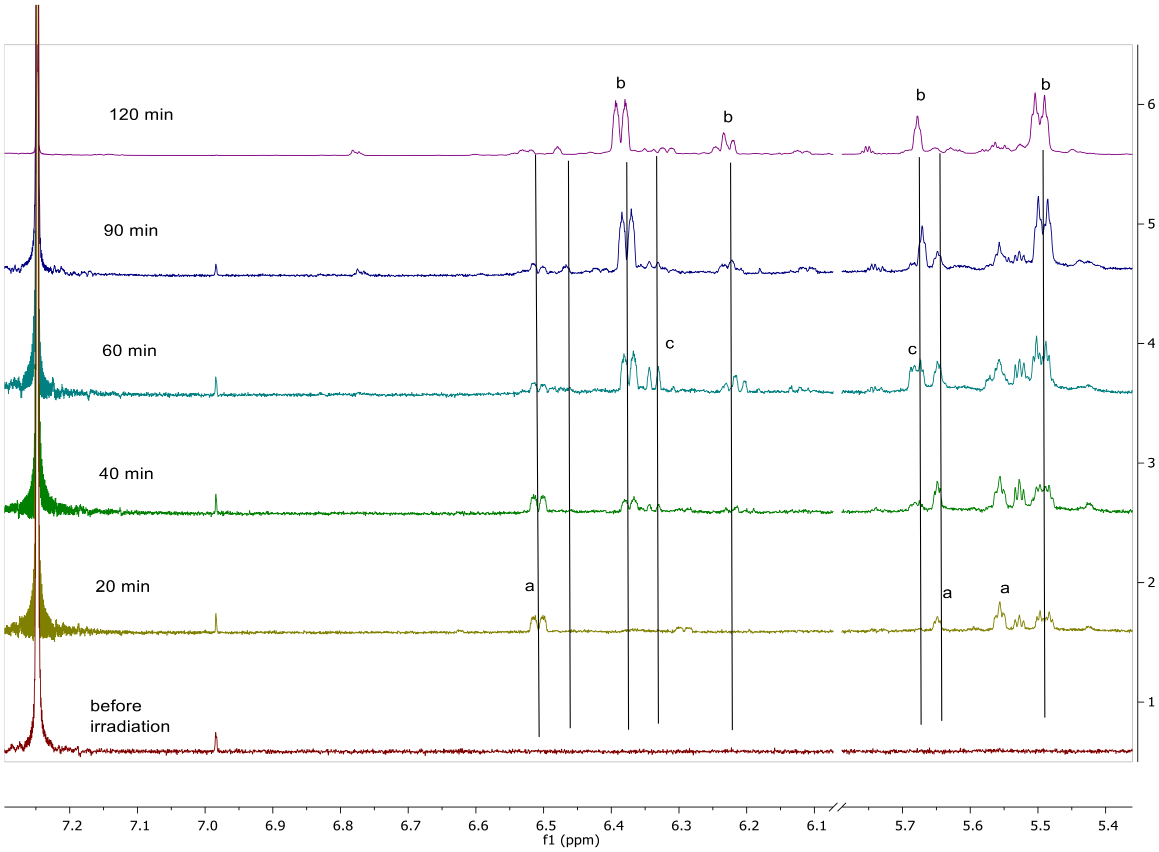

Figure S28: Photorearrangement of TMS-benzene catalysed by DCA monitored at short times (0 – 120 min) by ^{1}H NMR (zoom of the region with double bond protons) measured in $CDCl_3$. The initial photoproducts are described as a, intermediate photoproducts as c and final photoproducts as b.

4.2 Replacement of silyl group by TBAF

The stability of the rearranged adduct **1d** against desilylation has been tested by stirring a solution of **1d** (20 mg, 0.11 mmol, 1 eq.) in $CDCl_3$ (0.6 mL) with TBAF · $3H_2O$ (100 mg, 0.32

mmol, 2.9 eq.). The solution was found completely stable for 3 days (Figure S29) and even after wash with water (1 mL) no changes have been observed.

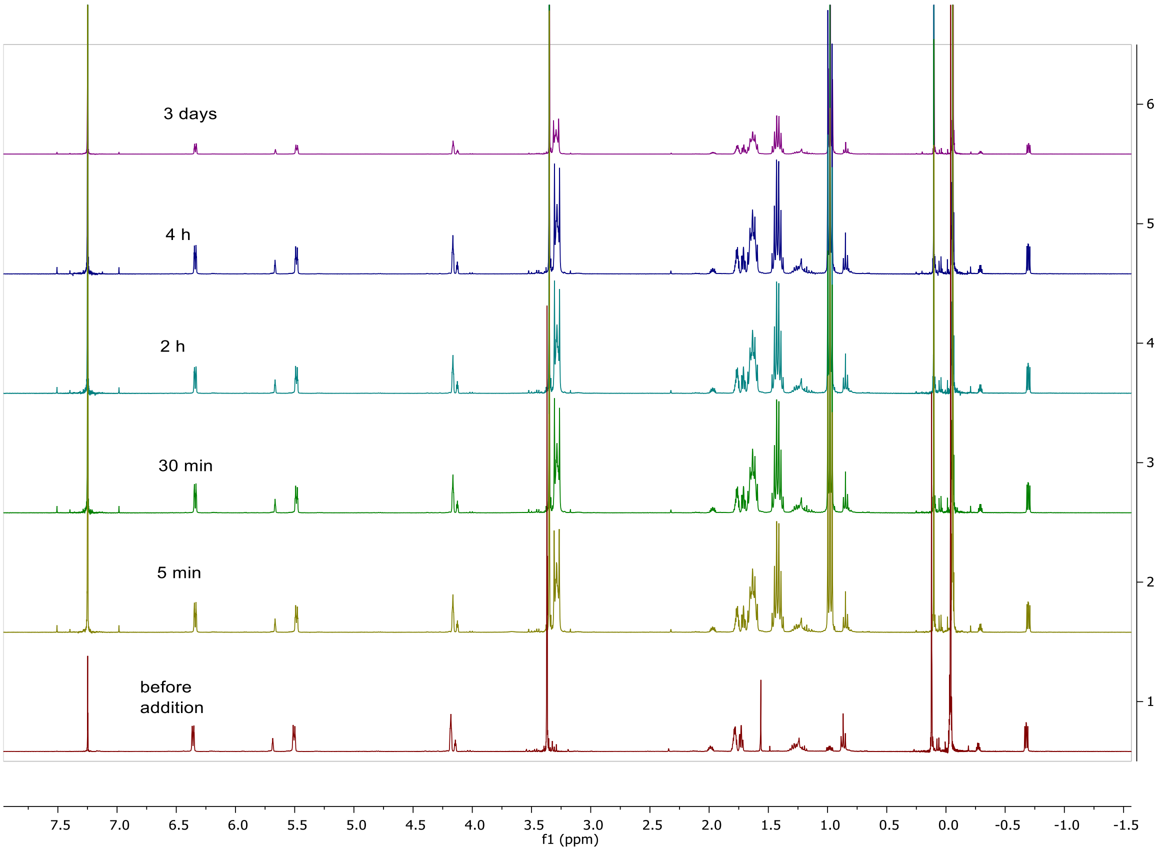

Figure S29: [1]H NMR spectra of **1d** in $CDCl_3$ in presence of TBAF. No changes were observed after 3 days of stirring at room temperature.

4.3 Demethylation

To test the reactivity of the product **1d**, we have demethylated it with BBr_3 (Scheme S3) by a following procedure:

To a solution of **1d** (337 mg. 1.85 mmol, 1.0 eq.) in anhydrous DCM (50 mL) boron tribromide (1 M solution in DCM, 3.69 mL, 3.69 mmol, 2.0 eq.) dropwise over 30 min at -78°C. The reaction was stirred for 15 min, quenched by pouring the reaction mixture on NH_4Cl (sat., aq., 50 mL). The organic phase was washed with water (50 mL) and brine (50 mL) and dried over $MgSO_4$. The solvent was carefully remover under reduced pressure to give crude (±)-(1*S*,2*S*,5*S*,6*R*)-6-(trimethylsilyl)bicyclo[3.1.0]hex-3-en-2-ol **1f**. The crude product was purified by column chromatography (pentane : Et_2O = 2:1, v/v, R_f = 0.4) to give 249 mg (80%) of the final product.

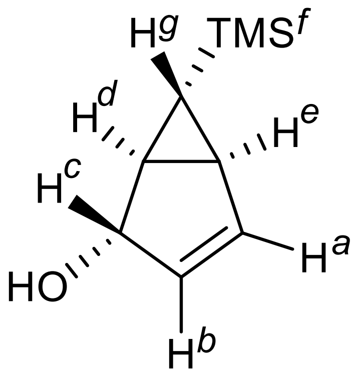

^{1}H NMR (400 MHz, Chloroform-*d*) δ (ppm) 6.38 – 6.27 (m, 1H. *a*), 5.52 (dt, *J* = 5.4, 1.6 Hz, 1H, *b*), 4.46 (s, 1H, *c*), 1.79 (dq, *J* = 6.3, 2.8, 2.4 Hz, 1H, *d*), 1.76 – 1.66 (m, 1H, *e*), -0.03 (s, 4H, *f*), -0.64 (dd, *J* = 5.7, 4.2 Hz, 1H, *g*).

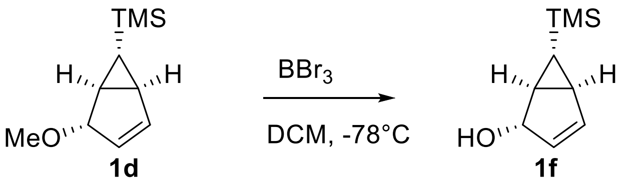

Scheme S3: Demethylation of **1d** by boron tribromide.

The bicyclic TMS-alcohol **1f** was identified by 1H NMR (Figure S30, bottom).

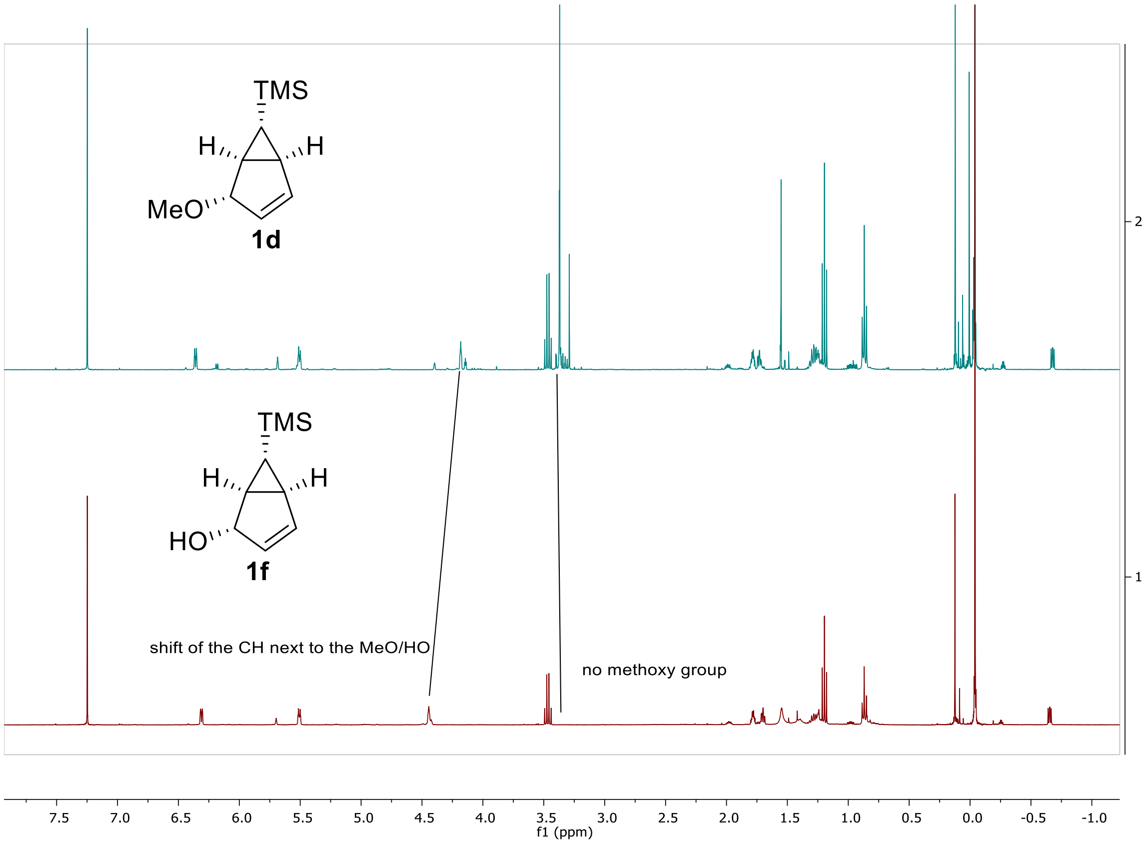

Figure S30: ^{1}H NMR of **1d** in $CDCl_3$ (top) and **1f** (bottom) with highlighted missing signal of the methoxy group and a shift of the adjacent proton.

4.4 Enzymatic esterification

Further derivatization of the rearrangement products has been done by acetylation of the alcohol **1a** (Scheme S4) by the immobilized lipase B from *Candida anctarctica* (Novozym 435). This lipase can efficiently transform alcohols to esters (and vice versa, depending on the conditions). The reaction was performed in isopropenyl acetate (irreversible acylation agent which produces acetone as a by-product). A full conversion of the product was observed after overnight reaction (Figure S31). However, kinetic resolution of enantiomers of **1a** by the enzyme was not successful, as we did not observe a difference in reactivity of different enantiomers.

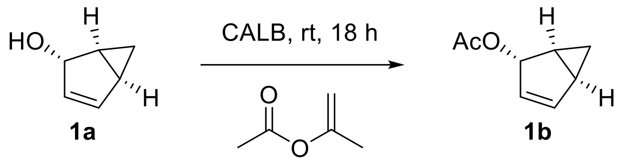

Scheme S4: Bioenzymatic esterification of the bicyclic alcohol **1a**.

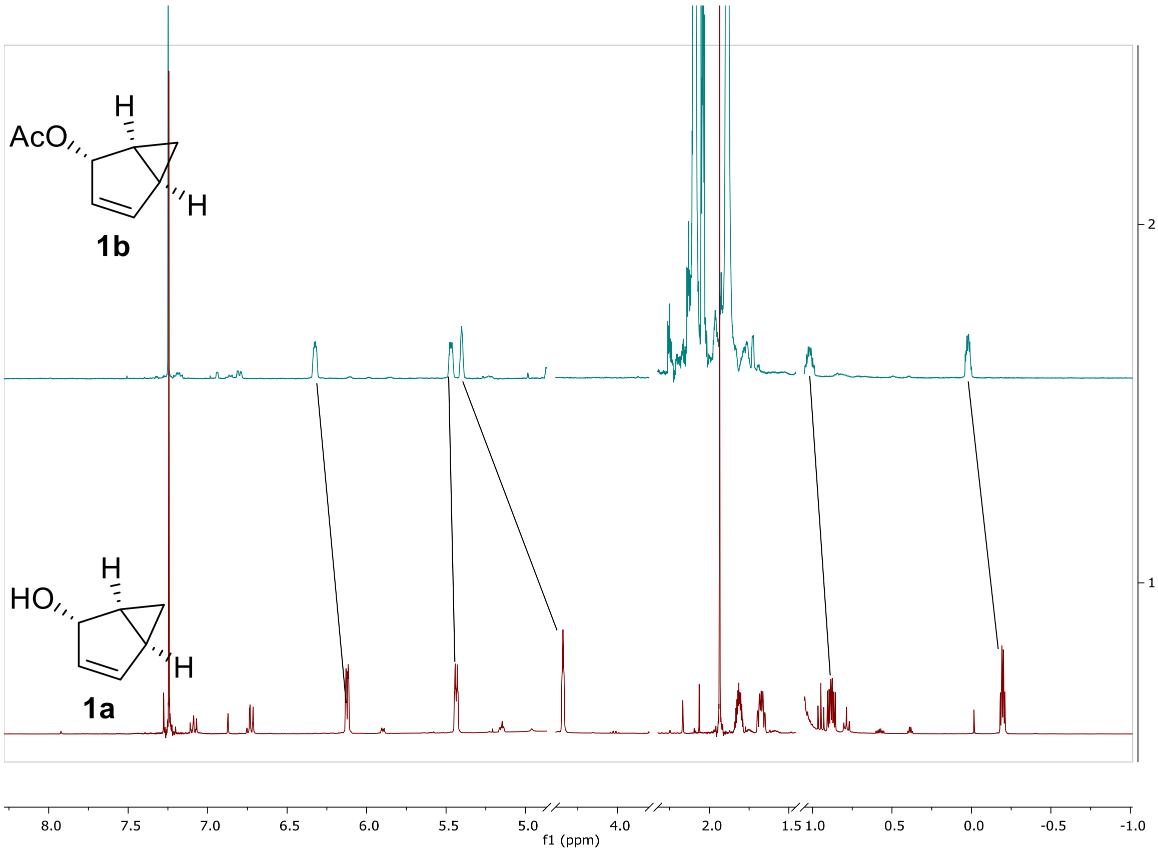

Figure S31: ^{1}H NMR spectrum of **1a** (bottom) and the corresponding acetylated product **1b** (top).

5. Mechanistic experiments

5.1 Fluorescence quenching

Similarly to TMS benzene, no quenching of benzene by HCl was found. The fluorescence and the absorption spectra of benzene in MeOH in absence and presence of different concentrations of anhydrous HCl (in cyclopentyl methyl ether) is shown in Figure S13.

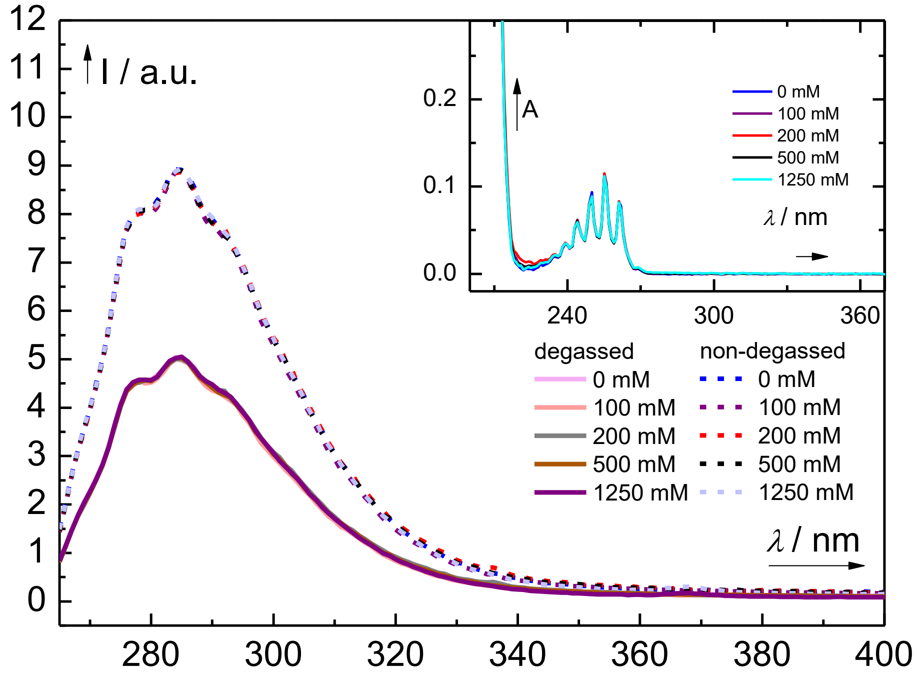

Figure S32: Fluorescence spectra of benzene (c = 1.0 mM, λ_{exc} = 254 nm) in anhydrous MeOH, degassed (solid line, purged with argon) and non-degassed (dashed line) in absence and presence of anhydrous HCl (c = 0 – 1250 mM). The absorption spectra are shown in the inlet.

Benzene fluorescence was further attempted by Lewis acid 9-borabicyclo[3.3.1]nonane (9-BBN). The solution of benzene (c = 1.0 mM) in anhydrous THF was quenched with different concentrations of 9-BBN (Figure S33). The observed decrease in emission was analysed by Stern-Volmer analysis and dynamic quenching was found. In case of non-nucleophilic polar solvent, the benzene fluorescence can be efficiently quenched by this Lewis acids.

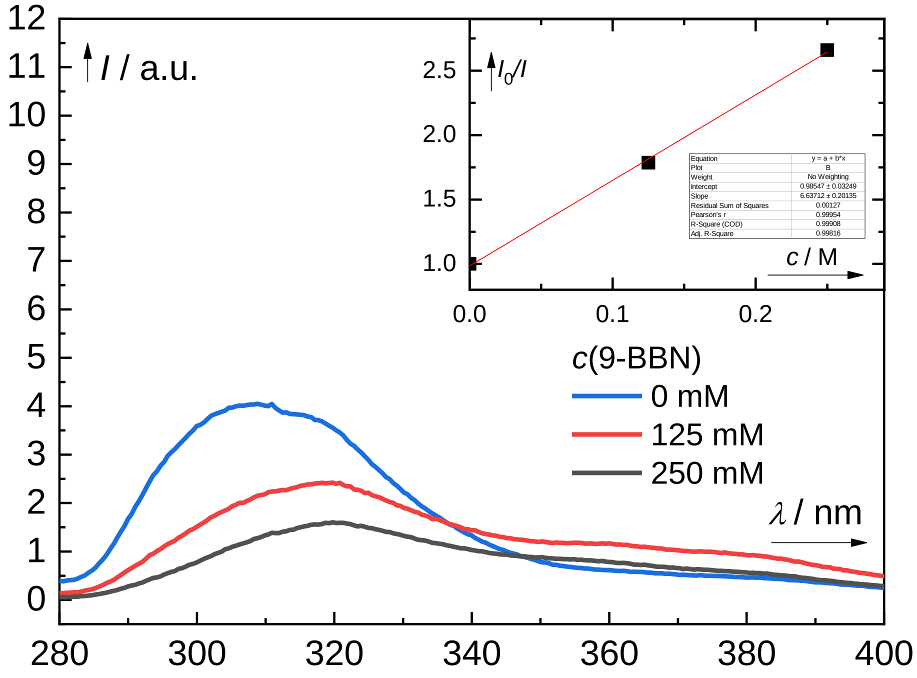

Figure S33: Fluorescence spectra of benzene (c = 1.0 mM, λ_{exc} = 254 nm) in anhydrous THF, in absence and presence of anhydrous 9-BBN (c = 0 –250 mM). The Stern-Volmer plot is shown in the inlet.

5.2 Stern Volmer analysis calculations

To estimate the quenching efficiency of HCl which is not an active quencher of benzene/TMS benzene fluorescence at concentrations up to 1.25 M, we calculated the hypothetical quenching constant if the fluorescence of benzene would by quenched from 20% at these extreme conditions. The quenching constant k_q was calculated from Equations S1 and S2:

$$\frac{I_0}{I_q} = \frac{100}{100-x} = 1 + \tau_s k_q \, [Q] \qquad \text{Eq. S1}$$

$$k_q = \frac{\frac{100}{100-x}-1}{\tau_s[Q]} = \frac{x}{(100-x)\tau_s[Q]} \qquad \text{Eq. S2}$$

Where x is the hypothetical percentual quenching (20%) at the concentration of quencher [Q] (1.25M) and τ_S is singlet lifetime of benzene (28 ns).

This gives $k_q = \frac{x}{(100-x)\tau_S[Q]} = \frac{20}{(100-20)\times 28\times 10^{-9}\times 1.25} = 7.14 \times 10^6 Lmol^{-1}\ s^{-1}$

We have estimated the diffusion constant in methanol at 298 K from the equation S3.

$$k_q^{diff} = \frac{8\times 8.314\times 298.15}{3\times 0.000553} = 1.19 \times 10^7 m^3 mol^{-1}\ s^{-1} = 1.19 \times 10^{10} Lmol^{-1}\ s^{-1} \qquad \text{Eq. S3}$$

This is four orders of magnitude higher than the hypothetical quenching constant. As we do not observe any quenching at this concentration, the real quenching constant must be even lower than $7.14 \times 10^6 Lmol^{-1}\ s^{-1}$. It is therefore highly unlikely that the quenching would be for some reason slower than diffusion by at least four orders of magnitude. We can conclude that the singlet state is not influenced by the quencher (HCl).

5.3 Deuterium experiments

To test the incorporation of water into the benzene molecule we performed a parallel experiment of irradiation of benzene and perdeuterated benzene in water (Figure S34). The products of the reaction were analysed by proton and deuterium NMR spectroscopy (Figure S35).

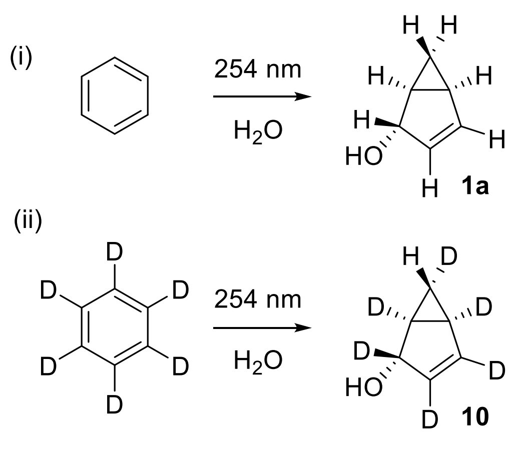

Figure S34: Photochemical rearrangement of benzene and perdeuterated benzene in water and their products.

The rearrangement of benzene resulted in the product **1a** (Figure S35, top) with characteristic set of multiplets corresponding to the diastereotopic protons of the bicyclic scaffold (vide supra). The irradiation of perdeuterated benzene in water lead to the product **10** that contains protium exclusively incorporated in the *endo* position of the cyclopropane CH_2 (signal at -0.13 ppm). This signal is not present in the deuterium spectrum (Figure S35, middle) and is the only present in the ^1H spectrum (Figure S35, bottom). *Note*: deuterium spectrum has only broad singlet signals instead of multiplets. This is caused by much smaller coupling constants ^2H-^2H in comparison to ^1H-^1H.

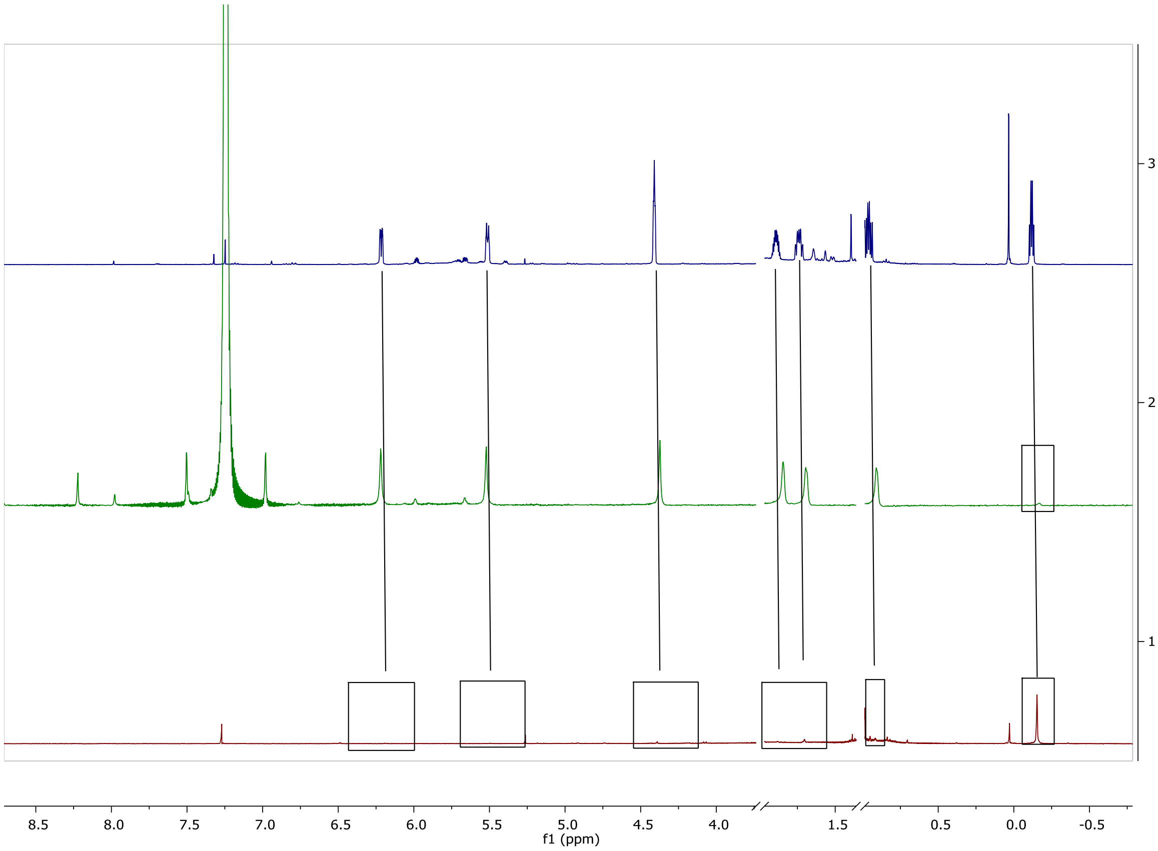

Figure S35: NMR spectra of the photorearrangement product of benzene (top, ^1H NMR) and per-deuterated benzene (middle: ^2H NMR; bottom: ^1H NMR). Rectangles emphasize the missing signals. Note: signal at ~0 ppm corresponds to the tetramethylsilane added as internal standard in $CDCl_3$.

5.4 Approximation of the concentration of excited molecules in a typical irradiation experiment

We have estimated the concentration of the excited molecules in a typical experiment in Rayonet reactor from the known photon flux of the Rayonet reactor (~1.65×10^{16} photons s^{-1} cm^{-3}) and from the known singlet state lifetime of benzene in polar solvents (28 ns).[7] Assuming that all incident light is being absorbed, the concentration of the excited states equals to c(excited state) = $I\tau$, where I is the photon flux of the light source (~1.65×10^{16} photons s^{-1} cm^{-3}) and τ is the lifetime of the excited state (28 ns). This corresponds to the upper limit of the excited molecules to be 4.62×10^{8} molecules/mL or **~8×10^{-13} M**.

5.5 Estimation of the concentration of benzvalene at photostationary state

Based on published results,[8] we have estimated the concentration of benzvalene in photostationary state. Wilzbach and co-workers have reported that a irradiation of a solution of 0.2 mL of benzene in cyclohexane in 25 mL leads to maximum 1% yield. This corresponds to 120 mM concentration of benzene (close to our experimental conditions with 70 mM) and the maximum achievable concentration of benzvalene at photostationary state irradiated at 254 nm in cyclohexane is **~1.2 mM**.

6. Pyridinium, pyrylium ion and silabenzene photochemical rearrangement

The photochemical rearrangement of pyridinium salts is analogous to simple arenes. It was first reported by Kaplan, Pavlik and Wilzbach in 1970s that irradiation of *N*-methylpyridinium chloride in basic aqueous solution leads to production of bicyclic aziridine derivative (Scheme **S5**).[9] Mariano and co-workers have observed an acid-promoted ring opening of photorearranged *N*-allylpyridinium perchlorate in 1980s.[10] The synthetic potential of the photoinduced rearrangement of pyridinium ions has been first identified in the mid-1990s when Mariano has demonstrated the generality of the process irradiating differently substituted pyridinium ions. The products of this reaction undergo stereocontrolled, acid-promoted ring opening with variety of nucleophiles.[11]

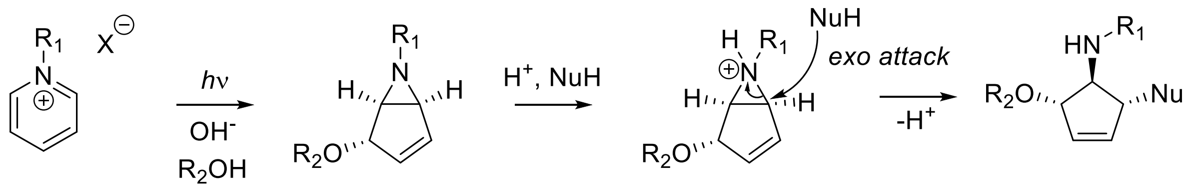

Scheme S5: Photochemistry and acid-promoted ring opening of the bicyclic product.

Number of other studies on this systems followed: synthesis of aminocyclopentitols,[12,13] (-)-allosamizoline aminocyclopentitol,[14] trehatolin aminocyclitol,[15] preparation of cyclopentenone ketals,[16] stereocontrolled synthesis of (+)-mannostatin A[9,17] and its analogues,[18] polyhydroxylated indolizidines,[19] synthesis of amino-sugars,[20] (+)-lactacystin,[21] highly substituted cyclopentanes,[22] (-)-cephalotaxine from 1,2-cyclopenta-fused pyridinium perchlorate[23] and synthetic utilization of other fused derivatives[24] scale-up of photochemical reactions in flow reactors[25,26] and other synthetic applications.[27,28] The pyridinium photochemistry, its mechanism and synthetic applications have been reviewed several times.[29,30,31,32,33,34]

Pyrylium salt photochemistry[32,35] and silabenzene photochemistry[36,37] are analogous to the pyridinium derivatives (Scheme **S6**). In the case of pyrylium, the oxygen atom is incorporated in the three-membered ring, silabenzene rearranges with bulky silicon atom as a part of the five-membered ring. However, their synthetic utility is much lower than in the case of pyridiniums.

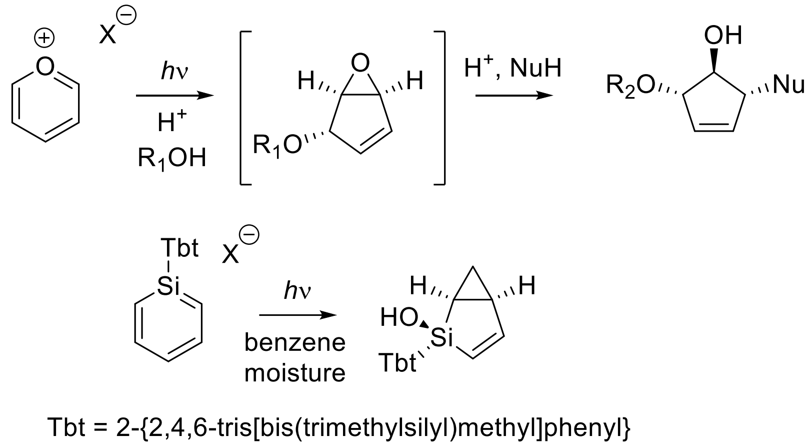

Scheme S6: Photochemistry of pyrylium salts and silabenzene.

7. Computational part

7.1 Computational details: DFT calculations

All DFT calculations were performed with the Gaussian 16 Revision B.01 program suite.[5] The geometries in the S_0, T_1, and S_1 states were optimized using, respectively, restricted B3LYP, unrestricted B3LYP (UB3LYP) and time-dependent (TD)-B3LYP with the 6-311+G(d,p) valence triple-zeta basis set of Pople and co-workers.[38,39] In calculations of the addition of MeOH and $MeOH_2^+$ to benzvalene in the S_0 state, implicit solvation was taken into account using the SMD model[40] simulating methanol as solvent. Dispersion corrections were added using Grimme's D3 model in calculations of activation energies for the proton transfer in the methanol cluster $(MeOH)_8H^+$ corresponding to a saturated cluster (see ref [41]).[42] All stationary points were verified by frequency calculations.
Proton affinities in the gas phase were computed at the same level as the geometry optimization. By definition, proton affinity (PA) is the negative of the reaction enthalpy for the gas phase addition of a proton to the chemical species in question.[43] It is calculated at 298.15 K according to the following Equation S4:

$$PA = -[H(MH^+) - (H(M) + H(H^+))] \qquad \text{Eq. S4}$$

7.2 Computational details: Calculations using multiconfigurational methods:

Geometry optimizations and energy calculations using multiconfigurational methods were performed using the OpenMolcas version 18.09 program (tag 50-g6d6e5e5).[44] In these calculations, all the optimized geometries were obtained through usage of state-average complete active space self-consistent field (SA-CASSCF)[45] using the ANO-RCC type basis set.[46] The dynamic electron correlation was included by single-point calculations using multi-state complete active space second-order perturbation (MS-CASPT2)[47] level at the optimized CASSCF geometries. Default IPEA[48] shift (0.25 a.u.) and imaginary shift[49] of 0.1 a.u. were applied to deal with intruder states at MS-CASPT2 level.

For benzene in the S_0 and T_1 states and for the S_1 state potential energy surface (PES) the ANO-RCC-VTZP basis set and an active space of six electrons and six orbitals including all the π orbitals were used. State average including three states (SA3-CASSCF) was used for optimizations of the S_0 and T_1 states. Due to the switch in the order of B_{1u} and E_g symmetric excited states at the S_1 D_{6h} minimum (1^1B_{2u}), four states were included in the average (SA4-CASSCF) for computation of the S_1 PES.[50] In the S_1 PES we computed the minimum energy path (MEP) from the vertically excited S_1 state, the transition state (TS) structure, the intrinsic reaction coordinate (IRC) path, and the S_1/S_0 conical intersection (CI). Frequency calculations were performed for all the stationary points to confirm that they were minima or saddle-points. For the IRC calculations steps of 0.1 a.u. and 0.025 a.u. were used in the reverse (towards the D_{6h} minimum) and forward (towards the CI) directions, respectively, since the TS structure is located near the CI. The same level of theory (MS3-CASPT2/ANO-RCC-VTZP//SA3-CASSCF/ANO-RCC-VTZP) was used to compute the C_{2v} symmetric S_0, S_1, and T_1 states of the benzenium cation. For those molecules, the active space was composed of four electrons in five π orbitals. Three states were included in the SA-CASSCF and MS-CASPT2 calculations.

The optimized geometries of the S_0 and S_1 states (S_1 minimum, TS, and conical intersections) for the pyridinium ion and silabenzene were obtained at SA3-CASSCF(6,6)/ANO-RCC-VTZP level and the dynamic electron correlation was included by single point calculations using MS3-CASPT2(6,6)/ANO-RCC-VTZP. For silabenzene, the reaction path was computed following the intrinsic reaction coordinate at CASSCF level, from the TS to the S_1 minimum, using 0.1 a.u. as step size. For the pyridinium ion it was not possible to find a TS leading from the S_1 minimum to the S_1/S_0 conical intersection because at CASSCF level the barrier towards the CI is too shallow or inexistent. Instead, linear interpolations in internal coordinates were used to build the PES in the S_1 state. The IPEA and imaginary shifts were the same as described for benzene. For cyclooctatetraene (COT) and protonated COT ($COTH^+$) the geometries of the S_0, S_1, and T_1 states were optimized at the same level described for the molecules above (MS3-CASPT2/ANO-RCC-VTZP//SA3-CASSCF/ANO-RCC-VTZP). The active space was composed by the π system, *i.e.*, 8 electrons in 8 orbitals for COT and 6 electrons in 7 orbitals for $COTH^+$.

Due to increase of the number of atoms, geometry optimizations and energy calculations for the substituted benzenes (TMS-benzene and *t*Bu-benzene) were performed using the ANO-RCC-VDZP basis set. Frequency calculations were done at the same level. For each one of the molecules, four different prefulvenic transition state structures in the S_1 state were computed, having the substituent group at either the *ipso, ortho, meta,* or *para* position relative to the puckered carbon atom of the ring. To be able to compare the energy barriers, stationary points of benzene in the different states were also computed using the ANO-RCC-VDZP basis set.

The potential energy surface for the protonation of benzene in the S_1 state by $MeOH_2^+$ was calculated using SA4-CASSCF(8,8)/ANO-RCC-VTZP optimizations followed by single-point energy calculations at MS4-CASPT2(8,8)/ANO-RCC-VTZP level. The active space includes the six benzene π and π* orbitals and one pair of σ and σ* orbitals corresponding to the O–H bond which will be broken. The starting geometry corresponds to an equilibrium geometry for the complex where the (O)H---C nonbonded distance is 2.561 Å. From this geometry, constrained optimizations were done reducing the OH–C distance in steps of 0.1 Å. The optimized complex between benzene and non-protonated methanol in the S_1 state was calculated at the same level of theory and used as a starting point for the calculation with protonated methanol. This optimization was done without geometric constraints and including eight electrons in eight orbitals, as described above.

7.3 Computational details: Aromaticity indices (NMR chemical shifts and electronic indices)

NMR chemical shifts (^1H and nucleus independent chemical shifts (NICS)) were obtained in the S_0 and T_1 states through calculations using the GIAO method[51] in Gaussian 16 Revision B.01 at B3LYP/6-311+G(d,p) level and in the S_1 state through the GIAO method using Dalton 16.02[52] at CASSCF/6-31++G(d,p) level. Restricted calculations were used for the S_0 state and unrestricted for the T_1 state. In order to take into account the multiconfigurational character of the S_1 states, NICS values were obtained using Dalton 16.02[52] at CASSCF/6-31++G(d,p) level.

$NICS(1)_{zz}$ values in the S_0 and T_1 states were also computed at the latter level of theory in a few cases. (U)DFT geometries were used for GIAO calculations at (U)DFT and at CASSCF levels, and SA-CASSCF geometries were used to obtain $NICS(1)_{zz}$ values at the CASSCF level. In all cases, the active spaces were kept as described for the molecules in the previous section.

The NICS values are the negative of the magnetic shieldings at specific positions, originally at the center of the rings. When probe atoms are inserted 1.0 Å above or below the molecular plane, along the *z*-axis of the coordinate system, the NICS values obtained at these points are called $NICS(1)_{zz}$. $NICS(1)_{zz}$ values were computed along the S_1 state PES of benzene, pyridinium ion, and silabenzene. $NICS(1)_{zz}$ were also computed for benzene, benzenium cation, COT, and $COTH^+$ in their S_0, S_1, and T_1 states, and for TMS-benzene and *t*-Bu-benzene in their S_1 vertical and S_1 minimum states.

For the prefulvenic structures of benzene, the position of the probe atom was chosen as the central position between the C1, C2, C4, and C5 atoms and the xy-plane was defined by these four atoms whereby the $NICS(1)_{zz}$ values were computed above and below that plane. For silabenzene and pyridinium ion the place of the probe atom was also chosen based on the plane comprising the corresponding four carbon atom. The $NICS(1)_{zz}$ values along the S_1 puckering coordinate from the S_1 minimum towards the CI (see Figure 1 in the manuscript and Figure S) were computed for each of the geometries along the PES. For the structures at (near) conical intersection it is not possible to compute NICS values due to the degeneracy of the states.

Finally, to help in the interpretation of the NMR data obtained experimentally, NMR chemical shift calculations of possible bicyclo[3.1.0]hexenyl photoproducts (**1a - f**) were performed with the GIAO method at B3LYP/6-311+G(2d,p) level.

Additionally, we also computed electronic aromaticity indices for benzene, benzenium cation, COT, and $COTH^+$ in the S_0 and S_1 states. The multicenter index (MCI)[53] and aromatic fluctuation index (FLU)[54] were obtained from SA-CASSCF/ANO-RCC-VTZP wavefunctions using the B3LYP/6-311+G(d,p) geometry. MCI quantifies the extent of cyclic delocalized conjugation while FLU describes the fluctuation of electronic charge between adjacent atoms in a given ring. Higher MCI values and smaller FLU values (typically close to zero) indicate increased aromaticity. These indices were computed using the AIMAll[55] and ESI[56] programs. For more details about these indices please check the references cited above.

7.4 Geometries, Cartesian coordinates, and energies

Table S13. Electronic energies (in a.u.), configurations, and configuration weights of benzene in the S_0 and along of puckering coordinate at SA-CASSCF(6,6)/ANO-RCC-VTZP level. Absolute energies at MS-CASPT2(6,6)/ANO-RCC-VTZP level. Three and four states were included in the average for the optimizations of the S_0 and S_1 species (S_1 minimum, TS, and CI). The optimized state is shown in italics while the remaining states are single point calculations at the respective optimized geometry.

Optimized Geometry	State	SA-CASSCF	MS-CASPT2	Conf	weight	Conf	weight
S_0	*S_0*	*-230.946618*	*-231.832480*	*222000*	*0.89*		
	S_1	-230.765931	-231.645541	2u2d00	0.40	u2200d	0.40
S_1	S_0	-230.939701	-231.825559	222000	0.87		
	S_1	*-230.774286*	*-231.652490*	*2u200d*	*0.38*	*u22d00*	*0.38*
TS	S_0	-230.788360	-231.691329	222000	0.72		
	S_1	*-230.742454*	*-231.637536*	*22ud00*	*0.74*		
CI	S_0	-230.744013	-231.655302	u2200d	0.76		
	S_1	-230.744012	-231.640988	222000	0.69		

Table S14. Cartesian coordinates of **benzene** in the S_0 state and along of puckering coordinate in the S_1 state (S_1 minimum, prefulvene TS and S_1/S_0 conical intersection) at SA-CASSCF(6,6)/ANO-RCC-VTZP level. Absolute energies at MS4-CASPT2(6,6)/ANO-RCC-VTZP level. Three and four states were included in the optimizations of the S_0 state and S_1 structures.

Benzene in the S_0 state

```
E : -231.83248030  a.u.

 C    -0.69626440    -1.20596594    -0.00021885
 C     0.69626601    -1.20596434     0.00022742
 C     1.39253068     0.00000376    -0.00000344
 C     0.69626437     1.20596555    -0.00022911
 C    -0.69626586     1.20596532     0.00023768
 C    -1.39252982    -0.00000272    -0.00001370
 H    -1.23271763    -2.13512115    -0.00073796
 H     1.23271198    -2.13512387     0.00076700
 H     2.46542942     0.00000224    -0.00000804
 H     1.23271838     2.13512072    -0.00077995
 H    -1.23271451     2.13512352     0.00080899
 H    -2.46542863    -0.00000307    -0.00005003
```

Benzene in the S_1 state

```
E : -231.65249029  a.u.

 C    -0.71521166    -1.23878523    -0.00002688
 C     0.71521158    -1.23878515     0.00002359
 C     1.43042486     0.00000004     0.00000327
 C     0.71521159     1.23878510    -0.00002686
 C    -0.71521155     1.23878509     0.00002360
 C    -1.43042483     0.00000006     0.00000326
 H    -1.25056433    -2.16603578    -0.00010249
 H     1.25056438    -2.16603576     0.00009016
 H     2.50112523    -0.00000002     0.00001234
 H     1.25056404     2.16603583    -0.00010250
 H    -1.25056411     2.16603583     0.00009015
 H    -2.50112520     0.00000003     0.00001235
```

Prefulvene TS in the S_1 state

```
E : -231.63753599  a.u.

 C    -0.75113820    -1.03504388    -0.02959979
 C     0.69802420    -1.16727634    -0.02324307
 C     1.44913370     0.00057440     0.08887811
 C     0.69737474     1.16801573    -0.02318332
 C    -0.75171068     1.03496600    -0.02958438
 C    -1.39929186    -0.00022324     0.75780701
```

S_1/S_0 conical intersection

```
E : -231.64098849  a.u.

 C    -0.74693586    -0.96731268    -0.06797895
 C     0.70199906    -1.15841480    -0.02507421
 C     1.46167420     0.00057453     0.08683577
 C     0.70134090     1.15914677    -0.02502981
 C    -0.74750214     0.96725396    -0.06789220
 C    -1.39019823    -0.00024181     0.80159738
```

H	-1.33625813	-1.69441821	-0.64421693	H	-1.34540764	-1.60607093	-0.69158605
H	1.14633676	-2.13304315	-0.14984932	H	1.12527551	-2.13732177	-0.12916580
H	2.51699374	0.00086847	0.16843638	H	2.52780219	0.00087696	0.18942845
H	1.14515163	2.13403720	-0.14974395	H	1.12406294	2.13829750	-0.12909337
H	-1.33719827	1.69405137	-0.64416017	H	-1.34631907	1.60576122	-0.69142322
H	-2.46970064	-0.00051837	0.83731570	H	-2.45807487	-0.00055898	0.90823828

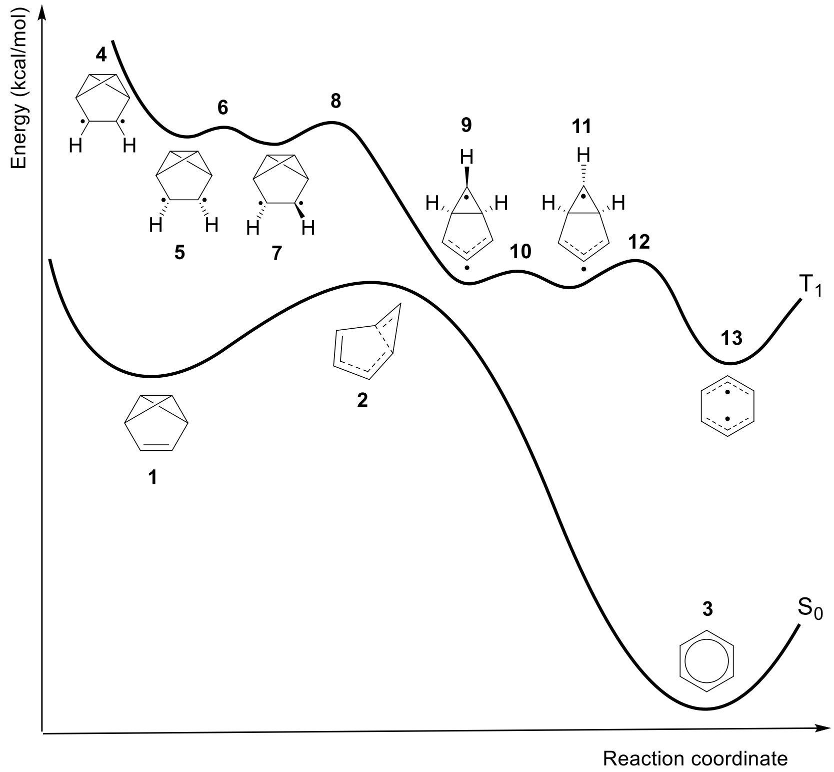

Figure S36: Compound numbering of minima and transition state structures on the T_1 and S_0 potential energy curves for the **rearrangement of T_1 state benzvalene to T_1 state benzene**. Structure **4** is the benzvalene vertically excited from its S_0 state structure to the T_1 state. It is worth to be noted that the rearrangement of T_1 state benzvalene to T_1 state benzene is highly exotermic (~60 kcal/mol). Moreover, the rearrangement in the S_0 state has a computed activation barrier of ~24 kcal/mol, resembling both previous experimental findings (26.7 kcal/mol)[57] and earlier computed results.[58,59]

Table S15. Electronic energies (without ZPE corrections) and cartesian coordinates for the structures shown in Figure S36 (**rearrangement of T_1 state benzvalene to T_1 state benzene**) calculated at B3LYP/6-311+G(d,p) level in the gas phase.

1 (Benzvalene (C_{2v}) in the S_0 state)

E : -232.180434003 a.u.

C	0.723750000	0.000000000	-1.011675000
C	-0.723750000	0.000000000	-1.011675000
C	0.000000000	1.076234000	-0.202173000
C	0.000000000	-1.076234000	-0.202173000
C	0.000000000	0.668799000	1.251754000
C	0.000000000	-0.668799000	1.251754000
H	1.482139000	0.000000000	-1.782197000
H	-1.482139000	0.000000000	-1.782197000
H	0.000000000	2.105997000	-0.537881000
H	0.000000000	-2.105997000	-0.537881000
H	0.000000000	1.347232000	2.092641000
H	0.000000000	-1.347232000	2.092641000

2 (TS benzvalene to benzene in the S_0 state)

E: -232.138507741 a.u.

C	0.543781000	-0.101597000	-1.010965000
C	-0.753460000	0.306817000	-1.335305000
C	-0.210293000	1.115596000	-0.143614000
C	-0.080547000	0.682619000	1.193401000
C	0.093878000	-0.712569000	1.257136000
C	0.327652000	-1.197081000	-0.006624000
H	1.493283000	0.062772000	-1.526624000
H	-1.003958000	0.814092000	-2.265718000
H	-0.087425000	2.166046000	-0.390957000
H	-0.126925000	1.357344000	2.038379000
H	-0.074972000	-1.315851000	2.139923000
H	0.254131000	-2.227820000	-0.328092000

Imaginary frequency : 264*i* cm^{-1}

3 (Benzene in the S_0 state)

E: -232.311270767 a.u.

C	0.000000000	1.394724000	0.000000000
C	1.207866000	0.697362000	0.000000000
C	1.207866000	-0.697362000	0.000000000
C	0.000000000	-1.394724000	0.000000000
C	-1.207866000	-0.697362000	0.000000000
C	-1.207866000	0.697362000	0.000000000
H	0.000000000	2.479163000	0.000000000
H	2.147018000	1.239581000	0.000000000
H	2.147018000	-1.239581000	0.000000000
H	0.000000000	-2.479163000	0.000000000
H	-2.147018000	-1.239581000	0.000000000
H	-2.147018000	1.239581000	0.000000000

4 (Benzvalene vertically excited to the T_1 state)

E : -232.047580612 a.u.

C	0.723750000	0.000000000	-1.011675000
C	-0.723750000	0.000000000	-1.011675000
C	0.000000000	1.076234000	-0.202173000
C	0.000000000	-1.076234000	-0.202173000
C	0.000000000	0.668799000	1.251754000
C	0.000000000	-0.668799000	1.251754000
H	1.482139000	0.000000000	-1.782197000
H	-1.482139000	0.000000000	-1.782197000
H	0.000000000	2.105997000	-0.537881000
H	0.000000000	-2.105997000	-0.537881000
H	0.000000000	1.347232000	2.092641000
H	0.000000000	-1.347232000	2.092641000

Imaginary frequencies : 652*i*, 350*i*, 273*i* cm^{-1}

5 (Benzvalene in the T_1 state - conformer 1)

E : -232.078530858 a.u.

C	-0.729612000	-0.965909000	0.000000000
C	0.715704000	-1.001633000	0.000000000
C	0.044302000	-0.198204000	1.100249000
C	0.044302000	-0.198204000	-1.100249000
C	0.044302000	1.234380000	0.768278000
C	0.044302000	1.234380000	-0.768278000
H	-1.564063000	-1.647769000	0.000000000
H	1.468299000	-1.773460000	0.000000000
H	0.027981000	-0.582509000	2.112134000
H	0.027981000	-0.582509000	-2.112134000
H	-0.470005000	1.978691000	1.366220000
H	-0.470005000	1.978691000	-1.366220000

6 (TS Benzvalene conf. 1 to conf. 2 in the T_1 state)

E : -232.075194849 a.u.

C	0.038251000	-0.722492000	-1.046256000
C	-0.052113000	0.714976000	-0.954612000
C	1.094721000	0.004993000	-0.209536000
C	-1.097997000	-0.154917000	-0.215775000
C	0.759920000	-0.118009000	1.210571000
C	-0.770137000	-0.160588000	1.221827000
H	0.094558000	-1.453582000	-1.836339000
H	-0.119475000	1.570551000	-1.606192000
H	2.103974000	0.091916000	-0.591360000
H	-2.109857000	-0.181656000	-0.599946000
H	1.420145000	-0.008613000	2.056198000
H	-1.361991000	0.417420000	1.928286000

Imaginary frequency: 332*i* cm^{-1}

7 (Benzvalene in the T_1 state - conformer 2)

E : -232.080902301 a.u.

C	0.003326000	0.722534000	0.967125000
C	-0.003615000	-0.722578000	0.967084000
C	1.097619000	-0.033469000	0.178949000

8 (TS Benzvalene to prefulvene in the T_1 state)

E : -232.073965923 a.u.

C	-0.130598000	0.746684000	1.045041000
C	0.060593000	-0.673130000	1.003091000

C	-1.097671000	0.033489000	0.178608000
C	0.757077000	0.035200000	-1.255513000
C	-0.756690000	-0.035109000	-1.255754000
H	0.030049000	1.513439000	1.698752000
H	-0.030565000	-1.513536000	1.698645000
H	2.110701000	-0.026791000	0.561317000
H	-2.110869000	0.026792000	0.560666000
H	1.316949000	0.666680000	-1.940041000
H	-1.316309000	-0.666650000	-1.940435000

C	1.146007000	-0.144688000	0.128292000
C	-1.108134000	-0.028724000	0.202962000
C	0.760889000	0.014344000	-1.221538000
C	-0.744893000	-0.008874000	-1.220569000
H	-0.040236000	1.621427000	1.664433000
H	0.030432000	-1.478909000	1.723381000
H	2.153248000	-0.032868000	0.508452000
H	-2.120068000	-0.171764000	0.561187000
H	1.364338000	0.536935000	-1.953727000
H	-1.371574000	-0.380430000	-2.021603000

Imaginary frequency : 519*i* cm^{-1}

9 (Prefulvene in the T_1 state - conformer 1)

E : -232.138529837 a.u.

C	1.430413000	0.000279000	-0.647324000
C	0.682220000	-0.783883000	0.364333000
C	-0.728875000	-1.145945000	0.061866000
C	0.681843000	0.784269000	0.364187000
C	-1.494720000	-0.000377000	-0.126492000
C	-0.729427000	1.145595000	0.061654000
H	2.494498000	0.000517000	-0.844595000
H	1.248371000	-1.378038000	1.077527000
H	-1.073034000	-2.167336000	-0.029659000
H	1.247707000	1.378828000	1.077272000
H	-2.539463000	-0.000655000	-0.411225000
H	-1.074077000	2.166803000	-0.030061000

10 (TS Prefulvene conf. 1 to conf.2 in the T_1 state)

E : -232.134377925 a.u.

C	-0.456150000	0.889998000	1.178158000
C	0.251357000	-0.380783000	0.974262000
C	1.310070000	-0.411410000	-0.079033000
C	-1.056345000	-0.022795000	0.196307000
C	0.757382000	-0.102287000	-1.318581000
C	-0.614417000	0.115318000	-1.223600000
H	-0.525778000	1.814786000	1.722530000
H	0.266926000	-1.119760000	1.773861000
H	2.353388000	-0.615288000	0.121119000
H	-2.011581000	-0.495719000	0.418896000
H	1.326435000	-0.016844000	-2.236405000
H	-1.275951000	0.378030000	-2.038148000

Imaginary frequency : 519*i* cm^{-1}

11 (Prefulvene in the T_1 state - conformer 2)

E : -232.138784256 a.u.

C	-0.524687000	0.825176000	1.249082000
C	0.206196000	-0.447864000	1.002979000
C	1.286056000	-0.382538000	-0.017325000
C	-1.088206000	-0.101793000	0.229731000
C	0.741478000	-0.021246000	-1.248704000
C	-0.641794000	0.133186000	-1.169114000
H	-0.199181000	1.854816000	1.164131000
H	0.218679000	-1.204988000	1.782161000
H	2.332740000	-0.559551000	0.188836000
H	-2.028133000	-0.604499000	0.440286000
H	1.320979000	0.129743000	-2.151424000
H	-1.298795000	0.412805000	-1.981272000

12 (TS Prefulvene to benzene in the T_1 state)

E : -232.129259148 a.u.

C	1.451129000	0.000294000	-0.557030000
C	0.707657000	-0.975380000	0.218484000
C	-0.717244000	-1.154432000	0.042651000
C	0.707176000	0.975755000	0.218308000
C	-1.470181000	-0.000364000	-0.160803000
C	-0.717813000	1.154100000	0.042410000
H	2.534729000	0.000556000	-0.515227000
H	1.243627000	-1.644544000	0.890637000
H	-1.152915000	-2.145414000	0.113077000
H	1.242811000	1.645242000	0.890404000
H	-2.529562000	-0.000646000	-0.378035000
H	-1.153956000	2.144890000	0.112607000

Imaginary frequency : 369*i* cm^{-1}

13 (Benzene in the T_1 state – antiquinoide)

E : -232.1699201 a.u.

C	-0.759873000	1.208112000	0.000000000
C	-1.440967000	0.000000000	0.000000000
C	-0.759873000	-1.208112000	0.000000000
C	0.759873000	-1.208112000	0.000000000
C	1.440967000	0.000000000	0.000000000
C	0.759873000	1.208112000	0.000000000
H	-1.286726000	2.153140000	0.000000000
H	-2.526366000	0.000000000	0.000000000
H	-1.286726000	-2.153140000	0.000000000
H	1.286726000	-2.153140000	0.000000000
H	2.526366000	0.000000000	0.000000000
H	1.286726000	2.153140000	0.000000000

7.5 Protonation of benzene

The vertical excitation energy of **2** (benzenium cation) is calculated to be 310 – 315 nm (at TD-B3LYP and CASPT2//CASSCF levels), in agreement with earlier experimental results (325 – 330 nm).[60,61] Methylated derivatives of **1** (bicyclo[3.1.0]hexene) have markedly red-shifted absorption maxima.[62] Interestingly, Olah *et al.* found that one of those, upon irradiation at its absorption maximum (390 nm)[63] rearranges to a bicyclo[3.1.0]hexenium cation **3** and this cation is further nucleophilically attacked by solvent from the *exo* face. [64]

Table S16. Cartesian coordinates and absolute energies of **protonated benzene** ($C_6H_7^+$): stationary points in the S_0, S_1, and T_1 states calculated with (TD/U)-B3LYP/6-311+G(d,p) in the gas phase (see Figure 2 in the main text).

2 Benzenium cation in the S_0 state

E : -232.611193322 a.u.

C	0.000000000	1.253008000	0.628502000
C	0.000000000	0.000000000	1.394693000
C	0.000000000	-1.253008000	0.628502000
C	0.000000000	-1.239290000	-0.740100000
C	0.000000000	0.000000000	-1.413014000
C	0.000000000	1.239290000	-0.740100000
H	0.000000000	0.000000000	-2.499042000
H	0.000000000	2.160328000	-1.309415000
H	0.000000000	2.188981000	1.177322000
H	0.000000000	-2.188981000	1.177322000
H	0.000000000	-2.160328000	-1.309415000
H	-0.849235000	0.000000000	2.106163000
H	0.849235000	0.000000000	2.106163000

3 Bicyclo[3.1.0]hexenium cation in the S_0 state

E : -232.568648213 a.u.

C	0.251961000	-0.749494000	0.743027000
C	-1.068866000	-1.112001000	0.000000000
C	0.251961000	-0.749494000	-0.743027000
C	0.251961000	0.655309000	-1.126982000
C	0.281886000	1.474598000	0.000000000
C	0.251961000	0.655309000	1.126982000
H	0.226366000	2.554010000	0.000000000
H	0.158387000	1.002855000	2.150408000
H	0.683817000	-1.529995000	1.356723000
H	0.683817000	-1.529995000	-1.356723000
H	0.158387000	1.002855000	-2.150408000
H	-1.361474000	-2.155879000	0.000000000
H	-1.874475000	-0.389209000	0.000000000

TS Benzenium cation to bicyclo[3.1.0]hexenium cation in the S_0 state

E : -232.534026829 a.u.

C	-0.244399000	1.128504000	0.631042000
C	0.309306000	-0.127223000	1.508319000
C	-0.330475000	-1.031586000	0.628683000
C	0.185721000	-1.212192000	-0.722788000
C	0.246146000	-0.072266000	-1.428342000
C	-0.146821000	1.157668000	-0.698155000
H	0.525169000	-0.044343000	-2.473933000
H	-0.346638000	2.074940000	-1.241121000
H	-0.580685000	1.936409000	1.269305000
H	-1.296074000	-1.468668000	0.896247000
H	0.355981000	-2.205770000	-1.125770000
H	-0.075644000	-0.071645000	2.521567000
H	1.398412000	-0.063830000	1.440855000

Benzenium cation in the S_1 state (C_{2v})

E : -232.466753410 a.u.

Benzenium cation in the S_1 state (C_s)

E : -232.471728622 a.u.

C	0.000000000	1.221113000	-0.644594000
C	0.000000000	0.000000000	-1.488474000
C	0.000000000	-1.221113000	-0.644594000
C	0.000000000	-1.209031000	0.765741000
C	0.000000000	0.000000000	1.503019000
C	0.000000000	1.209031000	0.765741000
H	0.000000000	0.000000000	2.583879000
H	0.000000000	2.159785000	1.286606000
H	0.000000000	2.185455000	-1.145698000
H	0.000000000	-2.185455000	-1.145698000
H	0.000000000	-2.159785000	1.286606000
H	0.855602000	0.000000000	-2.203367000
H	-0.855602000	0.000000000	-2.203367000

Imaginary frequencies : 774*i* cm^{-1} and 55*i* cm^{-1}

C	0.146977000	0.725876000	1.194069000
C	0.146977000	-0.689396000	1.088310000
C	0.146977000	-0.689396000	-1.088310000
C	0.146977000	0.725876000	-1.194069000
C	0.065429000	1.466286000	0.000000000
H	0.044718000	2.548302000	0.000000000
H	0.284328000	1.202207000	2.158190000
H	0.741289000	-1.307670000	1.757490000
H	0.741289000	-1.307670000	-1.757490000
H	0.284328000	1.202207000	-2.158190000
C	-0.630895000	-1.351330000	0.000000000
H	-0.548557000	-2.434386000	0.000000000
H	-1.682055000	-1.030488000	0.000000000

Benzenium cation in the T_1 state (C_{2v})

E : -232.527660223 a.u.

C	0.000000000	1.239300000	-0.650703000
C	0.000000000	0.000000000	-1.488010000
C	0.000000000	-1.239300000	-0.650703000
C	0.000000000	-1.201567000	0.770419000
C	0.000000000	0.000000000	1.491705000
C	0.000000000	1.201567000	0.770419000
H	0.000000000	0.000000000	2.572576000
H	0.000000000	2.145956000	1.306116000
H	0.000000000	2.203525000	-1.146559000
H	0.000000000	-2.203525000	-1.146559000
H	0.000000000	-2.145956000	1.306116000
H	0.863174000	0.000000000	-2.175227000
H	-0.863174000	0.000000000	-2.175227000

Imaginary frequency : 195*i* cm^{-1}

Benzenium cation minimum in the T_1 state (C_s)

E : -232.530897144 a.u.

C	-0.655223000	-1.195379000	-0.168952000
C	-1.452195000	0.000000000	0.263789000
C	-0.655223000	1.195379000	-0.168952000
C	0.751401000	1.198343000	-0.029433000
C	1.466649000	0.000000000	0.120738000
C	0.751401000	-1.198343000	-0.029433000
H	2.539583000	0.000000000	0.256290000
H	1.282060000	-2.145510000	-0.069342000
H	-1.158762000	-2.043934000	-0.621317000
H	-1.158761000	2.043934000	-0.621317000
H	1.282060000	2.145510000	-0.069342000
H	-1.572181000	0.000000000	1.361838000
H	-2.454860000	0.000000000	-0.163351000

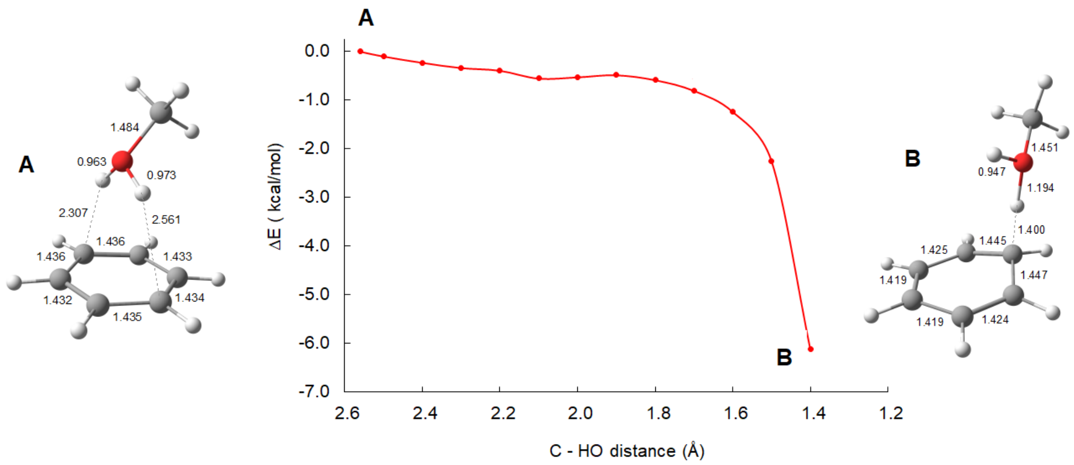

Figure S37. PES for **protonation of benzene in the S_1 state by $MeOH_2^+$** calculated at MS4-CASPT2(8,8)/ANO-RCC-VTZP//SA4-CASSCF(8,8)/ANO-RCC-VTZP level. The starting point (structure A) corresponds to the equilibrium geometry (without constraints) and the last point (structure B) corresponds to the last converged optimization with the C–OH distance constrained.

Table S17. Cartesian coordinates and energies for the first and last points of the PES for **protonation of benzene in the S_1 state by $MeOH_2^+$** calculated at MS4-CASPT2(8,8)/ANO-RCC-VTZP//SA4-CASSCF(8,8)/ANO-RCC-VTZP level.

Benzene + $MeOH_2^+$ (r C–OH = 2.561 Å)

E : -347.58058175 a.u.

C	-0.73832978	1.54526871	-0.73992927
C	-0.85261014	1.49948641	0.68678267
C	-1.02604109	0.24123028	1.35536011
C	-1.16314662	-0.96038237	0.58416120
C	-1.04360158	-0.91616600	-0.84321013
C	-0.78816178	0.33165218	-1.50572210
O	1.99174355	0.04314713	0.02222446
C	2.84529579	-1.17097299	0.00649127
H	-0.64686314	2.48743569	-1.23932722
H	-0.84989614	2.40925918	1.25045643
H	-1.18217651	0.21678747	2.41417369
H	-1.39589505	-1.88486732	1.07088088
H	-1.19108489	-1.80550185	-1.42061749
H	-0.77961346	0.37586455	-2.57569662
H	1.48129606	0.16296167	0.84205679
H	1.36397615	0.11321020	-0.70451307
H	2.20883985	-2.03331202	0.09247173
H	3.37023093	-1.13255452	-0.92990392
H	3.51272601	-1.05945710	0.84074175

Benzene + $MeOH_2^+$ (r C–OH = 1.400 Å)

E : -347.5903285 a.u.

C	-1.21132059	1.60732246	-0.86801895
C	-0.60988753	1.43103125	0.41078905
C	-0.22360544	0.12143738	0.88853108
C	-0.97171208	-0.94847314	0.26919224
C	-1.57616538	-0.78868382	-1.01159654
C	-1.63299579	0.48668994	-1.63045322
O	2.24611233	-0.06726469	0.12176769
C	3.03540648	-1.17354333	0.62925585
H	-1.37276642	2.60304731	-1.22654410
H	-0.43698555	2.28605099	1.03373158
H	-0.03202609	0.03070522	1.94770074
H	-1.08055314	-1.88052790	0.78787354
H	-2.02100398	-1.64264886	-1.47962583
H	-2.08529464	0.61270639	-2.59013674
H	1.10492623	-0.01725613	0.46928447
H	2.32589712	0.05003639	-0.81497298
H	2.69981714	-2.09627738	0.18555106
H	4.06512186	-0.97295841	0.38927877
H	2.89372364	-1.17830438	1.69527349

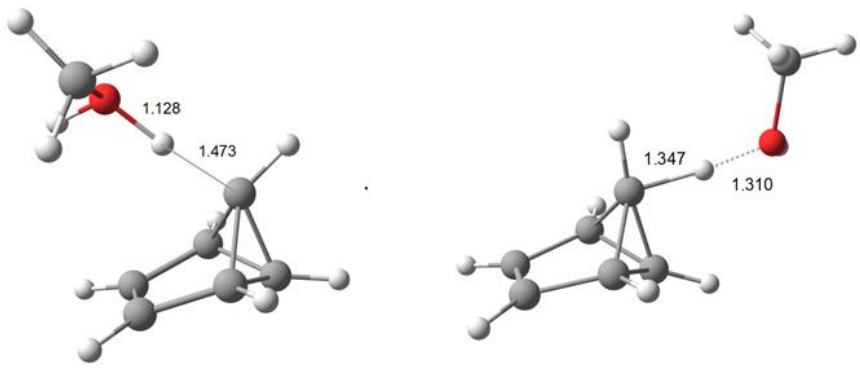

TS1_Endo

$\Delta G^{\ddagger}$ = 7.4 kcal/mol

TS1_Exo

$\Delta G^{\ddagger}$ = 21.8 kcal/mol

Figure S38. *Endo* and *exo* transition state structures for **protonation of benzvalene** in the S_0 state by $MeOH_2^+$ calculated with B3LYP/6-311+G(d,p) using SMD model and methanol as implicit solvent. The most stable transition state structure gives rise to the bicyclo[3.1.0]hexenium ion with the H atom incorporated in the 6-*endo* position.

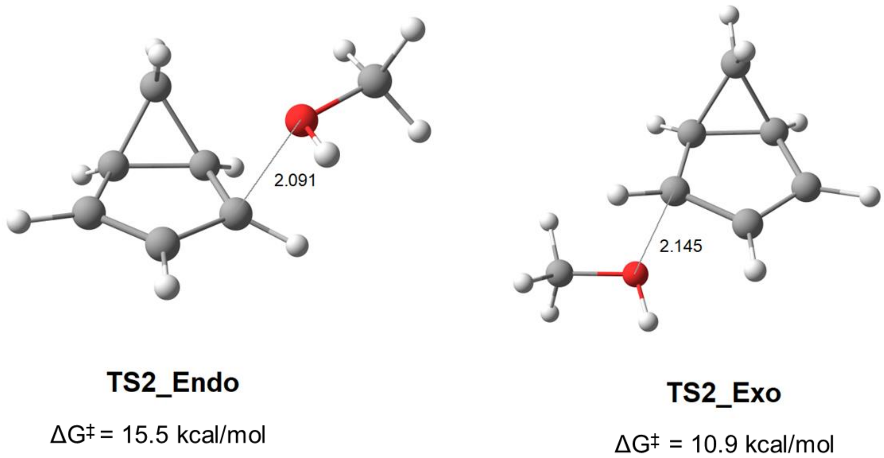

Figure S39. *Endo* and *exo* transition state structures for **nucleophilic attack of MeOH on the protonated bicyclo[3.1.0]hexenium ion** (primary photoproduct from protonation of benzvalene) in the S_0 state calculated with B3LYP/6-311+G(d,p) using SMD model and methanol as implicit solvent.

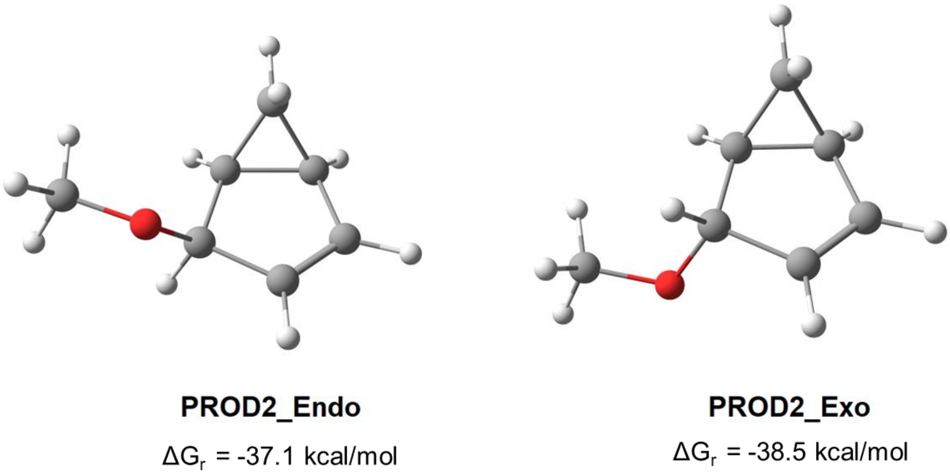

Figure S40. The most stable *endo* and *exo* products resulting from the **addition of MeOH to the bicyclo[3.1.0]hexenium cation** in the S_0 state calculated with B3LYP/6-311+G(d,p) using SMD model and methanol as implicit solvent.

Table S18. Geometries of the transition state for **protonation of benzvalene by $MeOH_2^+$** (TS1), transition state for nucleophilic attack of MeOH to the protonated benzvalene (TS2), and the products resulted from these reactions calculated at B3LYP/6-311+G(d,p) using SMD model and methanol as implicit solvent.

TS1_ENDO	**TS1_EXO**
E : -348.384164 a.u. G : -348.259382 a.u.	E : -348.359257 a.u. G : -348.236402 a.u.

C	1.872132000	-0.823711000	-0.174137000
C	0.414133000	-1.041338000	0.218670000
C	0.890924000	-0.289828000	-1.132554000
C	1.421810000	-0.025707000	0.976587000
C	0.713644000	1.169108000	-0.830323000
C	1.039192000	1.330910000	0.462162000
H	2.542525000	-1.666651000	-0.236784000
H	0.214076000	-2.094354000	0.400299000
H	0.714653000	-0.746301000	-2.096502000
H	1.739405000	-0.234762000	1.988577000
H	0.329215000	1.898117000	-1.529425000
H	0.983713000	2.223329000	1.069324000
H	-2.538816000	0.610770000	-1.146526000
C	-2.856204000	-0.111892000	-0.396745000
H	-2.813849000	-1.127171000	-0.782621000
H	-3.850235000	0.116016000	-0.018773000
O	-1.939604000	-0.075478000	0.748161000
H	-0.900391000	-0.440862000	0.503862000
H	-1.877246000	0.820440000	1.121318000

Imaginary frequency: -676*i* cm^{-1}

C	-0.084010000	0.053376000	-0.403389000
C	-0.564768000	-0.128318000	1.023671000
C	-1.085935000	-1.086014000	0.002138000
C	-1.085434000	1.056820000	0.286399000
C	-2.453819000	-0.612545000	-0.429215000
C	-2.452828000	0.712133000	-0.254796000
H	0.399058000	0.194926000	-1.366536000
H	0.055366000	-0.241514000	1.904952000
H	-0.763155000	-2.118370000	-0.016423000
H	-0.758833000	2.059161000	0.529149000
H	-3.231077000	-1.255972000	-0.815252000
H	-3.229160000	1.434703000	-0.460392000
H	3.124746000	1.155292000	-0.970691000
C	3.355406000	0.163442000	-0.587124000
H	4.363193000	0.147303000	-0.173555000
H	3.248707000	-0.586738000	-1.371942000
O	2.410238000	-0.092869000	0.489772000
H	1.156041000	-0.035108000	0.115586000
H	2.581532000	-0.964098000	0.880830000

Imaginary frequency : -1237*i* cm^{-1}

TS2_ENDO

E : -348.435965 a.u.
G : -348.304913 a.u.

C	-0.005440000	1.431527000	-1.372499000
C	0.049779000	-0.111898000	-1.166273000
C	-1.245994000	0.605023000	-1.485000000
C	-0.105786000	-0.597168000	0.200084000
C	-2.034105000	0.535076000	-0.226507000
C	-1.377170000	-0.169975000	0.726956000
H	0.454683000	1.785326000	-2.287270000
H	0.610879000	-0.682469000	-1.892273000
H	-1.719689000	0.476263000	-2.450171000
H	0.445268000	-1.446339000	0.580362000
H	-2.989767000	1.029576000	-0.098080000
H	-1.708945000	-0.350911000	1.739791000
H	2.878731000	-0.689374000	1.101636000
C	2.600526000	0.363059000	1.010720000
H	2.732470000	0.700347000	-0.016076000
H	3.215022000	0.972251000	1.677061000
H	0.143458000	2.042391000	-0.491418000
O	1.207872000	0.559689000	1.344342000
H	1.060140000	0.266706000	2.256956000

Imaginary frequency: 166*i* cm^{-1}

TS2_EXO

E : -348.440787 a.u.
G : -348.311916 a.u.

C	-1.532922000	-2.289139000	0.507757000
C	-2.091959000	-1.093497000	-0.279982000
C	-0.612669000	-1.332519000	-0.261719000
C	-2.295154000	0.073528000	0.589352000
C	-0.055302000	-0.278335000	0.590957000
C	-1.109058000	0.536698000	1.089522000
H	-1.659597000	-3.273247000	0.071652000
H	-2.725332000	-1.296961000	-1.132857000
H	-0.059284000	-1.746107000	-1.092657000
H	-3.274370000	0.451252000	0.860214000
H	-0.987248000	1.323540000	1.820397000
H	2.606090000	1.354928000	-1.956702000
C	2.239537000	0.665388000	-1.192472000
H	2.849841000	0.751418000	-0.290274000
H	2.280410000	-0.353953000	-1.574191000
H	-1.558345000	-2.238044000	1.588882000
H	0.921933000	-0.346520000	1.049990000
O	0.853989000	0.955316000	-0.910023000
H	0.790400000	1.847886000	-0.539083000

Imaginary frequency : 93*i* cm^{-1}

PROD2_ENDO

E : -348.021987 a.u.
G : -347.899957 a.u.

C	-0.997086000	-1.784201000	-0.197083000
C	-1.773886000	-0.596187000	-0.729552000
C	-0.319526000	-0.793076000	-1.113461000
C	-1.787717000	0.603397000	0.162504000
C	0.479160000	0.347765000	-0.464443000
C	-0.563776000	1.104885000	0.333915000
H	-1.222937000	-2.759187000	-0.614291000
H	-2.576625000	-0.764484000	-1.437551000
H	-0.058093000	-1.114156000	-2.113747000
H	-2.689063000	0.974762000	0.636490000
H	0.919199000	0.986690000	-1.248125000
H	-0.290623000	1.922804000	0.988508000
H	3.375360000	-0.879046000	0.501984000

PROD2_EXO

E : -348.024163 a.u.
G : -347.902211 a.u.

C	-1.127434000	-1.788671000	-0.113083000
C	-1.781849000	-0.584857000	-0.777433000
C	-0.309657000	-0.892203000	-1.001067000
C	-1.794283000	0.653181000	0.048995000
C	0.496354000	0.230330000	-0.339583000
C	-0.557582000	1.087680000	0.321376000
H	-1.376652000	-2.770536000	-0.501937000
H	-2.538260000	-0.752038000	-1.535124000
H	0.040595000	-1.284087000	-1.947914000
H	-2.709148000	1.106011000	0.416262000
H	-0.301269000	1.926232000	0.958724000
H	2.914935000	1.148910000	-2.411347000
C	2.453238000	0.446726000	-1.715403000

C	2.615370000	-0.672091000	-0.252112000	H	3.123076000	0.292120000	-0.860482000
H	2.321751000	-1.615440000	-0.730291000	H	2.299317000	-0.510499000	-2.226530000
H	3.041922000	-0.005969000	-1.016255000	O	1.218415000	1.029340000	-1.296090000
O	1.526818000	-0.059615000	0.413455000	H	-0.974435000	-1.745767000	0.960805000
H	-0.725340000	-1.781597000	0.851888000	H	1.220373000	-0.158228000	0.389632000

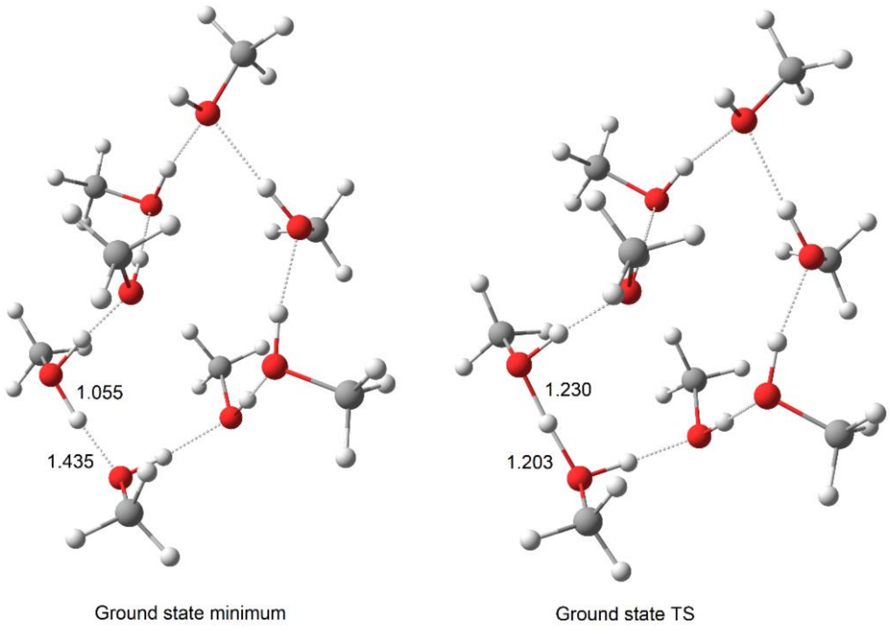

Figure S41. Protonation of **methanol cluster.** Ground state minimum and ground state transition state for proton transfer within a $(MeOH)_8H^+$ cluster calculated at B3LYP-D3/6-311+g(d,p) using SMD implicit solvation model and methanol as implicit solvent. The O–H bond lengths (in Å) involved in the proton transfer are also shown. The methanol cluster containing eight molecules of methanol was based conclusions drawn in reference 41 that this number corresponds to a saturated cluster with regard to the number of MeOH molecules.

Table S19. Vertical energies, adiabatic energies, and activation barriers, in kcal/mol, for **benzene**, **pyridinium ion**, and **silabenzene** optimized at SA-CASSCF(6,6)/ANO-RCC-VTZP level. Single point energies were computed at MS-CASPT2(6,6)/ANO-RCC-VTZP.

Energies (kcal/mol)	Benzene	Silabenzene	Pyridinium ion
SA-CASSCF(6,6)			
Vertical excitation	113.4	95.1	122.5
Adiabatic S_1 energy	108.1	78.4	117.4
S_1 Activation barrier	20.0	6.6	8.8
Adiabatic CI energy	127.1	85.0	126.1

MS-CASPT2(6,6)			
Vertical excitation	117.3	98.5	119.4
Adiabatic S_1 energy	112.9	93.6	114.2
S_1 Activation barrier	9.4	-3.5	-3.2
Adiabatic CI energy	120.2	89.9	111.0

Table S20. Electronic energies (in a.u.), configurations, and configuration weights for **silabenzene** in the S_0 and along of the puckering coordinate calculated at SA3-CASSCF(6,6)/ANO-RCC-VTZP level. Absolute energies at MS3-CASPT2(6,6)/ANO-RCC-VTZP level. The optimized state is shown in italics while the remaining states are single point calculations at the respective optimized geometry.

Optimized Geometry	State	SA-CASSCF	MS-CASPT2	Conf	weight	Conf	weight
S_0	*S_0*	*-482.544272*	*-483.422567*	*222000*	*0.80*		
	S_1	-482.392794	-483.265575	2u2d00	0.34	u220d0	0.40
S_1	S_0	-482.529189	-483.393063	222000	0.76		
	S_1	*-482.419347*	*-483.273376*	*2u2d00*	*0.46*	*u220d0*	*0.20*
TS	S_0	-482.415562	-483.294379	222000	0.58		
	S_1	-482.408812	-483.278886	2u2d00	0.74		
CI	S_0	-482.408836	-483.288959	222000	0.57		
	S_1	-482.408835	-483.279362	2u2d00	0.74		
C_{2v}[a)]	S_0	-482.540184	-483.418446	222000	0.78	u22d00	0.10
	S_1	*-482.397471*	*-483.269465*	*u220d0*	*0.40*	*2u2d00*	*0.32*

a) Optimized at B3LYP/6-311+G(d,p) level. Single point calculation at CASPT2//CASSCF level.

Table S21. Electronic energies (in a.u.), configurations, and configuration weights for **pyridinium ion** in the S_0 and along of puckering coordinate calculated at SA3-CASSCF(6,6)/ANO-RCC-VTZP level. Absolute energies at MS3-CASPT2(6,6)/ANO-RCC-VTZP level. The optimized state is shown in italics while the remaining states are single point calculations at the respective optimized geometry.

Optimized Geometry	State	SA-CASSCF	MS-CASPT2	Conf	weight	Conf	weight
S_0	*S_0*	*-247.335750*	*-248.244749*	*222000*	*0.90*		
	S_1	-247.140539	-248.054463	2u200d	0.59	22ud00	0.20
S_1[a)]	S_0	-247.327264	-248.238218	222000	0.88		
	S_1	*-247.148692*	*-248.062765*	*2u200d*	*0.59*	*22ud00*	*0.18*

TS	S_0				
	S_1	Not found			
CI	S_0	-247.134735	-248.076631	2u200d	0.85
	S_1	-247.134735	-248.067935	222000	0.83

a) At B3LYP/6-311+G(d,p) level S_1 minimum is puckered (C_s symmetric) and the planar structure (C_{2v}) has 2 imaginary frequencies corresponding to the out-of-plane vibrations.

Benzene	**Silabenzene**	**Pyridinium ion**
S_0 state 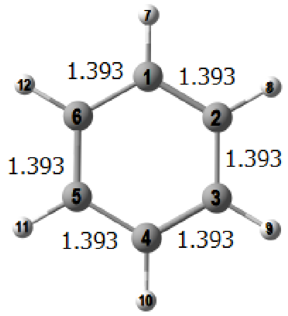 Angles (in degrees): C1-C2-C3 120.0 C2-C3-C4 120.0 C4-C5-C6 120.0 C6-C1-C2 120.0	S_0 state 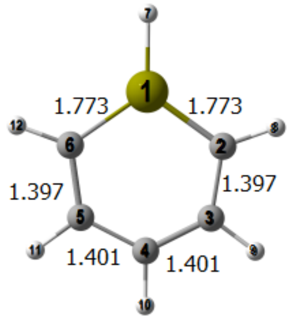 Angles (in degrees): Si1-C2-C3 116.8 C2-C3-C4 125.5 C4-C5-C6 125.7 C6-Si1-C2 109.6	S_0 state 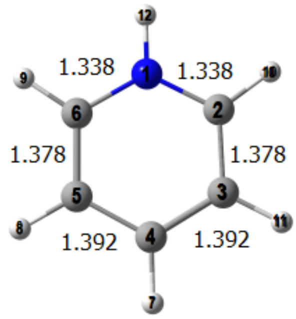 Angles (in degrees): N1-C2-C3 119.4 C2-C3-C4 118.9 C4-C5-C6 119.9 C6-N1-C2 123.5
S_1 state 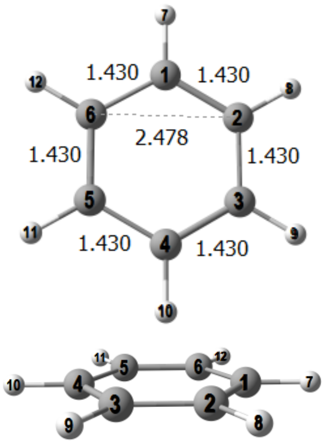 Angles (in degrees): C1-C2-C3 120.0 C2-C3-C4 120.0 C4-C5-C6 120.0 C6-C1-C2 120.0	S_1 state 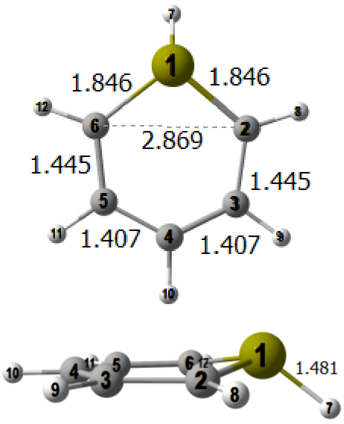 Angles (in degrees): Si1-C2-C3 120.7 C2-C3-C4 124.8 C4-C5-C6 125.2 C6-Si1-C2 101.9	S_1 state 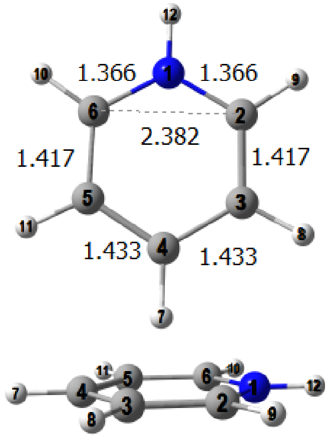 Angles (in degrees): N1-C2-C3 120.5 C2-C3-C4 120.4 C4-C5-C6 116.8 C6-C1-C2 121.4

<table>
<tr>
<td>TS in the S_1 PES
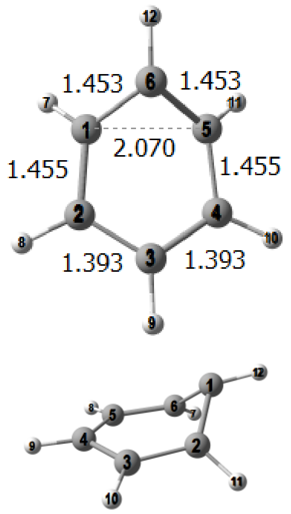
Angles (in degrees):
C1-C2-C3 120.4
C2-C3-C4 117.5
C4-C5-C6 113.9
C6-C1-C2 90.9</td>
<td>TS in the S_1 PES
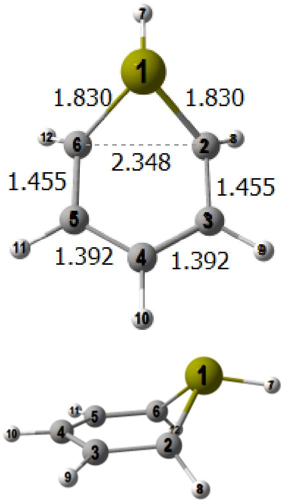
Angles (in degrees):
Si1-C2-C3 121.2
C2-C3-C4 120.2
C4-C5-C6 117.7
C6-C1-C2 79.8</td>
<td>TS in the S_1 PES
Not found</td>
</tr>
<tr>
<td>S_1/S_0
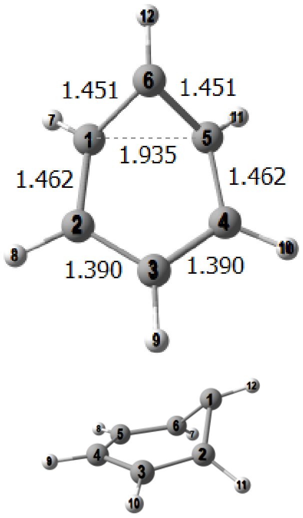
Angles (in degrees):
C1-C2-C3 120.6
C2-C3-C4 115.8
C4-C5-C6 112.9
C6-C1-C2 83.6</td>
<td>S_1/S_0
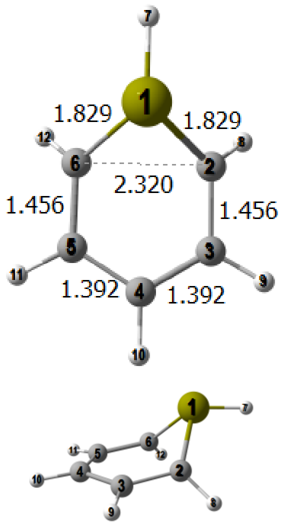
Angles (in degrees):
Si1-C2-C3 121.3
C2-C3-C4 119.9
C4-C5-C6 117.4
C6-C1-C2 78.7</td>
<td>S_1/S_0
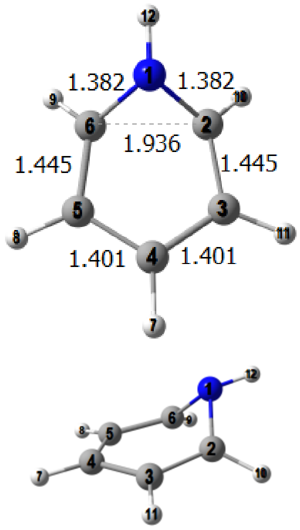
Angles (in degrees):
N1-C2-C3 120.2
C2-C3-C4 115.4
C4-C5-C6 112.8
C6-C1-C2 88.9</td>
</tr>
</table>

Figure S42. Bond lengths (in Ångstroms) and angles (in degrees) for benzene, silabenzene, and pyridinium ion in the S_0, S_1, TS, and CI. Geometries calculated at calculated at SA-CASSCF(6,6)/ANO-RCC-VTZP level.

Table S22. Cartesian coordinates of **silabenzene** in the S_0 state and along of puckering coordinate in the S_1 state (S_1 minimum, prefulvenic TS, and S_1/S_0 conical intersection) at SA3-CASSCF(6,6)/ANO-RCC-VTZP level. Absolute energies at MS3-CASPT2(6,6)/ANO-RCC-VTZP level.

Silabenzene in the S_0 state

E : -483.422567 a.u.

Si	0.00397010	0.00128188	0.00195789
C	-0.00225813	0.00345701	1.77476131
C	1.24191421	-0.00136847	2.40939506
C	2.48440445	-0.00861271	1.76314063
C	2.68489642	-0.01110276	0.37700159
C	1.67555585	-0.00810153	-0.58837460
H	-1.18847088	0.00402497	-0.84472580
H	-0.88323459	0.00907411	2.38766145
H	1.26140229	0.00027745	3.48509970
H	3.35952524	-0.01120865	2.38448087
H	3.70688610	-0.01620554	0.04078553
H	1.96374994	-0.00976476	-1.62218863

Silabenzene in the S_1 state

E : -483.273376 a.u.

Si	-0.09928873	-0.41136517	-0.06949249
C	-0.01686147	-0.09095587	1.74677910
C	1.25663499	0.00064969	2.42294650
C	2.50742218	0.02546843	1.77934031
C	2.70258695	-0.00881777	0.38648612
C	1.64399689	-0.10173672	-0.59235449
H	-1.08872693	0.43513478	-0.77584949
H	-0.89107193	-0.03603946	2.36884052
H	1.25514786	0.05688237	3.49537256
H	3.38030660	0.09662282	2.39878537
H	3.71480322	0.04084847	0.03122127
H	1.94339137	-0.05494058	-1.62308029

Silabenzene in the TS of S_1 state

E : -483.278886 a.u.

Si	0.21950127	-1.28276844	0.06046346
C	0.18656828	-0.13053037	1.48239935
C	1.33058944	0.00136183	2.37228464
C	2.62452699	-0.04504741	1.86143874
C	2.77390745	-0.04623444	0.47768201
C	1.60885117	-0.17736998	-0.38477970
H	-0.94726563	-1.08323695	-0.83334050
H	-0.64125389	0.53968151	1.64732963
H	1.16103478	0.15935570	3.42084923
H	3.47721265	0.00116982	2.50981670
H	3.74315236	0.07417888	0.03129551
H	1.56393321	0.46711659	-1.24751040

Imaginary frequency : 186.9*i* cm^{-1}

Silabenzene in S_1/S_0 conical intersection

E : -483.279362 a.u.

Si	0.22182186	-1.29194077	0.06248509
C	0.19511703	-0.12574054	1.47120995
C	1.33280650	0.00109195	2.37158183
C	2.62779990	-0.04715760	1.86402745
C	2.77377506	-0.04639221	0.47996336
C	1.60051817	-0.17204432	-0.37371852
H	-0.94579570	-1.10108554	-0.83175428
H	-0.62656528	0.55566450	1.62112295
H	1.15709959	0.15642319	3.41937299
H	3.48061191	-0.00662232	2.51265197
H	3.74056940	0.07130412	0.02794220
H	1.54299964	0.48417629	-1.22695630

Silabenzene in the S_1 state C_{2v} symmetric
(optimized at B3LYP/6-311+G(d,p))

E : -483.269465 a.u.

Si	0.00000000	0.00000000	1.39208000
C	0.00000000	1.44533000	0.36688000
C	0.00000000	1.24602000	-1.01823000
C	0.00000000	0.00000000	-1.65868000
C	0.00000000	-1.24602000	-1.01823000
C	0.00000000	-1.44533000	0.36688000
H	0.00000000	0.00000000	2.85562000
H	0.00000000	2.45641000	0.73413000
H	0.00000000	2.11588000	-1.65512000
H	0.00000000	0.00000000	-2.73452000
H	0.00000000	-2.11588000	-1.65512000
H	0.00000000	-2.45641000	0.73413000

Table S23. Cartesian coordinates of **pyridinium ion** in the S_0 state and along of the puckering coordinate in the S_1 state (S_1 minimum and S_1/S_0 conical intersection) at SA3-CASSCF(6,6)/ANO-RCC-VTZP level. Absolute energies at MS3-CASPT2(6,6)/ANO-RCC-VTZP level.

Pyridinium ion in the S_0 state

E : -248.244749 a.u.

C	1.37611153	-0.00000099	0.00000001
C	0.67900930	-1.20496279	-0.00000001
C	-0.69911538	-1.17814263	0.00000001
N	-1.33256409	0.00000065	-0.00000002
C	-0.69911464	1.17814382	0.00000002
C	0.67900984	1.20496233	-0.00000001
H	2.44736419	-0.00000018	0.00000003
H	1.18689626	-2.14643290	-0.00000003
H	-1.31269980	-2.05417369	0.00000005
H	-1.31270172	2.05417288	0.00000007
H	1.18689565	2.14643301	-0.00000004
H	-2.33150614	0.00000048	-0.00000008

Pyridinium ion in the S_1 state

E : -248.062765 a.u.

C	1.45036753	0.00000296	-0.00000008
C	0.69956644	-1.22011441	0.00000003
C	-0.71748448	-1.19097839	-0.00000000
N	-1.38553153	-0.00000238	0.00000001
C	-0.71748231	1.19097211	-0.00000004
C	0.69956712	1.22012132	0.00000009
H	2.51670444	0.00000031	-0.00000026
H	1.17599244	-2.17690049	0.00000015
H	-1.32278721	-2.07197491	-0.00000005
H	-1.32278342	2.07197008	-0.00000021
H	1.17600068	2.17690414	0.00000030
H	-2.38454467	-0.00000034	0.00000007

Pyridinium ion in the S_1/S_0 conical intersection

E : -248.067935 a.u.

C	1.48749814	0.02316709	0.14479044
C	0.74222781	-1.15579705	0.00945472
C	-0.68932500	-0.97871246	-0.07313844
N	-1.31715011	-0.02051358	0.69971867
C	-0.71946820	0.95677043	-0.07313845
C	0.70587308	1.17834959	0.00945494
H	2.54932448	0.03970564	0.25950056
H	1.15545589	-2.13334780	-0.12364239
H	-1.31620754	-1.65223215	-0.62661628
H	-1.36701942	1.61044147	-0.62661664
H	1.08845754	2.16829438	-0.12364199
H	-2.31741661	-0.03609153	0.67145756

Table S24. Electronic configurations and configuration weights for the S_1 vertical and S_1 minimum and activation barriers (in kcal/mol) from the S_1 state minimum at CASSCF and CASPT2/CASSCF levels.

Molecule	State	Conf	weight	Conf	weight	ΔE CASSCF	ΔE CASPT2
Benzene	S_1*vert*	2u2d00	0.40	u2200d	0.40		
	S_1 *min*	2u200d	0.38	u22d00	0.38	20.0	9.4
Silabenzene	S_1*vert*	u220d0	0.40	2u2d00	0.34	6.6	-3.5
	S_1 *min*	2u2d00	0.46	u220d0	0.20		
Pyridinium ion	S_1*vert*	2u200d	0.59	22ud00	0.20	8.8	-3.2
	S_1 *min*	2u200d	0.59	22ud00	0.18		
TMS-benzene	S_1*vert*	2u2d00	0.43	22u0d0	0.35		
	S_1 *min*	2u2d00	0.42	22u0d0	0.34	16.4 –18.5	7.6 – 9.7
t-Bu-benzene	S_1*vert*	22ud00	0.41	2u20d0	0.37		
	S_1 *min*	2u2d00	0.40	22u0d0	0.36	15.0 – 18.5	7.9 – 10.0

Table S25. Vertical and adiabatic (min-min) excitation energies (in kcal/mol) in the gas phase calculated for **benzene**, **TMS-benzene** and ***t*-Bu-benzene** at B3LYP/6-311+G(d,p) and MS-CASPT2(6,6)/ANO-RCC-VDZP//SA-CASSCF(6,6)/ANO-RCC-VDZP levels. For benzene, the results calculated with ANO-RCC-VTZP basis set are also shown (in italics).

Molecule	**TD-DFT**	**TD-DFT**	**MS-CASPT2**	**MS-CASPT2**
	ΔE (S_1-S_0)	**ΔE (S_1-S_0)**	**ΔE (S_1-S_0)**	**ΔE (S_1-S_0)**
	vertical	**min-min**	**vertical**	**min-min**
Benzene	124.2	121.3	118.4	113.4
			117.3	*113.0*
t-Bu-benzene	122.1	119.1	117.6	112.7
TMS-benzene	121.0	118.0	116.1	111.4

Table S26. Activation barriers, ΔE (without ZPE corrections) and ΔG, in kcal/mol, in the S_1 states of **benzene**, **TMS-benzene** and ***t*-Bu-benzene** in the gas phase. For substituted benzene, the four possible TS structures were considered as shown in Figure S43 and Figure S44**.** The calculations were performed at MS-CASPT2(6,6)/ANO-RCC-VDZP//SA-CASSCF(6,6)/ ANO-RCC-VDZP level using, respectively, four and three states in the state-average for benzene and substituted benzene. For benzene, the results obtained with the ANO-RCC-VTZP basis set are also shown (italics).

Molecule	**Prefulvene 1**		**Prefulvene 2**		**Prefulvene 3**		**Prefulvene 4**	
	Δ*E*	Δ*G*	Δ*E*	Δ*G*	Δ*E*	Δ*G*	Δ*E*	Δ*G*
Benzene	9.9	19.9						
	9.4	*20.7*						
t-Bu-benzene	7.9	15.0	8.9	18.8	8.5	17.8	10.0	18.8
TMS-benzene	8.1	13.4	7.6	17.0	9.7	16.2	9.6	17.5

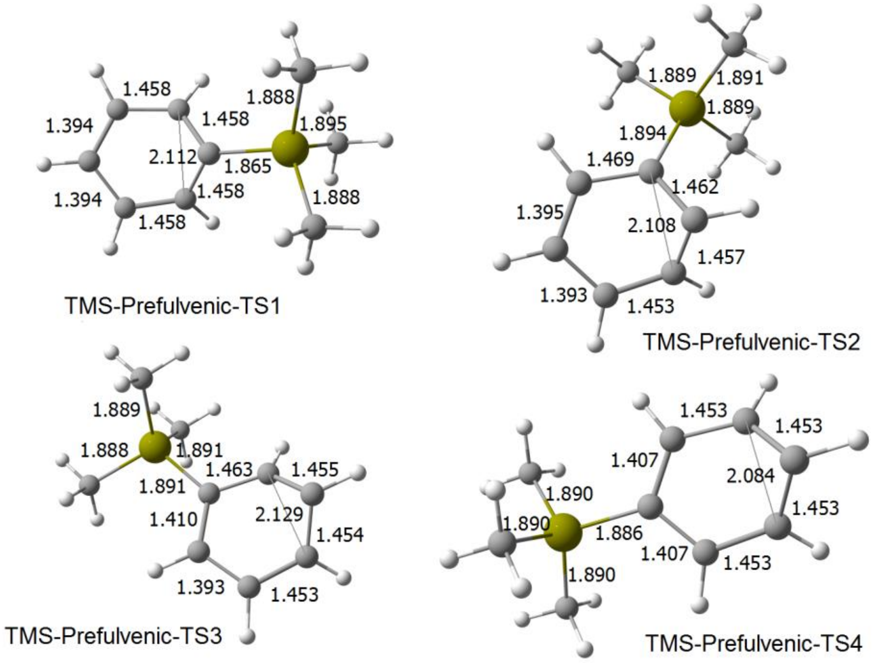

Figure S43. Optimized transition state structures, C – C, and C – Si bond lengths for the S_1 state of **TMS-benzene** showing the TMS group at different positions. Calculations at SA3-CASSCF(6,6)/ANO-RCC-VDZP level.

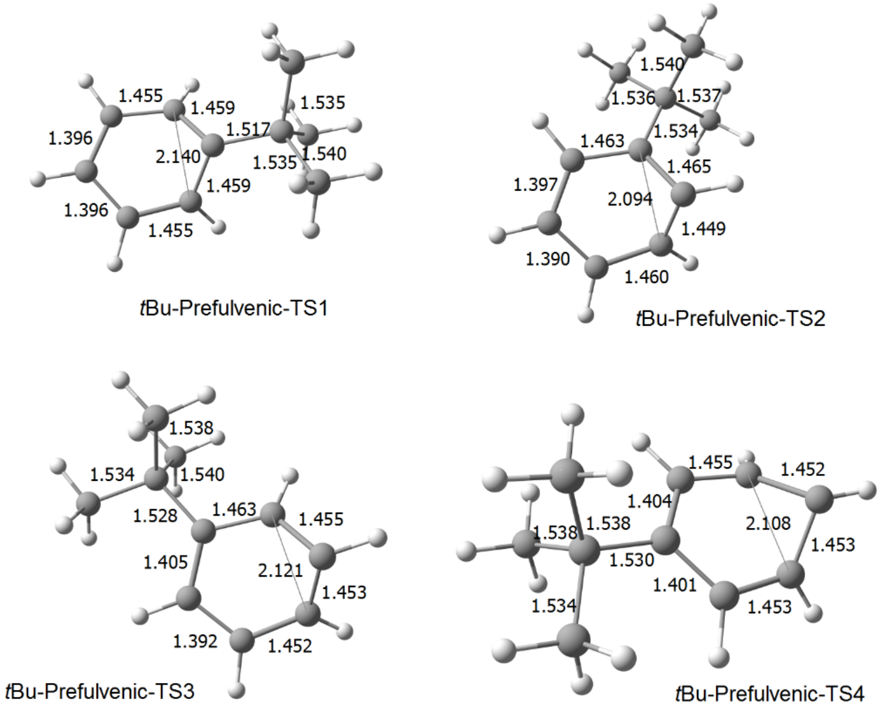

Figure S44. Optimized transition state structures and C – C bond lengths for the S_1 state of ***t*Bu-benzene** showing the *t*-Bu group at different positions. Calculations at the SA3-CASSCF(6,6)/ANO-RCC-VDZP level.

Table S27. Cartesian coordinates for **TMS-benzene** in the S_0 and S_1 states and the prefulvenic transition state in S_1 calculated with SA3-CASSCF(6,6)/ANO-RCC-VDZP. Absolute energies at MS3-CASPT2(6,6)/ANO-RCC-VDZP level.

TMS-benzene in the S_0 state

E : -640.16262487 a.u.

C	0.41542099	0.21256595	0.00340498
C	1.12402769	0.02125047	1.20087832
C	2.47689288	-0.31890998	1.20157254
C	3.15781862	-0.47688987	-0.00300889
C	2.47654205	-0.29236096	-1.20837466
C	1.12730186	0.04677873	-1.19910295
H	0.62288375	0.13688526	2.14520221
H	2.99275992	-0.45885988	2.13480310
H	4.20047308	-0.73901450	-0.00589227
H	2.99344371	-0.41205645	-2.14378289
H	0.62572180	0.18324568	-2.14222663
Si	-1.42509044	0.67567783	-0.02907538
C	-2.09258586	0.82418151	1.73219532
H	-3.14770796	1.08972487	1.70852224
H	-2.00297142	-0.11138861	2.27935391
H	-1.57403528	1.59463257	2.29807124
C	-1.63863347	2.32956162	-0.91890015
H	-1.26769643	2.28547654	-1.94039017
H	-2.68784106	2.61537632	-0.96157123
H	-1.09778614	3.12220613	-0.40668521
C	-2.39074641	-0.66184401	-0.95171303
H	-2.29171124	-1.62639705	-0.45876830
H	-3.45014217	-0.41655345	-0.99483446
H	-2.03776318	-0.77735709	-1.97398452

TMS-benzene minimum in the S_1 state

E : -639.98512393 a.u.

C	0.40262916	0.26627669	-0.01831646
C	1.12157365	0.05681491	1.21844620
C	2.50150891	-0.32971611	1.23494863
C	3.21172745	-0.52134551	0.01208981
C	2.53013788	-0.32268423	-1.22586074
C	1.15012807	0.06382187	-1.23917604
H	0.62015323	0.19541361	2.15769571
H	2.99966333	-0.47370282	2.17511397
H	4.24489849	-0.81061827	0.02327743
H	3.05001552	-0.46130978	-2.15500335
H	0.67064686	0.20770572	-2.18905649
Si	-1.43436081	0.68632999	-0.03938126
C	-1.88312790	1.68013171	1.50507474
H	-2.93216658	1.96846135	1.47449957
H	-1.73131981	1.10820039	2.41730636
H	-1.29137642	2.58963136	1.57972328
C	-1.84059717	1.71032098	-1.57590890
H	-1.66258846	1.15660593	-2.49462296
H	-2.89033563	1.99765297	-1.56927966
H	-1.24769650	2.62125233	-1.61591461
C	-2.46343881	-0.90082185	-0.06943270
H	-2.26393600	-1.51555291	0.80571591
H	-3.52891566	-0.67849472	-0.08333754
H	-2.23771458	-1.49930918	-0.94946283

TMS-Prefulvenic-TS1 in the S_1 state

E : -639.97220041 a.u.

C	-0.29396273	0.09561514	0.00000110
C	-1.16986137	-0.39886650	-1.05612854
C	-2.55153792	0.05141188	-1.17091596
C	-3.23138689	0.38508492	-0.00001991
C	-2.55154688	0.05149288	1.17090444
C	-1.16986865	-0.39879176	1.05615908
H	-0.82279975	-1.15431369	-1.74379520
H	-3.02357057	0.06762804	-2.13645724
H	-4.22670476	0.78637251	-0.00003748
H	-3.02358771	0.06777288	2.13644064
H	-0.82281193	-1.15419023	1.74388176
Si	1.57149631	0.08485547	0.00000027
C	2.17211809	0.97927803	-1.55093027
H	3.25932572	1.00270055	-1.59175228
H	1.82022578	0.48583859	-2.45450564
H	1.81488166	2.00617126	-1.57531656
C	2.17212638	0.97923349	1.55095343
H	1.82025740	0.48575702	2.45451760
H	3.25933433	1.00267187	1.59175810
H	1.81487455	2.00612039	1.57538116
C	2.26720837	-1.67810963	-0.00002970
H	1.94419204	-2.23378784	-0.87807125
H	3.35581411	-1.66783386	-0.00004152
H	1.94421045	-2.23381113	0.87800393

Imaginary frequency : 356*i* cm^{-1}

TMS-Prefulvenic-TS2 in the S_1 state

E : -639.97299881 a.u.

C	0.43252725	1.22352711	0.85266300
C	1.64349684	1.27998908	0.03546568
C	2.41216301	2.53124941	0.07729451
C	1.71914518	3.73781412	0.17954364
C	0.33615294	3.61734048	0.06309515
C	-0.21569092	2.27345341	0.07729739
H	-0.08036557	0.28534324	0.98232126
H	3.48212537	2.50266600	-0.01749975
H	2.21666048	4.68607126	0.25607258
H	-0.31143998	4.46296407	-0.07913222
H	-1.07356530	2.04641211	-0.53330518
Si	2.13263829	-0.18480564	-1.06114231
C	2.50046813	-1.67244635	0.04714882
H	1.63679693	-1.94529757	0.64931079
H	2.77466786	-2.54155524	-0.54797385
H	3.32286781	-1.46303127	0.72766350
C	3.67612612	0.24456002	-2.06232125
H	4.52689823	0.46129243	-1.42020834
H	3.95493429	-0.59076263	-2.70178997
H	3.51103463	1.10932126	-2.70066719
C	0.72104112	-0.62907207	-2.23572628
H	0.98033033	-1.49975512	-2.83536390
H	-0.19091075	-0.86460987	-1.69195097
H	0.50065938	0.19096812	-2.91473489

Imaginary frequency : 255*i* cm^{-1}

TMS-Prefulvenic-TS3 in the S_1 state

E : -639.9696909 a.u.

C	0.33466349	1.04045856	-0.17358021
C	1.62921239	1.46792858	-0.68125265
C	2.48153093	2.38882600	0.07180734

TMS-Prefulvenic-TS4 in the S_1 state

E : -639.96984094 a.u.

C	0.75587414	0.98038199	0.59324325
C	1.39402609	1.39989185	-0.64230489
C	2.17296942	2.62570269	-0.69488724

C	1.79234501	3.33538572	0.85795441
C	0.41622736	3.41168503	0.65868724
C	-0.21732654	2.38529040	-0.15221640
H	-0.19805397	0.27454073	-0.71068336
H	1.94660976	1.13913127	-1.65735537
H	2.30152514	4.02068374	1.50876522
H	-0.17516537	4.21743591	1.05498676
H	-1.04854187	2.64790021	-0.78504865
Si	4.36575709	2.26949109	-0.04294245
C	4.93605706	0.60155483	0.63628699
H	4.65414028	0.48546273	1.68032936
H	4.49305224	-0.22305664	0.08232756
H	6.01781660	0.50227098	0.56966597
C	5.15382889	3.66428174	0.95603728
H	4.89303020	3.60150832	2.00989091
H	6.23834320	3.61056694	0.88356359
H	4.84728087	4.64213247	0.59231335
C	4.88860288	2.41501459	-1.85406788
H	5.97162029	2.35698528	-1.94518157
H	4.46756222	1.61725507	-2.46149799
H	4.56921726	3.36229058	-2.28248410

Imaginary frequency : 337*i* cm^{-1}

C	1.79677931	3.71220150	0.11565756
C	0.54473188	3.49319036	0.71848335
C	-0.06586391	2.17768619	0.62493030
H	0.26882395	0.02091773	0.62103763
H	1.27078415	0.81893053	-1.54144576
H	2.98495451	2.68772762	-1.39705764
H	-0.00628253	4.28138549	1.19946217
H	-1.13815628	2.10236740	0.54959689
Si	2.79552858	5.30274246	0.29040277
C	3.98745671	5.16603428	1.75061865
H	3.44988882	4.99396710	2.68062029
H	4.68049133	4.33855088	1.61473496
H	4.57373128	6.07549600	1.86826865
C	3.78734936	5.60440847	-1.29042212
H	4.34506527	6.53593307	-1.21561088
H	4.50717423	4.81014761	-1.47455087
H	3.13876050	5.67525057	-2.16067313
C	1.62368313	6.75690377	0.58355505
H	0.90882369	6.86296436	-0.22931126
H	1.06278927	6.64477466	1.50860912
H	2.18451910	7.68676736	0.65560417

Imaginary frequency : 356*i* cm^{-1}

Table S28. Cartesian coordinates for ***t*Bu-benzene** in the S_0 and S_1 states, and the prefulvenic transition state structure in S_1 calculated with SA3-CASSCF(6,6)/ANO-RCC-VDZP. Absolute energies at MS3-CASPT2(6,6)/ANO-RCC-VDZP level.

***t*Bu-benzene in the S_0 state**

E : -388.51489601 a.u.

C	-2.42468118	1.36079246	-0.01549959
C	-1.02021456	1.35033833	0.03743874
C	-0.37419536	2.58645995	0.09768955
C	-1.09428667	3.78738301	0.10537091
C	-2.48242904	3.77497439	0.05273005
C	-3.14705728	2.55232887	-0.00808180
H	-2.96748103	0.43541676	-0.06296514
H	0.69557355	2.64115834	0.13960157
H	-0.56349527	4.72136607	0.15257972
H	-3.03621442	4.69645881	0.05847063
H	-4.22122094	2.52317397	-0.04938700
C	-0.26539559	0.00951707	0.02587714
C	-0.58741964	-0.75272411	-1.27095782
H	-0.05528459	-1.70012776	-1.29635526
H	-1.64653459	-0.96818023	-1.36266428
H	-0.29035935	-0.17704948	-2.14310524
C	-0.69498662	-0.83615053	1.23701423
H	-0.16039314	-1.78242431	1.24745982
H	-0.47975409	-0.31841036	2.16754897
H	-1.75636415	-1.05902826	1.22093056
C	1.25563688	0.19677928	0.09784008
H	1.63514549	0.76115164	-0.74844671
H	1.55866329	0.70401209	1.00875088
H	1.74245757	-0.77384308	0.08722901

***t*Bu-benzene minimum in the S_1 state**

E : -388.33534965 a.u.

C	-2.44845897	1.33985733	-0.02155610
C	-1.00969446	1.33129494	0.03722510
C	-0.34202847	2.61004967	0.10484692
C	-1.08483195	3.83980389	0.11363079
C	-2.51074259	3.82411336	0.05501108
C	-3.19488840	2.57065170	-0.01294244
H	-2.99017547	0.41588760	-0.07306784
H	0.72600475	2.66341587	0.14973783
H	-0.55784901	4.77373282	0.16457258
H	-3.06411800	4.74391201	0.06150949
H	-4.26693223	2.54153234	-0.05766881
C	-0.25820163	-0.00460450	0.02567302
C	-0.58347335	-0.77319142	-1.27068003
H	-0.05144833	-1.72015774	-1.29485771
H	-1.64202519	-0.99009504	-1.35921639
H	-0.28876530	-0.20055539	-2.14462623
C	-0.68453219	-0.85197645	1.24105953
H	-0.15996092	-1.80342164	1.24406763
H	-0.45468887	-0.33938475	2.17002622
H	-1.74769417	-1.06417438	1.23516222
C	1.26583711	0.18242314	0.09299511
H	1.64194534	0.74575716	-0.75474887
H	1.57094797	0.69085350	1.00176286
H	1.75362947	-0.78703790	0.08242458

***t*Bu-Prefulvenic-TS1 in the S_1 state**

E : -388.32279877 a.u.

C	0.16146768	0.84778902	0.64897859
C	1.46452347	0.95575081	0.00165690
C	2.25250528	2.17125226	0.14223967
C	1.57375840	3.38217188	0.28900448
C	0.19594662	3.30808775	0.07755941

***t*Bu-Prefulvenic-TS2 in the S_1 state**

E : -388.32117491 a.u.

C	0.34094544	0.97433083	0.45047627
C	1.63582855	0.99517286	-0.23426543
C	2.49771814	2.14744917	0.02845394
C	1.89948729	3.40039837	0.18615895
C	0.53632612	3.42596907	-0.08588517

C	-0.40759143	1.99062880	-0.05722545
H	1.82386427	0.18105872	-0.65551347
H	3.32418949	2.12015754	0.07624505
H	2.08226925	4.31180557	0.45995468
H	-0.41289211	4.18596146	-0.04128950
H	-1.22218263	1.86487039	-0.75132343
C	-0.57173197	-0.46857454	0.82496963
C	-0.89907753	-1.13718934	-0.52305417
H	-1.42306515	-2.07614914	-0.36267818
H	-1.53533125	-0.50853885	-1.13884080
H	0.00009634	-1.35717379	-1.09077485
C	0.30580630	-1.41643483	1.65444307
H	0.54980586	-0.97592781	2.61683330
H	-0.20930479	-2.35634870	1.83450411
H	1.23884863	-1.64276621	1.14704747
C	-1.87933786	-0.20849299	1.58593287
H	-2.54161548	0.44725552	1.02859455
H	-2.41002397	-1.13982670	1.76534907
H	-1.68226469	0.25779629	2.54692911

Imaginary frequency : 337*i* cm^{-1}

C	-0.11951233	2.13667550	-0.28219367
H	-0.25697178	0.08164347	0.43055954
H	3.56431268	2.03519091	0.04959497
H	2.46348278	4.28125622	0.42721742
H	-0.02760995	4.33673055	-0.16892155
H	-0.94992622	2.06371777	-0.96486179
C	2.10477766	-0.19857023	-1.07530747
C	2.38992743	-1.37929847	-0.12875424
H	1.50135422	-1.67096506	0.42211212
H	2.73386411	-2.24519223	-0.68906894
H	3.15894879	-1.12308615	0.59488446
C	3.38269073	0.12157116	-1.86423039
H	4.22928336	0.31144793	-1.21275008
H	3.64650871	-0.72190100	-2.49581029
H	3.24781137	0.98856322	-2.50399132
C	1.02235423	-0.61160276	-2.08601605
H	0.09151344	-0.88150336	-1.60042273
H	0.81567144	0.19464191	-2.78319479
H	1.35576875	-1.47411071	-2.65697133

Imaginary frequency : 270*i* cm^{-1}

***t*Bu-Prefulvenic-TS3 in the S_1 state**

E : -388.32175177 a.u.

C	0.70197164	1.12092846	0.56609178
C	1.99725577	1.22212065	-0.08822035
C	2.83134202	2.41495861	0.05451472
C	2.13178648	3.62519614	0.19570785
C	0.75938910	3.56047774	-0.03046160
C	0.14426030	2.25163286	-0.15595986
H	0.18248467	0.17887556	0.52514007
H	2.32872075	0.41828984	-0.72212901
H	2.61929202	4.56080260	0.38078058
H	0.15847653	4.44459499	-0.14321394
H	-0.68724561	2.11844986	-0.82792348
C	4.35099805	2.28857275	-0.03620248
C	4.84611589	1.23318398	0.96763661
H	4.58238201	1.51002983	1.98446160
H	4.41701913	0.25654941	0.76906942
H	5.92743020	1.13729423	0.91470045
C	5.04759840	3.61815879	0.27893291
H	4.79919318	3.97352502	1.27445006
H	6.12480804	3.48758888	0.23425136
H	4.78201553	4.39187423	-0.43425463
C	4.74775966	1.86155486	-1.46156486
H	5.82882453	1.78410554	-1.54339047
H	4.33070739	0.89631726	-1.72840166
H	4.40613289	2.58708933	-2.19412515

Imaginary frequency : 334*i* cm^{-1}

***t*Bu-Prefulvenic-TS4 in the S_1 state**

E : -388.31944652 a.u.

C	1.26144674	0.87049945	0.54295012
C	1.84306394	1.35189984	-0.69706542
C	2.54320139	2.62678269	-0.74129330
C	2.13245773	3.66364847	0.11209797
C	0.92751786	3.36705640	0.76343130
C	0.38550855	2.02265513	0.67048139
H	0.82028843	-0.11136916	0.55494570
H	1.70809077	0.80080347	-1.61310903
H	0.35683922	4.10755864	1.28935484
H	-0.68427867	1.89629557	0.64234889
C	2.89280539	4.98701931	0.22423392
C	2.18149612	5.96678531	1.16587649
H	2.75402088	6.88653013	1.24194182
H	1.19172300	6.22762627	0.80300106
H	2.07957487	5.55895555	2.16704469
C	4.30246378	4.72142791	0.77884848
H	4.25275111	4.26118772	1.76158786
H	4.86623325	4.05696176	0.13154213
H	4.86062568	5.65009730	0.86900261
C	3.00849165	5.64908047	-1.15918013
H	3.55207702	5.02640988	-1.86207909
H	2.02622887	5.84495873	-1.57985934
H	3.53765289	6.59563807	-1.08492182
H	3.33142756	2.75142295	-1.46027498

Imaginary frequency : 373*i* cm^{-1}

Table S29. Electronic energies (in a.u.), configurations, and configuration weights for **COT** at SA3-CASSCF(8,8)/ANO-RCC-VTZP level. Absolute energies at MS3-CASPT2(8,8)/ANO-RCC-VTZP level. The optimized state is shown in italics and the remaining states are single point energies from the optimized state.

Geometry	State	SA-CASSCF	MS-CASPT2	Conf	weight	Conf	weight
S_0, D_{8h} a)	*S_0*	*-307.838915*	*-309.004902*	*22220000*	*0.40*	*222ud000*	*0.40*
	S_1	-307.790473	-308.973939	22220000	0.39	22202000	0.39
	S_2	-307.731516	-308.963461	222ud000	0.93		
S_0, D_{2d} b)	*S_0*	*-307.859909*	*-309.034762*	*22220000*	*0.83*		
	S_1	-307.641484	-308.892022	222ud000	0.93		
	S_2	-307.624044	-308.814408	22202000	0.54		
S_1	S_0	-307.838911	-309.004935	22220000	0.33	22202000	0.33
	S_1	*-307.790481*	*-308.973916*	*22220000*	*0.39*	*22202000*	*0.39*
	S_2	-307.731679	-308.963946	222ud000	0.78		
T_1	*T_1*	*-307.816374*	*-308.994109*	*222uu000*	*0.81*		
	T_2	-307.711955	-308.881235	2u2u2000	0.18	22u2u000	0.18
	T_3	-307.711955	-308.881234	2u22u000	0.18	22uu2000	0.18

a) The D_{8h} symmetric structure is antiaromatic as evidenced by NICS (see the next section).
b) Geometry optimized at B3LYP/6-311+G(d,p) level. This structure is the global minimum for COT in the S_0 state.

Table S30. Electronic energies (in a.u.), configurations, and configuration weights for **COTH⁺** at SA3-CASSCF(6,7)/ANO-RCC-VTZP level. Absolute energies at MS3-CASPT2(6,7)/ANO-RCC-VTZP level. The optimized state is shown in italics and the remaining states are single point energies.

Geometry	State	SA-CASSCF	MS-CASPT2	Conf	weight	Conf	weight
S_0, C_{2v} a)	*S_0*	*-308.1626015*	*-309.3452757*	*2220000*	*0.871*		
	S_1	-308.0731349	-309.2695129	22ud000	0.810		
	S_2	-308.0285916	-309.2171277	2202000	0.507	2u2d000	0.17
S_0, HA b)	*S_0*	*-308.1626015*	*-309.3452757*	*2220000*	*0.87*		
	S_1	-308.0731349	-309.2695129	22ud000	0.81		
	S_2	-308.0285916	-309.2171277	2202000	0.51	2u2d000	0.17
S_1	S_0	-308.151338	-309.338617	2220000	0.86		
	S_1	*-308.082981*	*-309.280353*	*22ud000*	*0.81*		
	S_2	-308.041510	-309.233301	2202000	0.58	2u2d000	0.11
T_1	*T_1*	*-308.1193603*	*-309.3001756*	*22uu000*	*0.87*		
	T_2	-308.0480381	-309.2271692	2u2u000	0.65	22u00u0	0.20
	T_3	-308.0142358	-309.1915291	u22u000	0.64		

a) The C_{2v} symmetric structure is antiaromatic as evidenced by NICS (see the next section).
b) Geometry optimized at B3LYP/6-311+G(d,p) level. This structure is homoaromatic and it is the global minimum in the S_0 state.

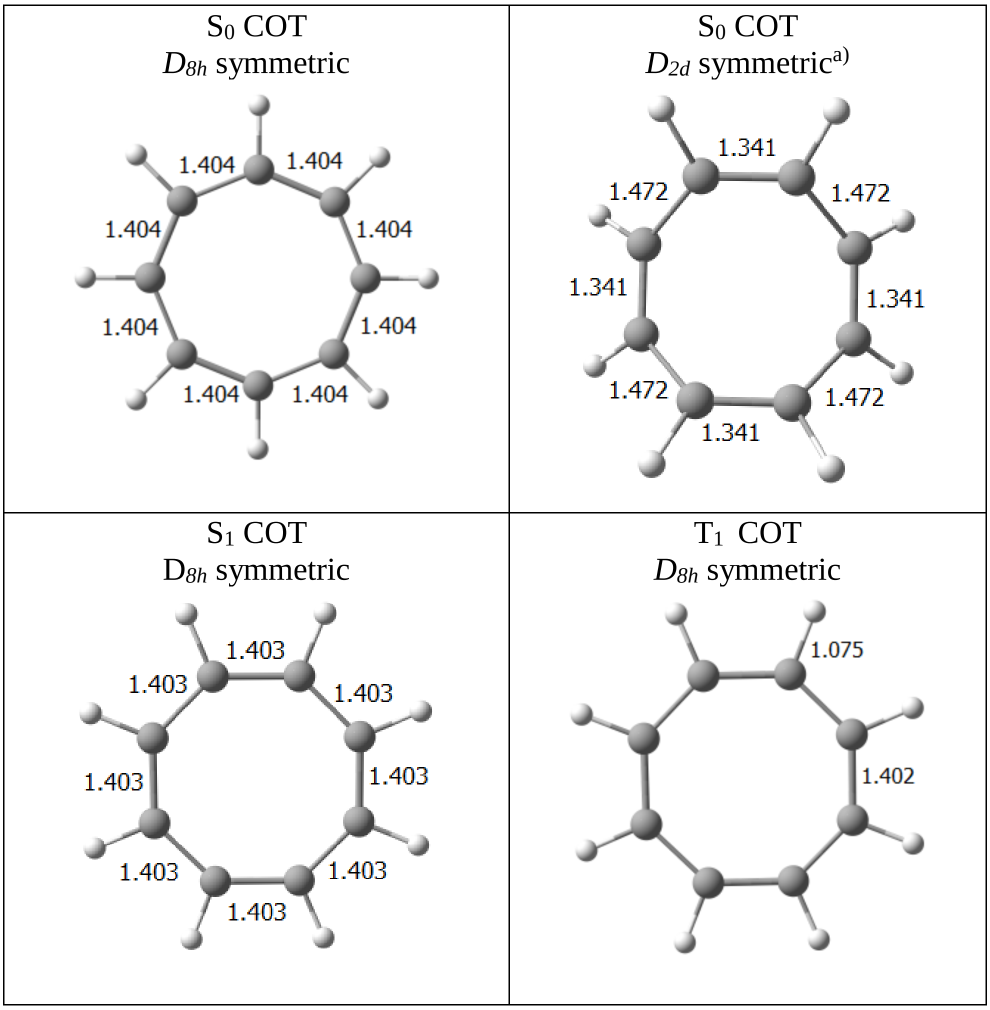

Figure S45. Optimized geometries for **cyclooctatetraene** (**COT**) in the S_0, S_1, and T_1 states optimized at SA3-CASSCF/ANO-RCC-VTZP level. [a] S_0 D_{2d} symmetric was optimized at B3LYP/6-311+G(d,p).

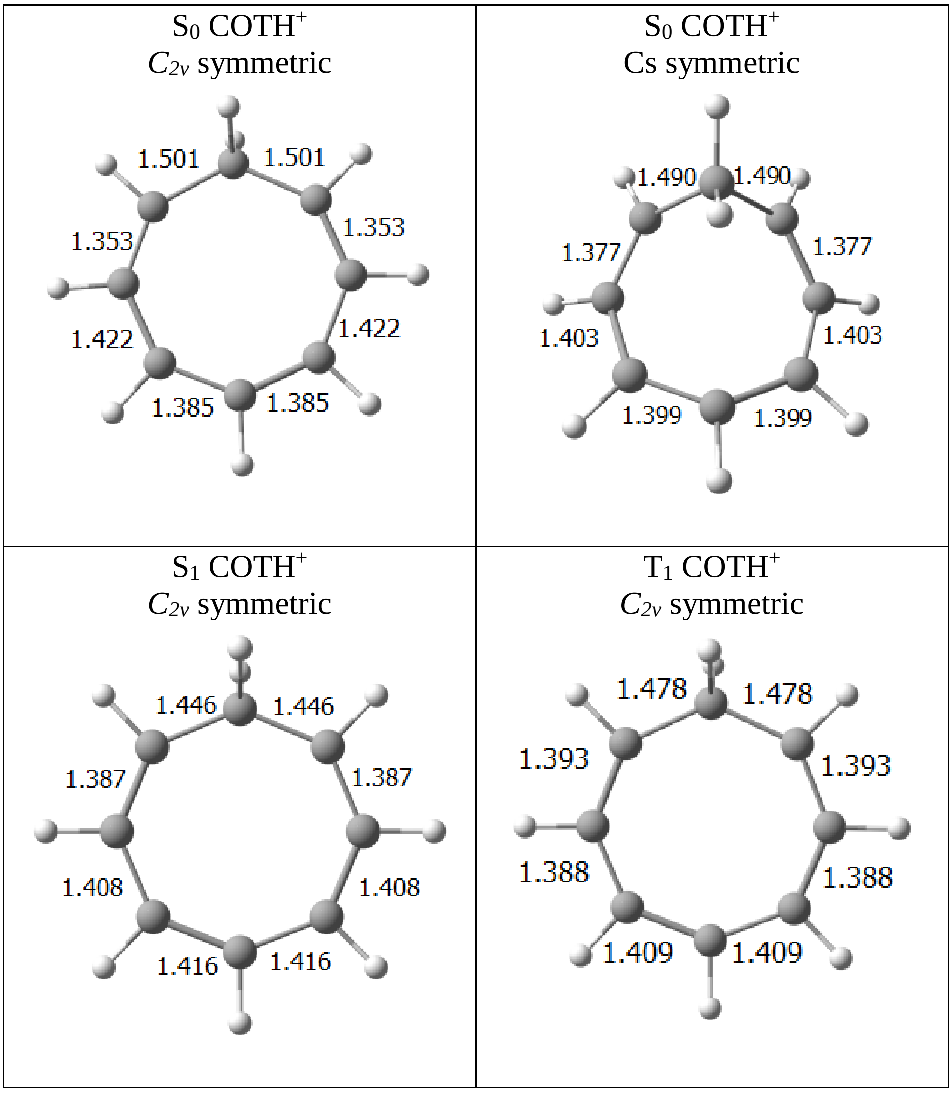

Figure S46. Optimized geometries for **protonated cyclooctatetraene** (**COTH$^+$**) in the S_0, S_1, and T_1 states optimized at SA3-CASSCF/ANO-RCC-VTZP level. [a)] S_0 C_s symmetric was optimized at B3LYP/6-311+G(d,p).

Table S31. Cartesian coordinates for **cyclooctatetraene** (**COT**) in the S_0, S_1, and T_1 states calculated at SA3-CASSCF(8,8)/ANO-RCC-VTZP and respective energies. The absolute energies are given at MS3-CASPT2(8,8)/ANO-RCC-VTZP level.

COT S_0 D_{8h} state

E : -309.00490189 a.u.

C	-1.29713112	1.29713230	-0.00000000
C	-0.00000034	1.83442179	0.00000000
C	0.00000047	-1.83442201	0.00000000
C	1.29713372	1.29713236	-0.00000000
C	1.29713124	-1.29713255	-0.00000000
C	1.83442208	0.00000110	0.00000000
C	-1.83442215	-0.00000073	-0.00000000
C	-1.29713376	-1.29713242	0.00000000
H	0.00000037	-2.90909007	0.00000000
H	2.05703637	-2.05703683	-0.00000000
H	2.90909019	0.00000059	0.00000000
H	2.05703758	2.05703775	-0.00000000
H	-0.00000023	2.90908980	0.00000000
H	-2.05703629	2.05703657	-0.00000000
H	-2.05703786	-2.05703758	-0.00000000
H	-2.90909025	-0.00000006	0.00000000

COT S_0 D_{2d} state (optimized at B3LYP/6-311+G(d,p) level)

E : -309.03476196 a.u.

C	-0.37388000	-0.67058000	1.56754000
C	-0.37388000	0.67058000	1.56754000
C	-0.37388000	-0.67058000	-1.56754000
C	0.37388000	1.56754000	0.67058000
C	-0.37388000	0.67058000	-1.56754000
C	0.37388000	1.56754000	-0.67058000
C	0.37388000	-1.56754000	0.67058000
C	0.37388000	-1.56754000	-0.67058000
H	-0.91859000	-1.17285000	-2.36589000
H	-0.91859000	1.17285000	-2.36589000
H	0.91859000	2.36589000	-1.17285000
H	0.91859000	2.36589000	1.17285000
H	-0.91859000	1.17285000	2.36589000
H	-0.91859000	-1.17285000	2.36589000
H	0.91859000	-2.36589000	1.17285000
H	0.91859000	-2.36589000	-1.17285000

COT S_1 state

E : -308.97391627 a.u.

C	-1.29627773	1.29627779	-0.00000000
C	-0.00000036	1.83321427	0.00000000
C	-0.00000026	-1.83321255	0.00000000
C	1.29627892	1.29627838	-0.00000000
C	1.29627858	-1.29627841	-0.00000000
C	1.83321494	0.00000050	-0.00000000
C	-1.83321412	-0.00000074	0.00000000
C	-1.29627995	-1.29627911	-0.00000000
H	-0.00000058	-2.90768508	0.00000000
H	2.05604458	-2.05604485	-0.00000000
H	2.90768747	0.00000002	0.00000000
H	2.05604490	2.05604510	0.00000000
H	0.00000016	2.90768665	-0.00000000
H	-2.05604436	2.05604381	-0.00000000
H	-2.05604562	-2.05604588	-0.00000000
H	-2.90768657	0.00000011	0.00000000

COT T_1 state

E : -308.99410912 a.u.

C	-1.29546180	1.29546171	-0.00000001
C	0.00000021	1.83205922	-0.00000000
C	-0.00000008	-1.83205890	-0.00000001
C	1.29546168	1.29546163	0.00000001
C	1.29546151	-1.29546171	-0.00000002
C	1.83205841	-0.00000067	0.00000000
C	-1.83205916	-0.00000000	0.00000000
C	-1.29546084	-1.29546137	0.00000002
H	0.00000095	-2.90668732	-0.00000002
H	2.05533759	-2.05533831	-0.00000006
H	2.90668685	-0.00000015	0.00000003
H	2.05533841	2.05533767	0.00000005
H	-0.00000087	2.90668765	-0.00000002
H	-2.05533762	2.05533869	-0.00000005
H	-2.05533773	-2.05533726	0.00000006
H	-2.90668751	-0.00000088	0.00000001

Table S32. Cartesian coordinates for **protonated cyclooctatetraene cation ($COTH^+$)** in the S_0, S_1, and T_1 states calculated at SA3-CASSCF(6,6)/ANO-RCC-VTZP and respective energies. For CASSCF geometries absolute energies are given at MS3-CASPT2(6,6)/ANO-RCC-VTZP level.

$COTH^+$ S_0 D_{8h} state

E : -309.3452757 a.u.

C	1.26986703	1.31107644	0.00000220
C	-0.00000008	1.86284728	0.00000260
C	0.00000007	-1.92790583	0.00000464
C	-1.26986740	1.31107682	0.00000030
C	-1.33932817	-1.24944599	-0.00000305
C	-1.83983760	0.00794082	-0.00000191
C	1.83983756	0.00794060	-0.00000372
C	1.33932838	-1.24944625	-0.00000414
H	0.00000117	-2.59432758	0.85616854
H	-2.11195836	-1.99786074	-0.00000641
H	-2.91183487	0.04378638	-0.00000751
H	-2.03215126	2.06904473	0.00000150
H	0.00000014	2.93506701	0.00000597
H	2.03215096	2.06904421	0.00000637

$COTH^+$ S_0 C_{2v} state (optimized at B3LYP/6-311+G(d,p) level)

E : -309.38985452 a.u.

C	0.14721000	1.42683000	0.00000000
C	1.16483000	0.47386000	-0.12045000
C	-1.45827000	-0.59324000	-1.69215000
C	1.10145000	-0.91886000	0.00000000
C	-1.19429000	-1.64530000	-0.67099000
C	0.00000000	-1.78868000	0.00000000
C	-1.24866000	1.28071000	0.00000000
C	-2.00369000	0.34433000	-0.67099000
H	-2.20458000	-0.89684000	-2.42267000
H	-1.98072000	-2.36982000	-0.48375000
H	0.13967000	-2.72939000	0.52685000
H	2.05090000	-1.38718000	0.24748000
H	2.16975000	0.88267000	-0.08620000

H	2.11195872	-1.99786091	-0.00000913
H	2.91183478	0.04378653	-0.00000770
H	-0.00000108	-2.59434138	-0.85614856

H	0.50009000	2.42495000	0.24748000
H	-3.07256000	0.31409000	-0.48375000
H	-1.80536000	2.05178000	0.52685000
H	-0.55461000	-0.22562000	-2.17632000

$COTH^+$ S_1 state

E : -309.28035320 a.u.

C	1.312432420	1.311617210	-0.000052310
C	0.000000150	1.844370290	-0.000022680
C	-0.000000040	-1.832817660	0.000058230
C	-1.312432400	1.311616950	0.000002580
C	-1.329021990	-1.261811510	0.000042180
C	-1.866202430	0.016832760	0.000004720
C	1.866202340	0.016832820	0.000038150
C	1.329021830	-1.261811410	0.000090300
H	-0.000004000	-2.558936700	0.829864800
H	-2.070567400	-2.039017130	-0.000004710
H	-2.939161830	0.016381240	0.000015350
H	-2.064364120	2.076002410	0.000013710
H	0.000000040	2.916416710	-0.000017160
H	2.064364310	2.076002600	-0.000099770
H	2.070567360	-2.039016960	0.000165180
H	2.939161730	0.016381170	-0.000040500
H	0.000004060	-2.558620640	-0.830058060

$COTH^+$ T_1 state

E : -309.30017557 a.u.

C	1.31119789	1.30837836	-0.00000164
C	-0.00000086	1.82418312	-0.00001114
C	0.00000014	-1.89066291	-0.00000800
C	-1.31119856	1.30837846	-0.00000281
C	-1.33836565	-1.26306570	0.00000813
C	-1.85330041	0.03094043	0.00000975
C	1.85330107	0.03094009	0.00000974
C	1.33836634	-1.26306630	0.00000955
H	-0.00000052	-2.57557916	0.84968722
H	-2.10224647	-2.01759316	0.00001353
H	-2.92701113	0.04269736	0.00001308
H	-2.05228304	2.08331155	-0.00000452
H	-0.00000001	2.89869522	-0.00001976
H	2.05228271	2.08331138	-0.00000472
H	2.10224675	-2.01759415	0.00001214
H	2.92701177	0.04269755	0.00001570
H	-0.00000003	-2.57555001	-0.84972625

7.6 Rationalization of the barrier in the S_1 state

Table S24 above shows the electron configurations of the S_1 states and their respective weights at the vertically excited and at the minima of the investigated molecules. As mentioned in the main text, due its high symmetry (D_{6h}) benzene in the S_1 state (the 1^1B_{2u} state) is described by two degenerate configurations of equal weights in an in-phase coupling. The out-of-phase coupling of the two configurations contributes to the $^1E_{1u}$ state which is of higher energy. Thus, the splitting between the $^1B_{2u}$ and $^1E_{1u}$ states reflects the strengths of the coupling between the two configurations, and as pointed by Sobolewski *et al.*,[50] it stabilizes the S_1 state of benzene at its D_{6h} minimum. However, as there is a symmetry reduction along the reaction coordinate the energies of the two configurations become unequal and as a consequence the weights of the two configurations describing the S_1 state (the former $^1B_{2u}$ state) become unequal.

Silabenzene and the pyridinium ion have lower symmetry (their highest symmetry is C_{2v}), and as a consequence, the two configurations have *per se* different weights at their S_1 state minimum geometries. Thus, as seen in **Table S24** the difference in weights between the two configurations increases as one goes from silabenzene to the pyridinium ion. The stabilizing in-phase coupling between the two configurations in the S_1 state should be smaller in silabenzene and the pyridinium ion than in benzene, and as a result, the activation barrier will be lower or even negligible. The different in the weights in the S_1 states of the two substituted benzenes (TMS-benzene and *t*Bu-benzene) is smaller than in the two heterocycles, yet, it is still noticeable. Of the two substituted benzenes, the difference in weights of the configurations is slightly larger for TMS-benzene.

This explains the reduced activation barriers for TMS-benzene and *t*-Bu benzene, and the lack of activation barriers for silabenzene and the pyridinium ion. Thus, it seems that the larger barrier in benzene is an effect of the stabilization created by the two degenerated configurations at D_{6h} symmetry: while the avoided crossing creates a barrier, the presence of two degenerated configurations at the D_{6h} dictates the height of the barrier.

7.7 Aromaticity index (NICS(1)$_{zz}$, MCI and FLU values)

Table S33. NICS(1)$_{zz}$ values for benzene in the S_1 and S_0 states computed at the CASSCF/6-311++G(d,p)//CASSCF/ANO-RCC-VTZP level.

State	Geometry	NICS(1)$_{zz}$
S_0	S_0 min	-27.4
S_1	S_0 min	99.5
S_1	S_1 min	80.9
S_0	S_1 min	-25.5
TS-S_1 a)	TS in S_1	-21.2
“TS”-S_0 a)	TS in S_1	-10.0

a) The structure that corresponds to the CASSCF maximum on the S_1 state potential energy surface. See Figure 4.

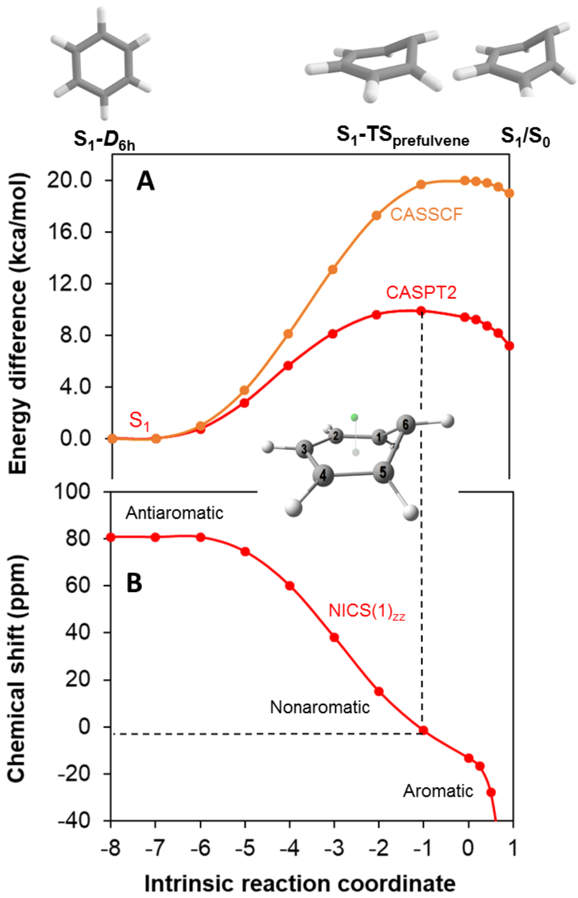

Figure S47. (A) Intrinsic reaction coordinate for benzene from the planar S_1 state minimum (D_{6h} symmetry) to the S_1/S_0 conical intersection. (B) The corresponding NICS(1)$_{zz}$ values towards the upper direction, as shown in the inserted picture. Geometries calculated at SA4-CASSCF(6,6)/ANO-RCC-VTZP level and energies obtained at MS4-CASPT2(6,6)/ANO-RCC-VTZP level and NICS(1)$_{zz}$ values at CASSCF(6,6)/6-31++G(d,p) level. It is noteworthy that the TS geometry optimization and IRC calculations were performed at SA4-CASSCF level and the respective energies were computed at MS4-CASPT2 level. This is the reason why the TS at the CASSCF level does not corresponds exactly to the maximum energy point at CASPT2 level.

Table S34 NICS(1)$_{zz}$ values (in ppm) for benzene, benzenium cation, COT, and COTH$^+$ computed at three different levels: B3LYP/6-311+G(d,p)//B3LYP/6-311+G(d,p), CASSCF/6-31++G(d,p)//B3LYP/6-311+G(d,p), and CASSCF/6-31++G(d,p)//SA-CASSCF/ANO-RCC-VTZP. Unrestricted wavefunction was used to compute the triplets and TD-DFT was used for the singlet geometries. The symmetry of each specie is given in parenthesis.

State	Level of calculation (NICS(1)$_{zz}$//geometry)	Benzene	Benzenium cation	COT	COTH$^+$
	B3LYP/B3LYP	-29.2	-14.1	6.2	36.4

		(D_{6h})	(C_{2v})	(D_{2d})	(C_{2v}, *i*)
					-27.4 (C_s, HA)
S_0	CASSCF/B3LYP	-27.3 (D_{6h})	-11.3 (C_{2v})	99.1 (D_{8h})	21.0 (C_{2v}, *i*)
				1.27 (D_{2d})	-5.5 (C_s,HA)
	CASSCF/CASSCF	-27.4 (D_{6h})	-10.8 (C_{2v})	99.1 (D_{8h})	20.1 (C_{2v})
S_1	CASSCF/B3LYP	83.2 (D_{6h})	27.6 (C_{2v}, *i*)	-26.3 (D_{8h})	-45.0 (C_{2v})
	CASSCF/CASSCF	80.9 (D_{6h})	24.0 (C_{2v})	-26.4 (D_{8h})	-42.6 (C_{2v})
T_1	B3LYP/B3LYP	66.9 (D_{2h}, AQ)	16.6 (C_{2v}, *i*)	-32.5 (D_{8h})	-13.3 (C_{2v})
			-5.3 (C_s, HA)		
	CASSCF/B3LYP	40.4 (D_{2h}, AQ)	12.1 (C_{2v}, *i*)	-25.6 (D_{8h})	-10.3 (C_{2v})
			-7.8 (C_s, HA)		
	CASSCF/CASSCF	49.7 (D_{2h} ,AQ)	11.4 (C_{2v})	-25.6 (D_{8h})	-9.6 (C_{2v})

HA = homoaromatic structure; AQ = antiquinoidal; *i* = structure presents imaginary frequency.

Table S35 NICS(1)$_{zz}$ values for the S_1 state of TMS-benzene, *t*-Bu benzene, toluene, and silylbenzene computed at CASSCF(6,6)/6-31++G(d,p) level at the geometries obtained with SA-CASSCF/ANO-RCC-VDZP for TMS-benzene and *t*-Bu-benzene and at SA-CASSCF/ANO-RCC-VTZP for benzene, pyridinium ion, and silabenzene.

NICS(1)$_{zz}$	**Benzene**	**Pyridinium ion**	**Silabenzene**	**TMS-benzene**	***t*-Bu-benzene**
S_1 vertical	99.5	113.3	99.3	97.0	97.1
S_1 minimum	80.9	91.2	33.0	78.8	79.0

Table S36 MCI and FLU computed for benzene, benzenium ion, COT, and $COTH^+$ at CASSCF/ANO-RCC-VTZP//B3LYP/6-311+G(d,p) level. Normalized values for MCI are shown in italics between parenthesis and given as $MCI^{1/n}$.[65]

		Benzene	**Benzenium ion**	**COT**	**$COTH^+$**
S_0	MCI	0.0429 *(0.592)* (D_{6h})	0.0034 *(0.388)* (C_{2v})	0.00053 *(0.389)* (D_{2d})	0.0217 *(0.578)* (C_s)
	FLU	0.0062	0.0284	0.0316	0.0278
S_1	MCI	0.0038 *(0.395)* (D_{6h})	*0.0166* *(0.505)* (C_{2v})	0.00353 *(0.493)* (D_{8h})	0.00061 *(0.396)* (C_{2v})
	FLU	0.0249	0.0392	0.0102	0.0218

*Larger MCI values and smaller FLU values (typically close to zero) indicates larger aromaticity character.

7.8 Approximate estimate of the S_1 state ESAA relief energy

The barrier in the S_1 state is a composite energy which we here consider as split into (*i*) one component representing the increase in strain in the σ-orbital framework when going from the hexagonal structure, which is ideal four six sp^2 hybridized C atoms, to a puckered structure, and (*ii*) one component that represents the energy relieved upon alleviation of ESAA. From our CASSCF calculations we observe that the C-C σ-orbitals are not involved in the excitation representing the S_1 state. Based on this we can conclude that the σ-strain in the puckered structure of the S_1 state TS is the same in the S_1 and S_0 states. Now, if we assume that the benzene molecule in its S_0 state loses all its aromatic stabilization energy upon the puckering, then we can set the GSA loss to 36 kcal/mol.[66] Based on this value, together with the energy differences between the two structures in S_1 (84.3 kcal/mol) and in S_0 (9.4 kcal/mol), we can deduce in an approximate manner that the σ-strain energy equals ~53 kcal/mol and that the ESAA relief should be ~43 kcal/mol.

Moreover, in the S_1 state the ESAA relief when going from the S_1 state minimum to the S_1 transition state structure at CASSCF level is revealed through a change in the NICS(1)$_{zz}$ values from 80.9 ppm (strongly antiaromatic) to -21.2 ppm (aromatic). Indeed, a slight ESAA relief is already established when going from the vertically excited S_1 state structure (99.5 ppm) to the relaxed S_1 state structure. In contrast, when using the S_1 state minimum structure and the S_1 state TS structure for S_0 state NICS calculations we observe a significant aromaticity loss as the NICS(1)$_{zz}$ value changes from -25.5 ppm to -10.0 ppm. Interestingly, the S_0 state aromaticity loss according to NICS when going from the S_0 state minimum structure (-27.4 ppm) to the structure which is the optimum in the S_1 state is minute (ΔNICS = 1.9 ppm).

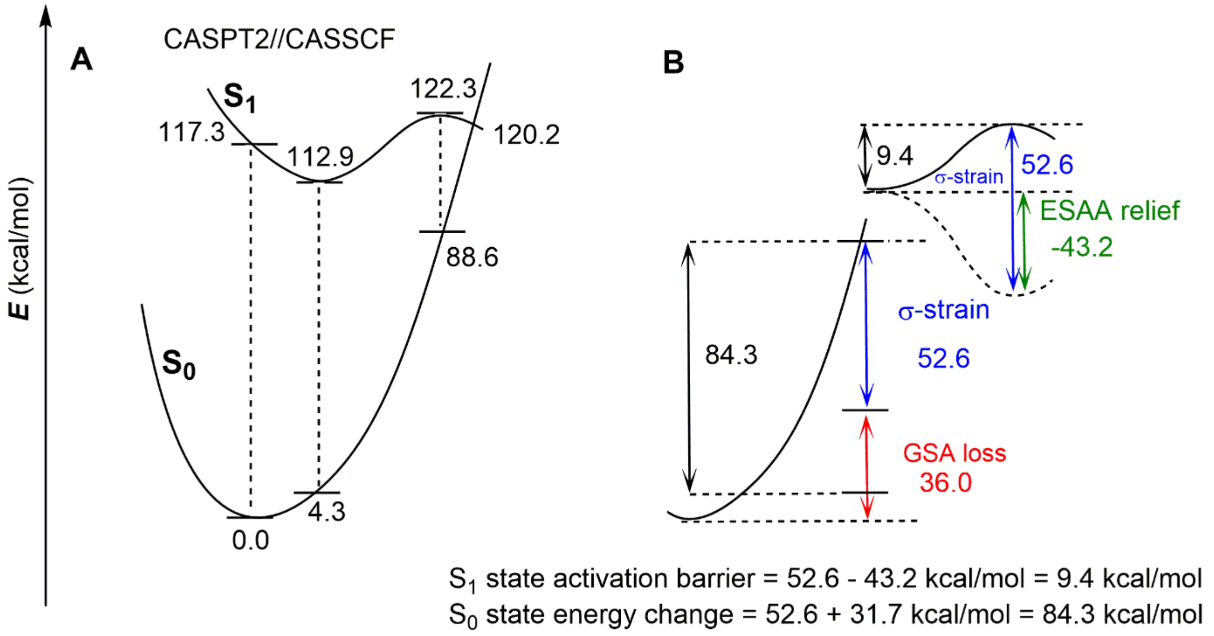

Figure S48. (A) Schematic drawing of the potential energy surfaces of benzene in the S_1 state and with the corresponding S_0 state energies as single-point energies at the S_1 state structures. Electronic energies at MS-CASPT2/ANO-RCC-VTZP//SA-CASSCF/ANO-RCC-VTZP level relative to the energy of the S_1 state minimum structure. (B) Estimation of the excited state antiaromaticity (ESAA) relief and σ-strain energies based on the calculated energy difference between the two structures in S_1 and S_0 as well as the ground state aromaticity (GSA) loss taken as the experimentally determined aromatic stabilization energy of benzene in the S_0 state, reported as 36 kcal/mol.[66]

7.9 Protonation of benzene and COT

Table S34 above shows the computed NICS(1)$_{zz}$ values for benzene, benzenium cation, COT, and COTH$^+$ computed at three different levels and respective symmetries of the species. First of all, one can notice the sensibility of NICS(1)$_{zz}$ values with the levels of calculation.[67] However, the overall behavior remains the same, *i.e.* ΔNICS(1)$_{zz}$ values (computed as the difference between protonated and non-protonated species at each state) are positive when aromaticity is lost and negative when aromaticity is gained under protonation. In this way, one can notice an inverse behavior for benzene and COT in the ground and excited states, also reflected in their proton affinities (**Table S37**). The only exception occurs for the protonation of COT in the S_1 state where one should expect a less negative value upon protonation. In fact, MCI values reveal the expected (opposite) behavior (**Table S36)** with a decrease in aromaticity after protonation. The outlying NICS(1)$_{zz}$ value could be attributed to an underestimated value of COT in the S_1 state due to methodological constraints (the S_1 state in COT is doubly excited (see **Table S29**) and (nearly)degenerated with the S_2 state). Noteworthy, when comparing the hydrogen isotropic shieldings between $C_6H_7^+$ in the S_0 and $COTH^+$ in the S_1 their ”equivalent” protons are shifted in the same direction and Mulliken charge distribution presents the same distribution pattern in both species indicating similar chemical environment.

Another feature to note is that for $COTH^+$ in the S_0 and benzenium cation in the T_1 state two NICS(1)$_{zz}$ values are given and associated with two different geometries. One can see dramatic changes in their NICS(1)$_{zz}$ values, going from positive to negative values. The reason is that these molecules become homoaromatic (HA), *i.e.*, they present cyclic through-space conjugation, as already investigated by Jorner *et. al*.[68] and represented in **Figure S49.** Based on the similarities with the T_1 state (minimum energy structure is puckered with similar C---C through-space distance, imaginary frequency at C_{2v} symmetric structure), one can argue that the benzenium cation in its S_1 state is also homoaromatic. However, for methodologic limitations, it is impossible to obtain the NICS(1)$_{zz}$ value for this species as it is located very close to the conical intersection, *i.e.*, it would need a state-average description which is not available in the Dalton program.

Benzenium ion S_1, C_{2v}	**Benzenium ion T_1, C_{2v}**	**$COTH^+$ S_0, C_{2v}**
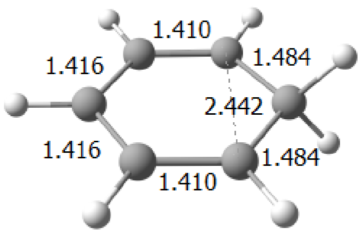	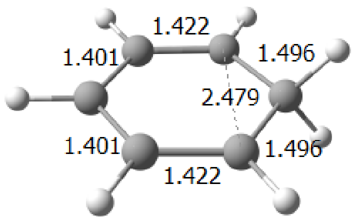	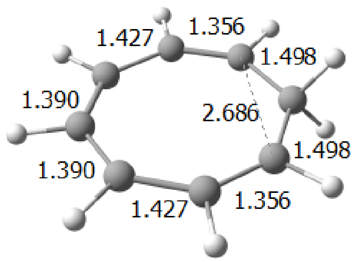
Benzenium ion S_1, HA	**Benzenium ion T_1, HA**	**$COTH^+$ S_0, HA**

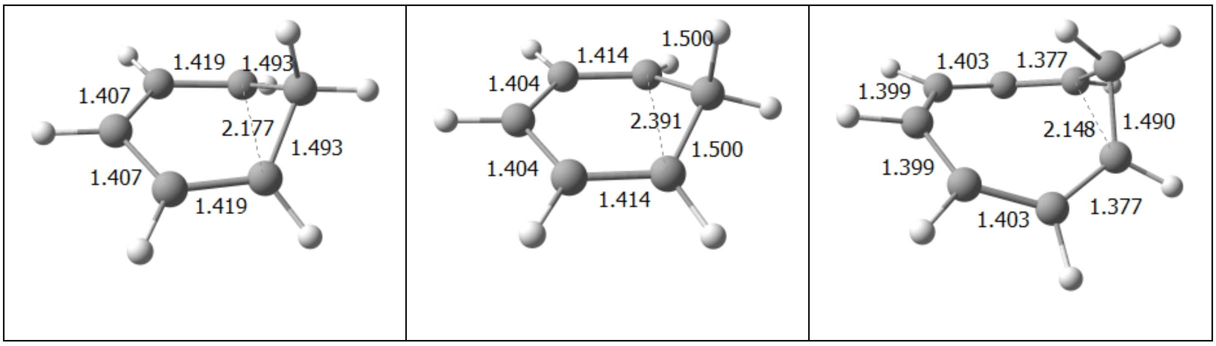

Figure S49. Geometries for benzenium cation in the S_1 and T_1 state and $COTH^+$ in the S_0 state: C_{2v} structures (above) presenting imaginary frequencies and homoaromatic (HA) geometries (below) which are global minima calculated at B3LYP/6-311+G(d,p) level.

7.10 Proton affinities

Table S37 Calculated gas phase proton affinities (kcal/mol) in the S_0, S_1, and T_1 states calculated at (U)- and (TD-)B3LYP/6-311+G(d,p) levels.

Compound	S_0	S_1	T_1
Benzene	183.1	214.7 (C_{2v}, *i*)	217.0 (C_{2v}, *i*)
		232.1 (C_s)	218.4 (C_s)
Cyclooctatetraene	220.8	182.8	195.0
Benzvalene	243.6		

The calculated gas phase proton affinity in the S_1 state increases further for TMS and *t*Bu monosubstituted benzenes as their gas phase proton affinities, varying with the protonation site (*ortho*-, *meta*- or *para*-), are found in the ranges 258 – 265 and 243 – 248 kcal/mol, respectively (**Table S38).** The protonated TMS-benzene in the S_1 state would relax to either an S_1 state homoaromatic minimum or to a conical intersection located very nearby.

Table S38. Proton affinities (kcal/mol) in the S_1 states of substituted benzenes calculated at B3LYP/6-311+G(d,p) level in the gas phase.

Molecule	Ipso	Ortho	Meta	Para
TMS-benzene	257.9	260.9	265.4	262.1
t-*Bu*-Benzene	242.8	243.3	247.9	245.0

8. Spectra

Figure S50: ^{1}H NMR spectrum of **1d** in $CDCl_3$. Signals with asterisk symbol depicts minor stereoisomers inseparable by repeated chromatography.

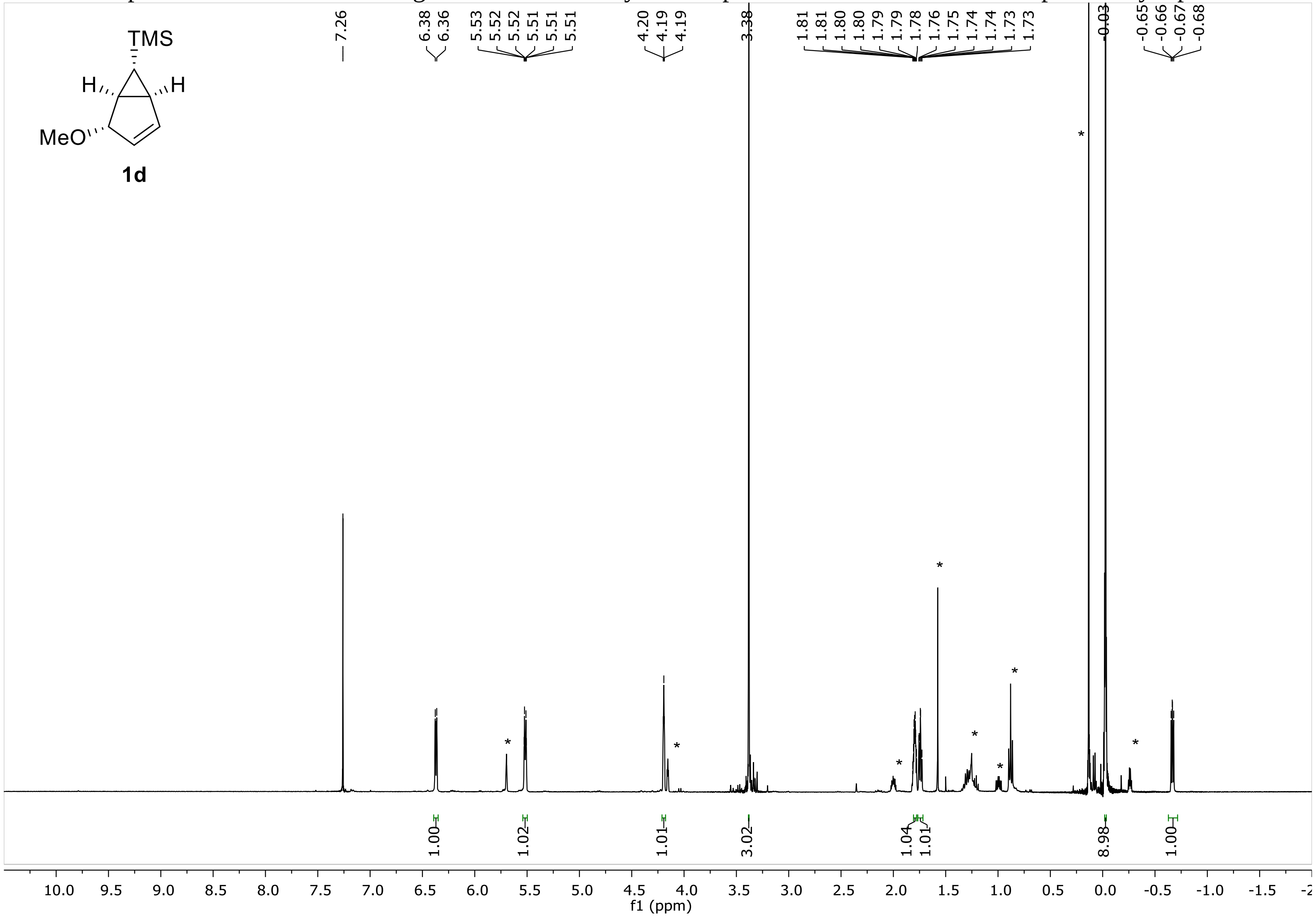

Figure S51: ^{13}C NMR spectrum of **1d** in $CDCl_3$. Signals with asterisk symbol depicts minor stereoisomers inseparable by column chromatography.

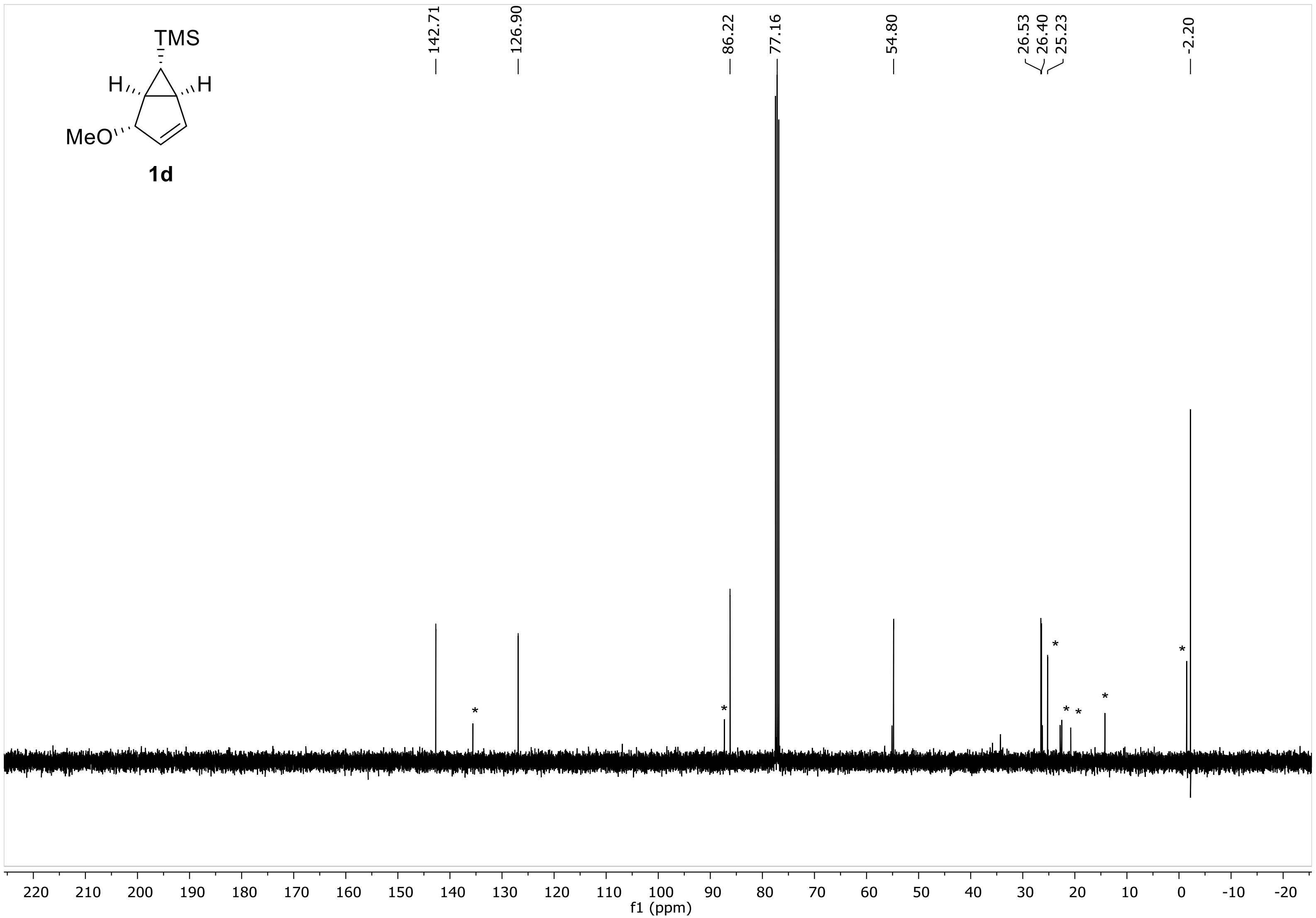

Figure S52: COSY spectrum of **1d** in $CDCl_3$. Important correlations are highlighted.

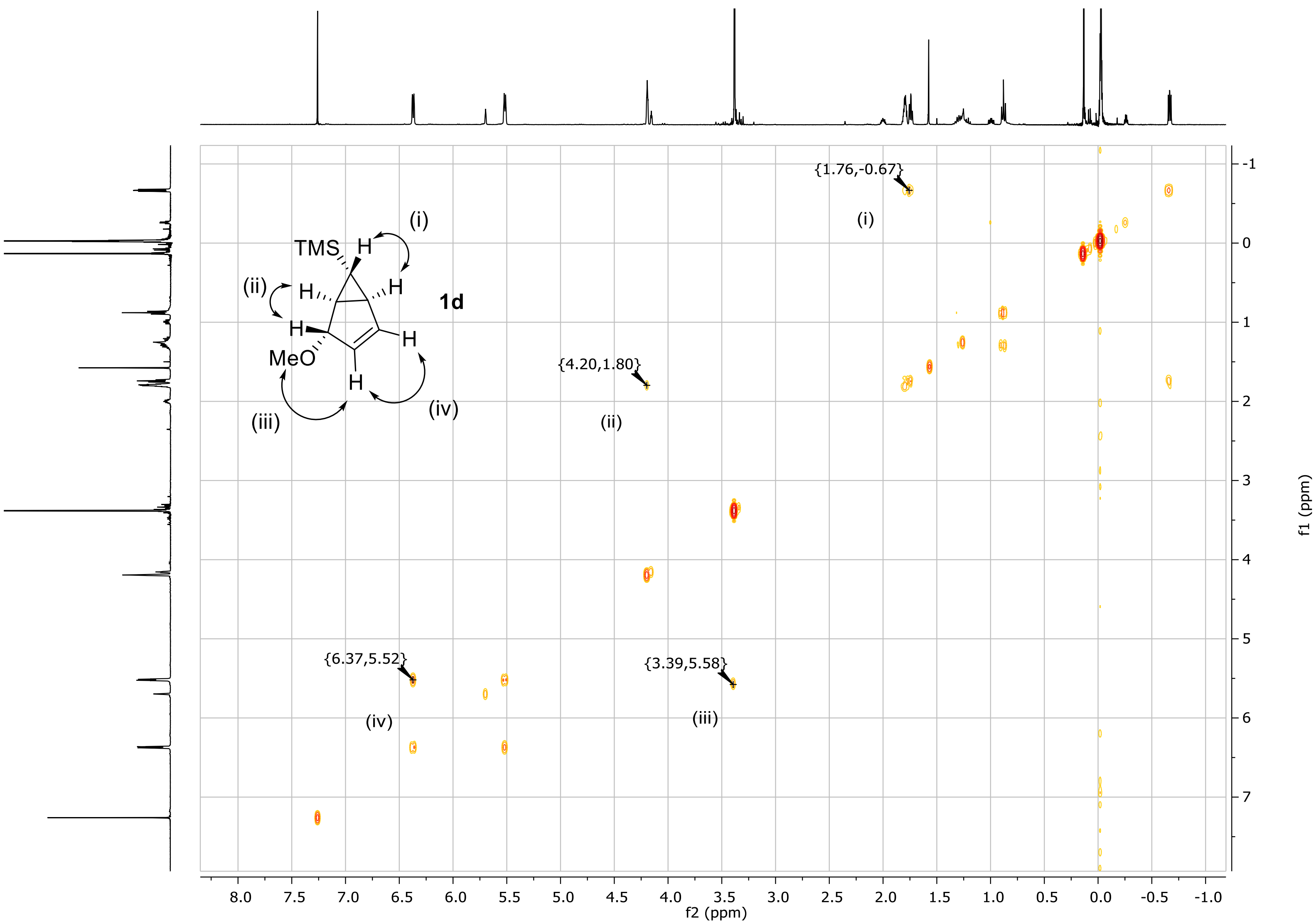

Figure S53: HSQC spectrum of **1d** in $CDCl_3$.

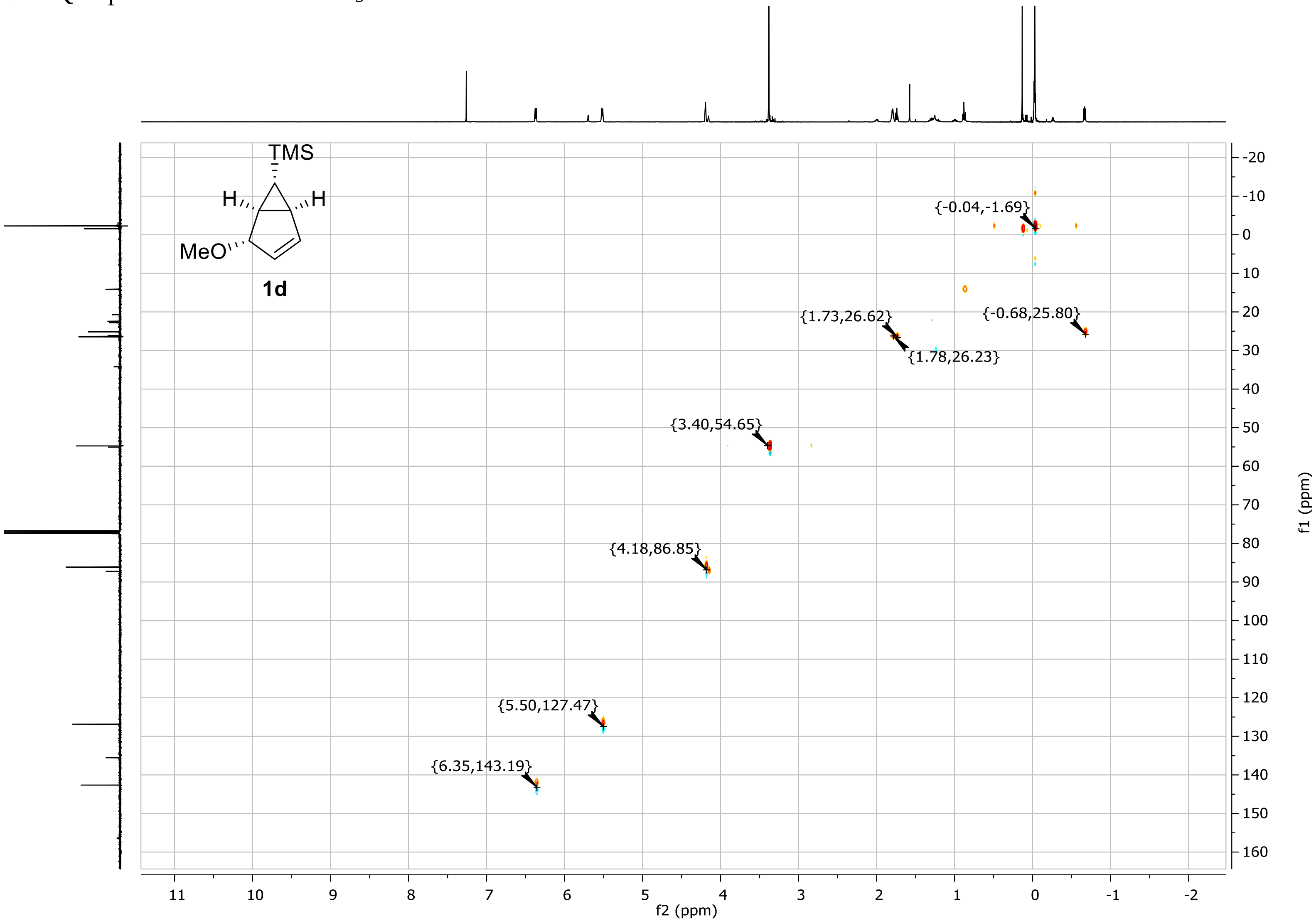

Figure S54: HMBC spectrum of **1d** in $CDCl_3$. Important correlations are highlighted.

Figure S55: [1]H NMR spectrum of mixture of **1d** (a), **1e** (b), unknown bicyclic product (c) and TMS benzene in $CDCl_3$.

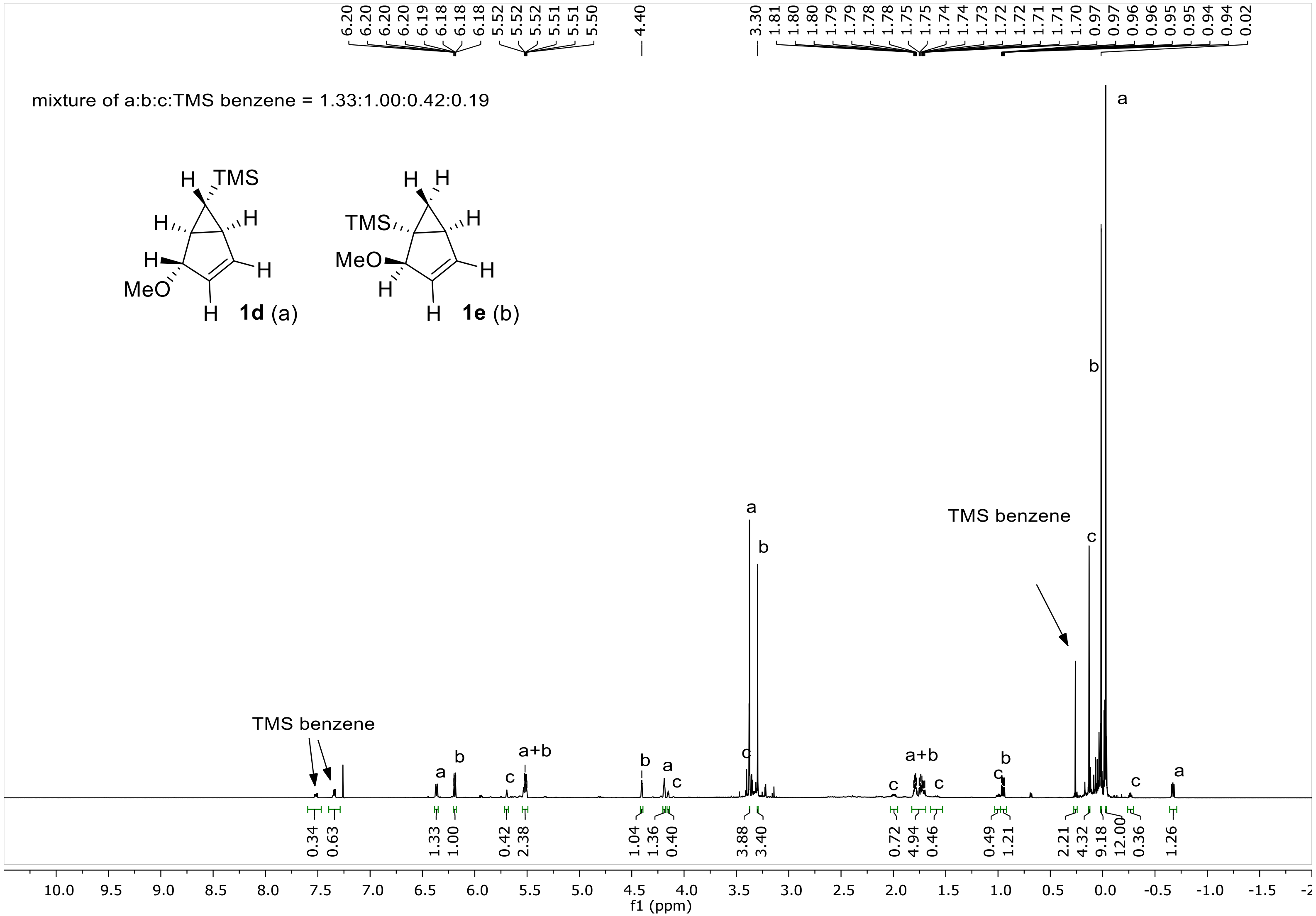

Figure S56: COSY spectrum of a mixture of **1d** (a), **1e** (b) and an unknown bicyclic product (c) in $CDCl_3$. Important correlations of b are highlighted.

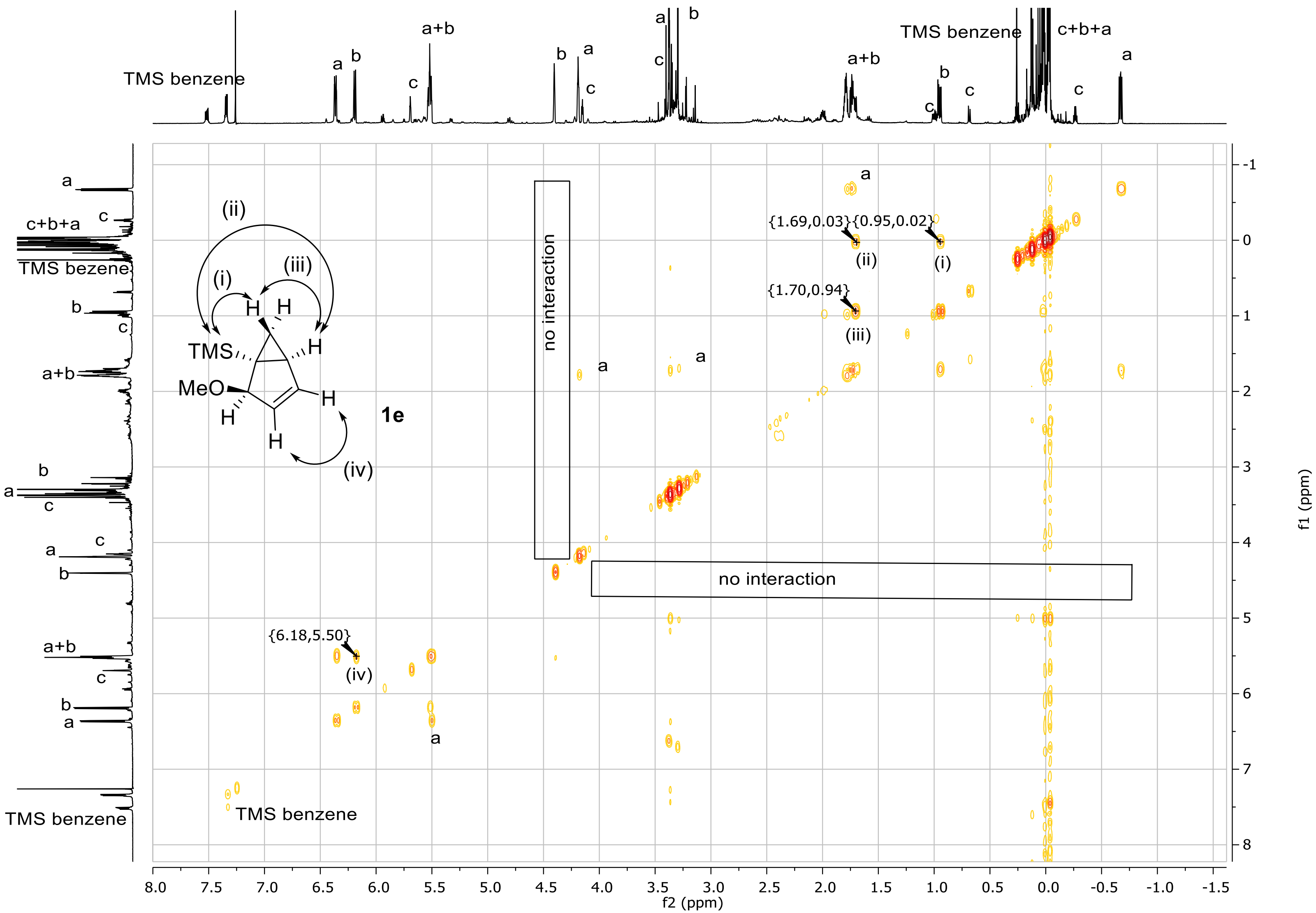

Figure S57: HSQC spectrum of **1e** in $CDCl_3$.

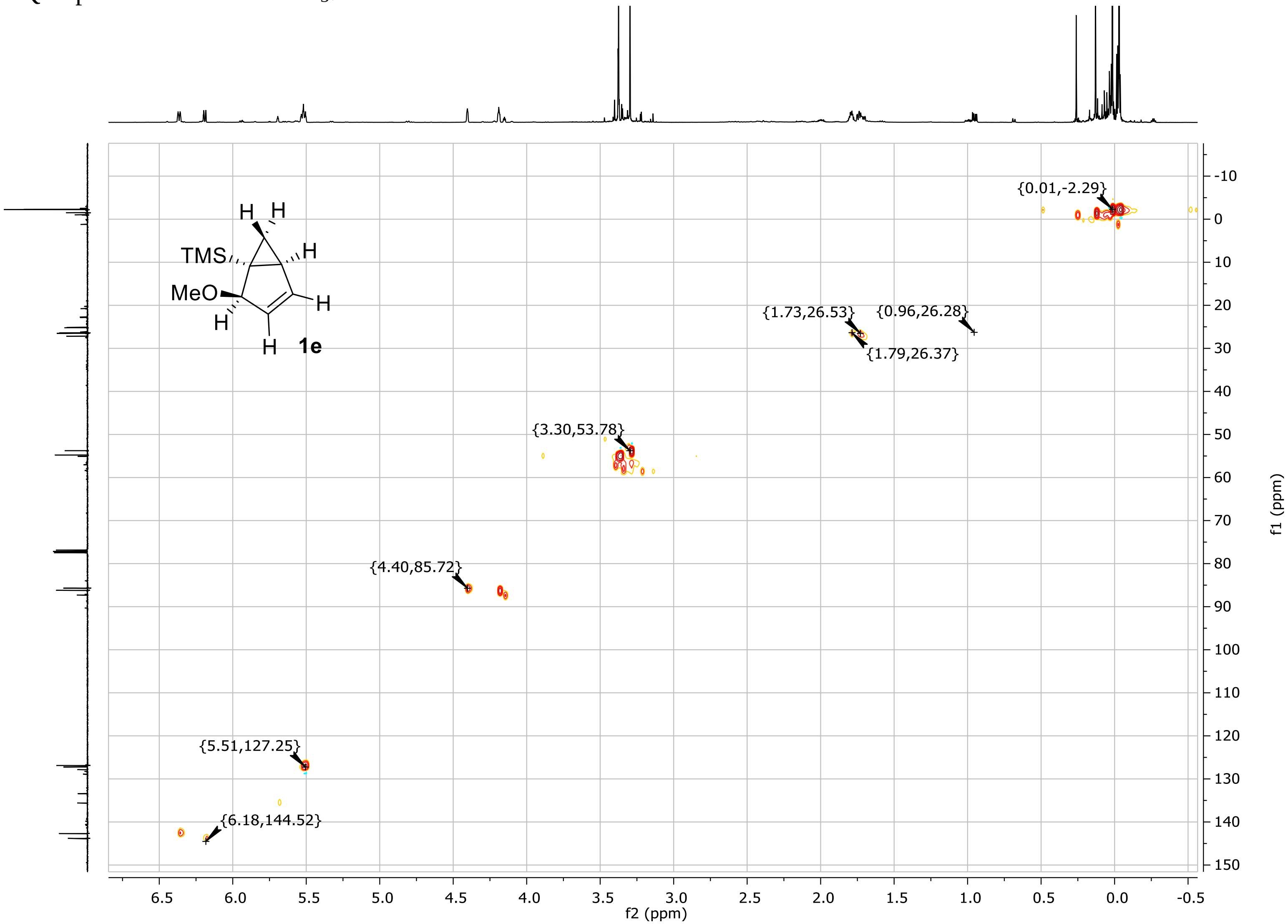

Figure S58: HMBC spectrum of **1e** in $CDCl_3$.

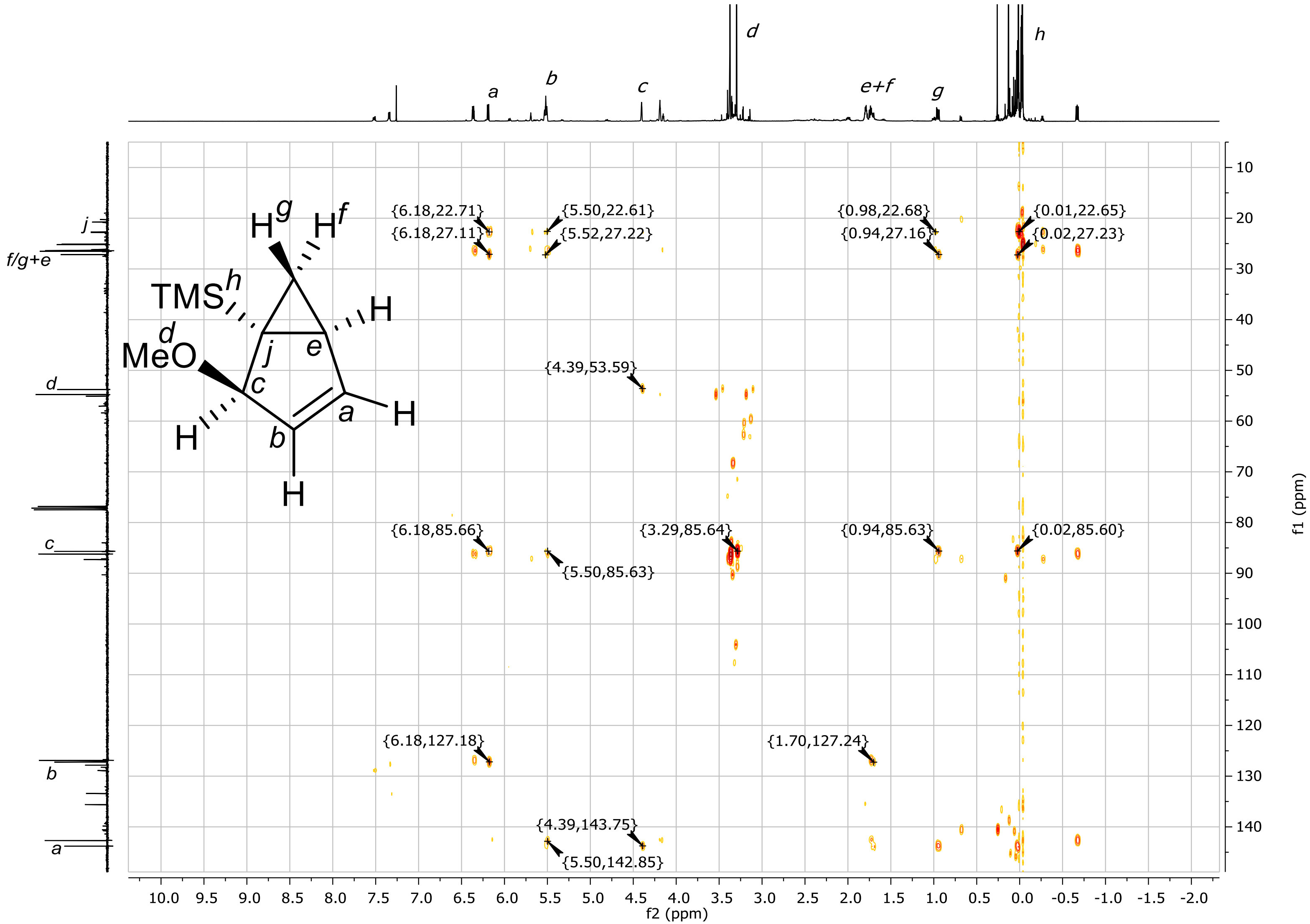

Figure S59: HRMS (GC coupled with TOF) of **1d**.

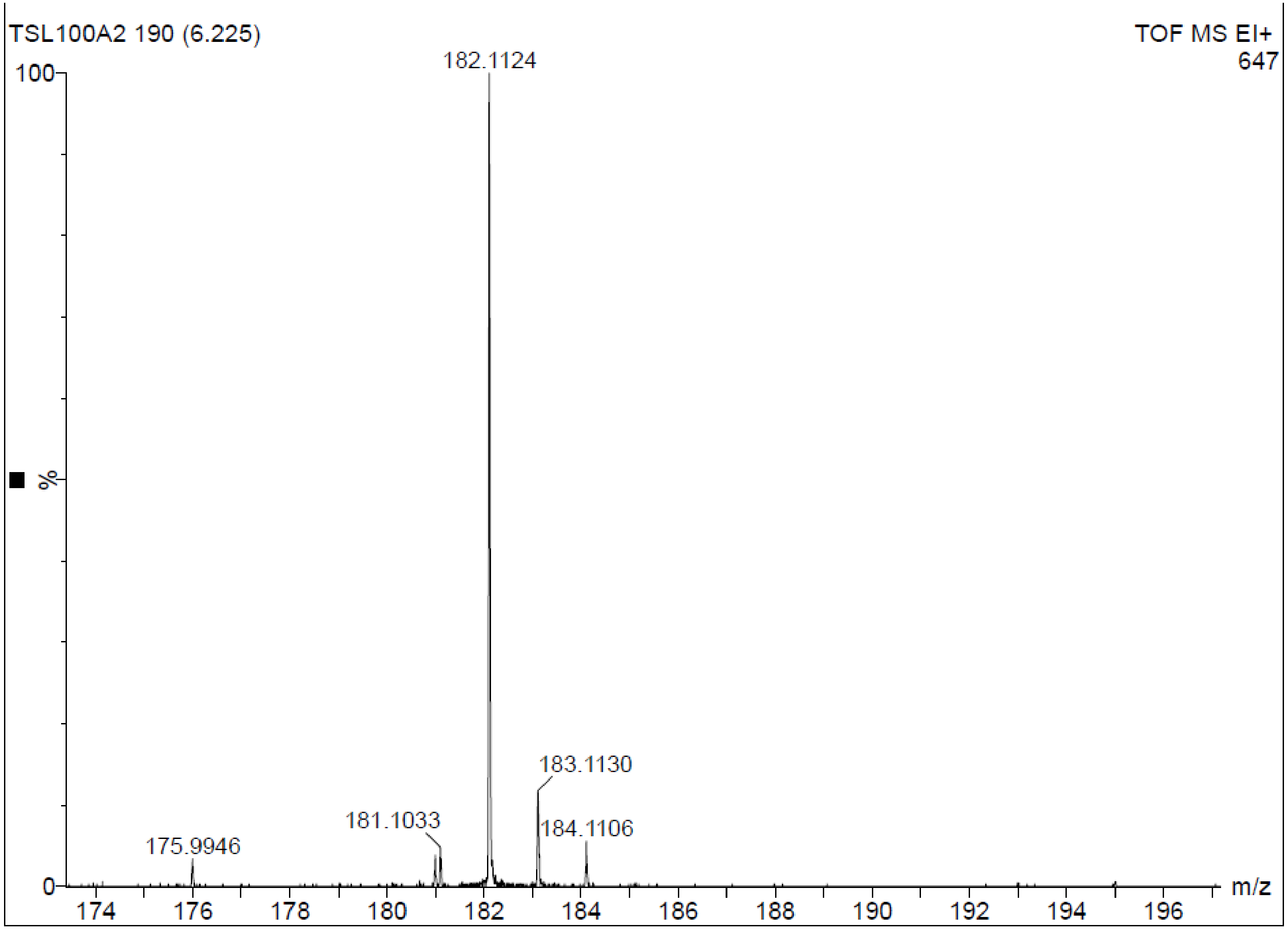

Figure S60: Predicted HRMS spectrum for $C_{10}H_{18}OSi$.

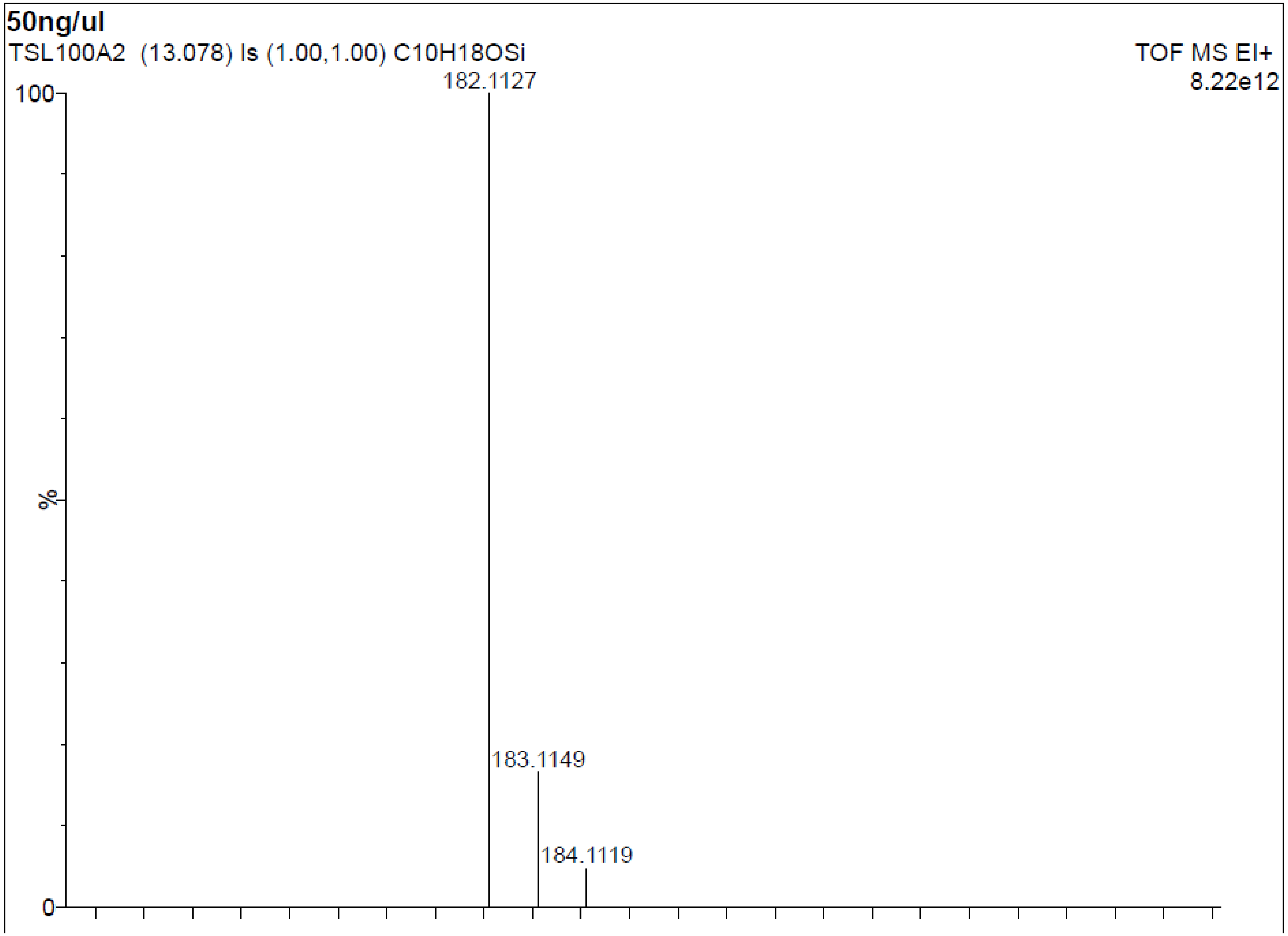

Figure S61: ^{1}H NMR spectrum of **1c** in $CDCl_3$. Signals with asterisk symbol depict minor stereoisomers inseparable by repeated chromatography.

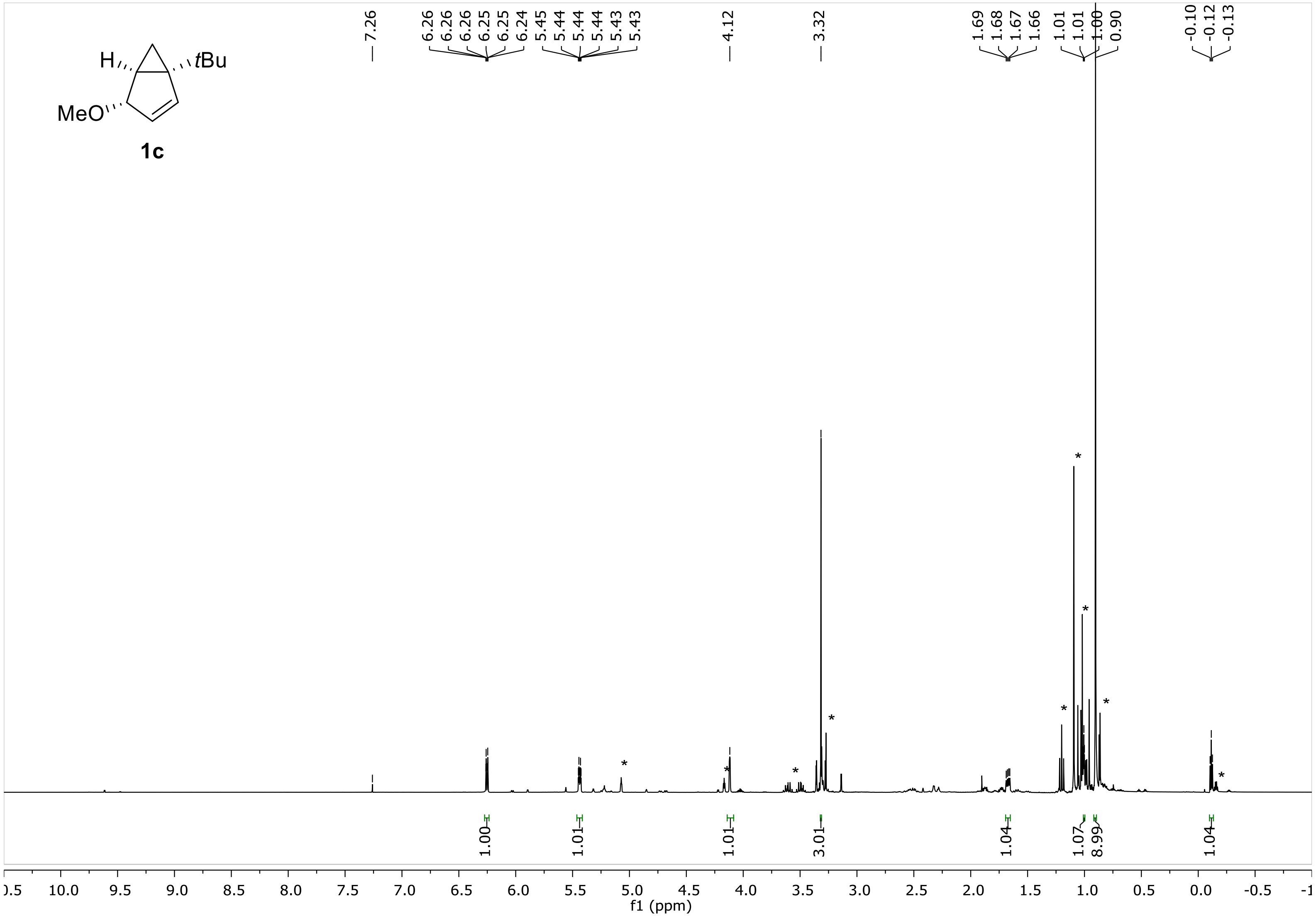

Figure S62: COSY spectrum of **1c** in $CDCl_3$. Important correlations are highlighted.

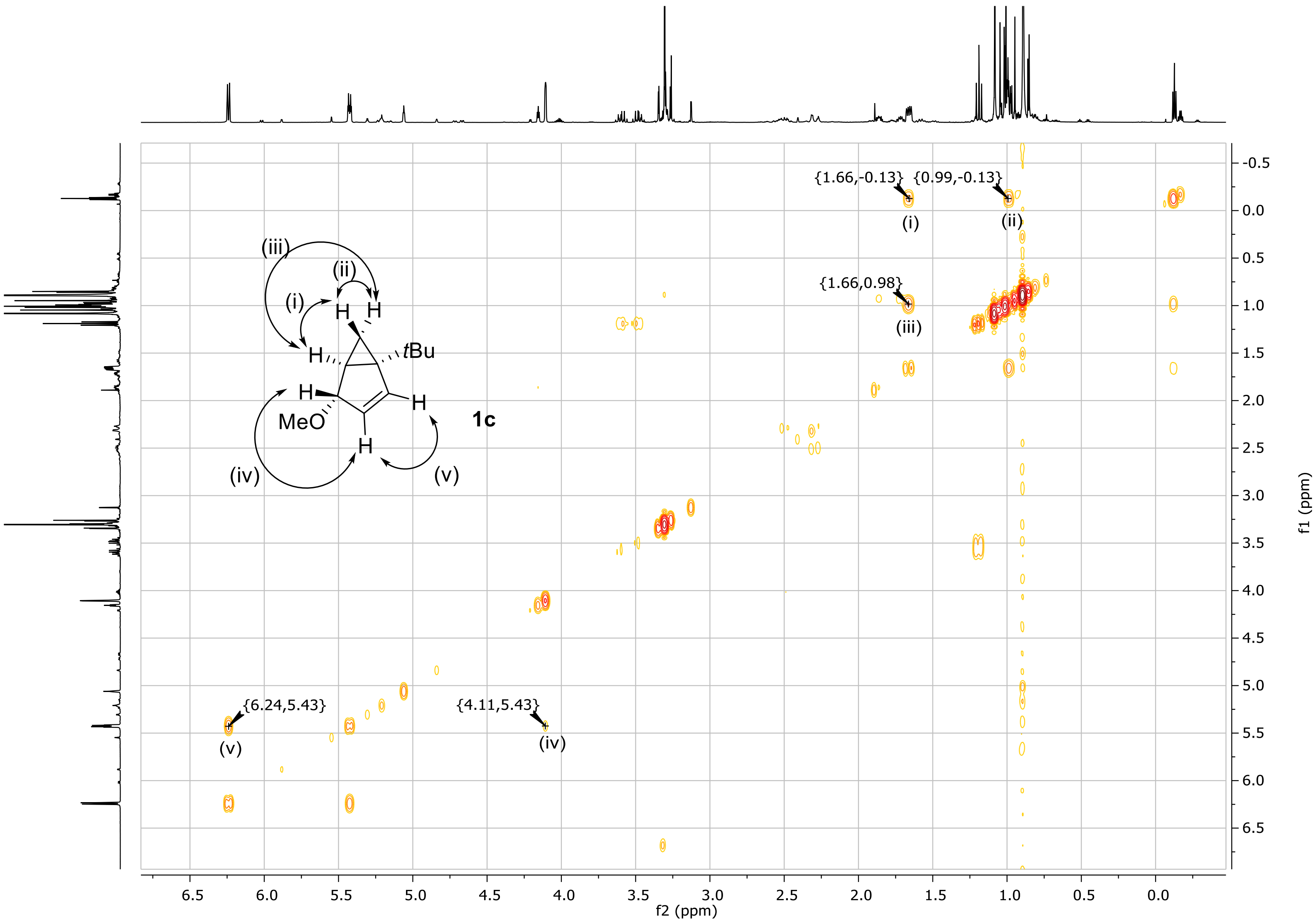

Figure S63: [1]H NMR spectrum of **1a** in $CDCl_3$. Signals with asterisk symbol depict residual diethyl ether signals.

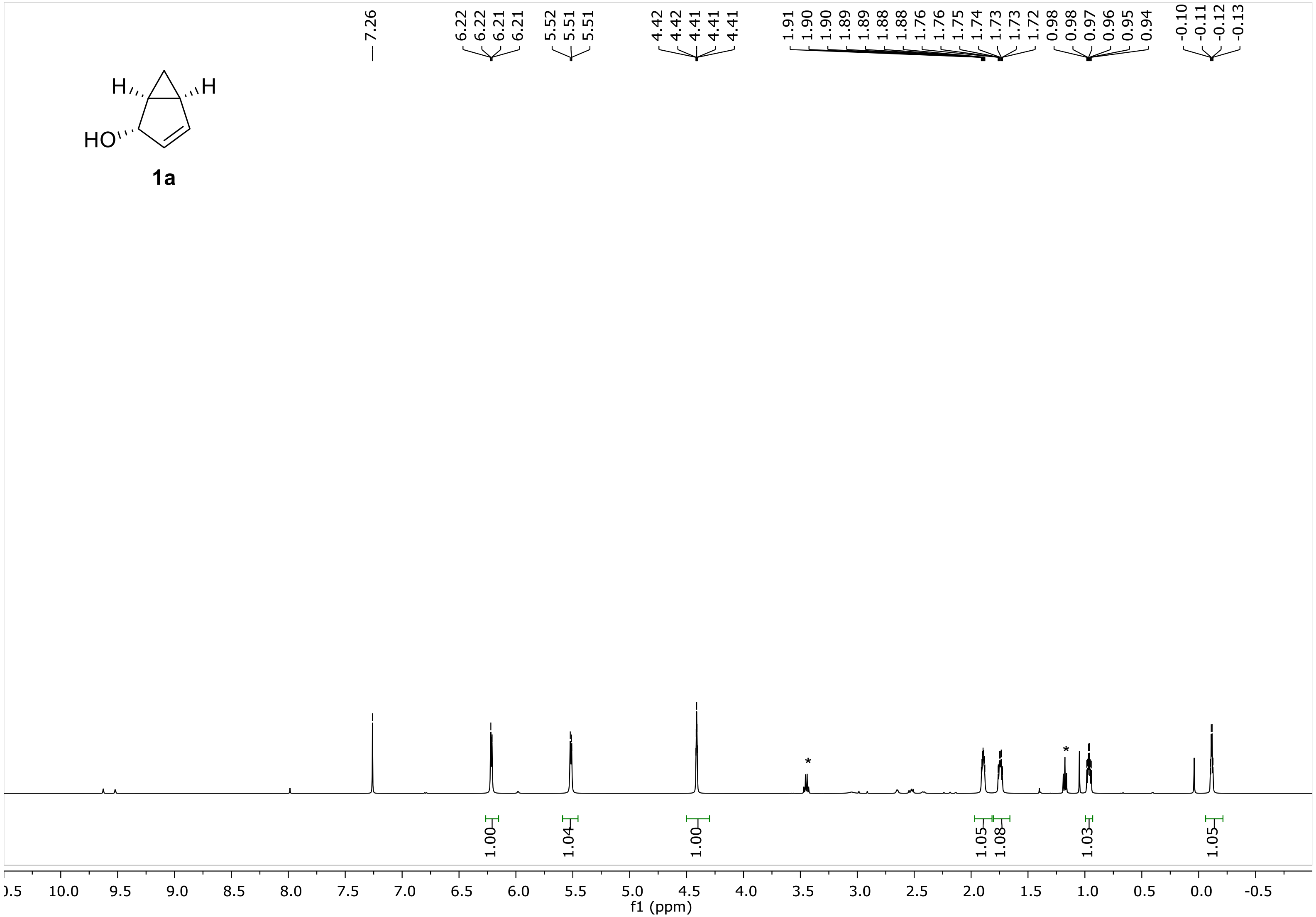

Figure S64: COSY spectrum of **1a** in $CDCl_3$. Important correlations are highlighted.

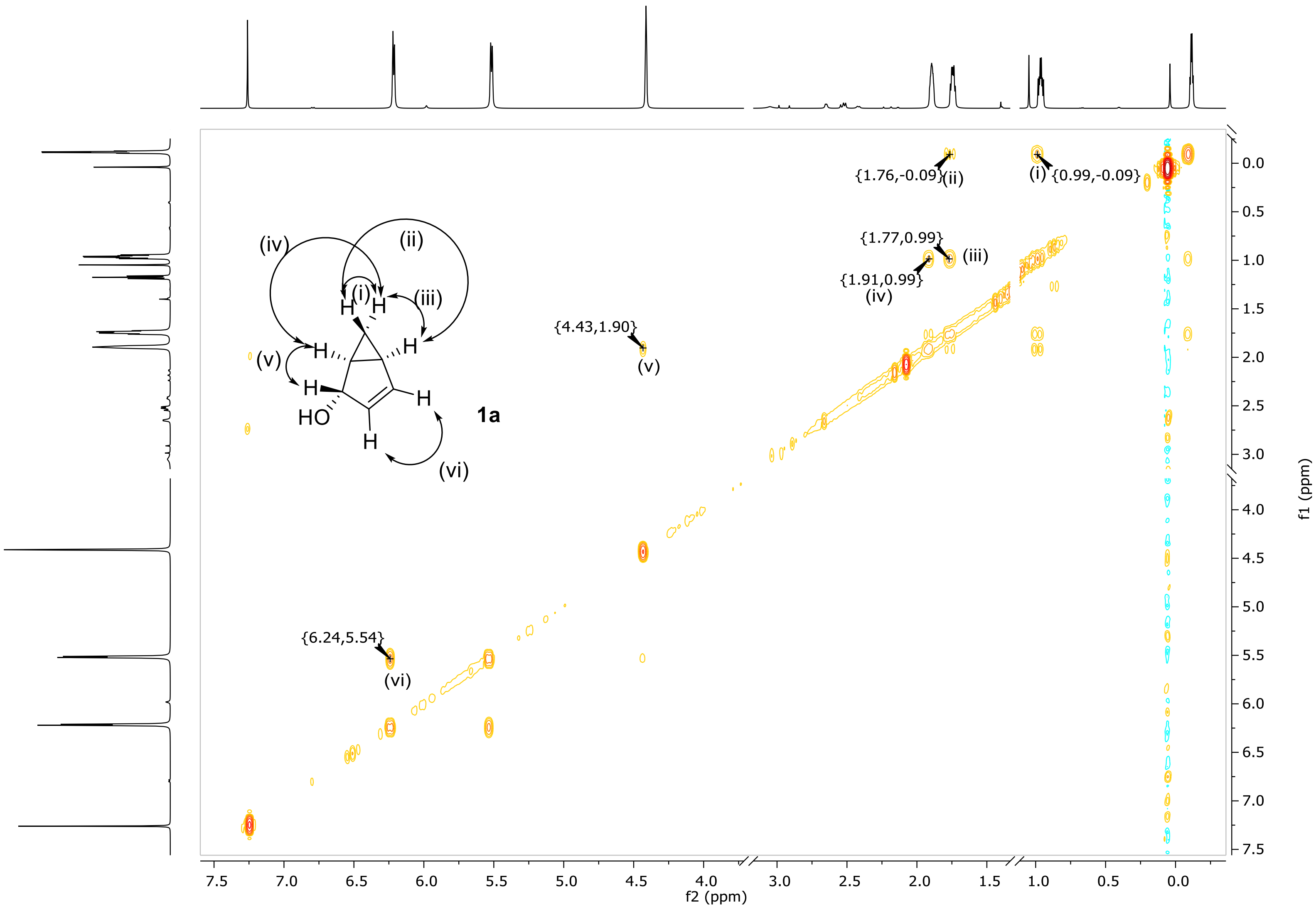

Figure S65: ^{1}H NMR spectrum of **1b** (a) and an inseparable bicyclic isomer (b, ~20%) in $CDCl_3$. Signals with asterisk symbol depict residual diethyl ether signals.

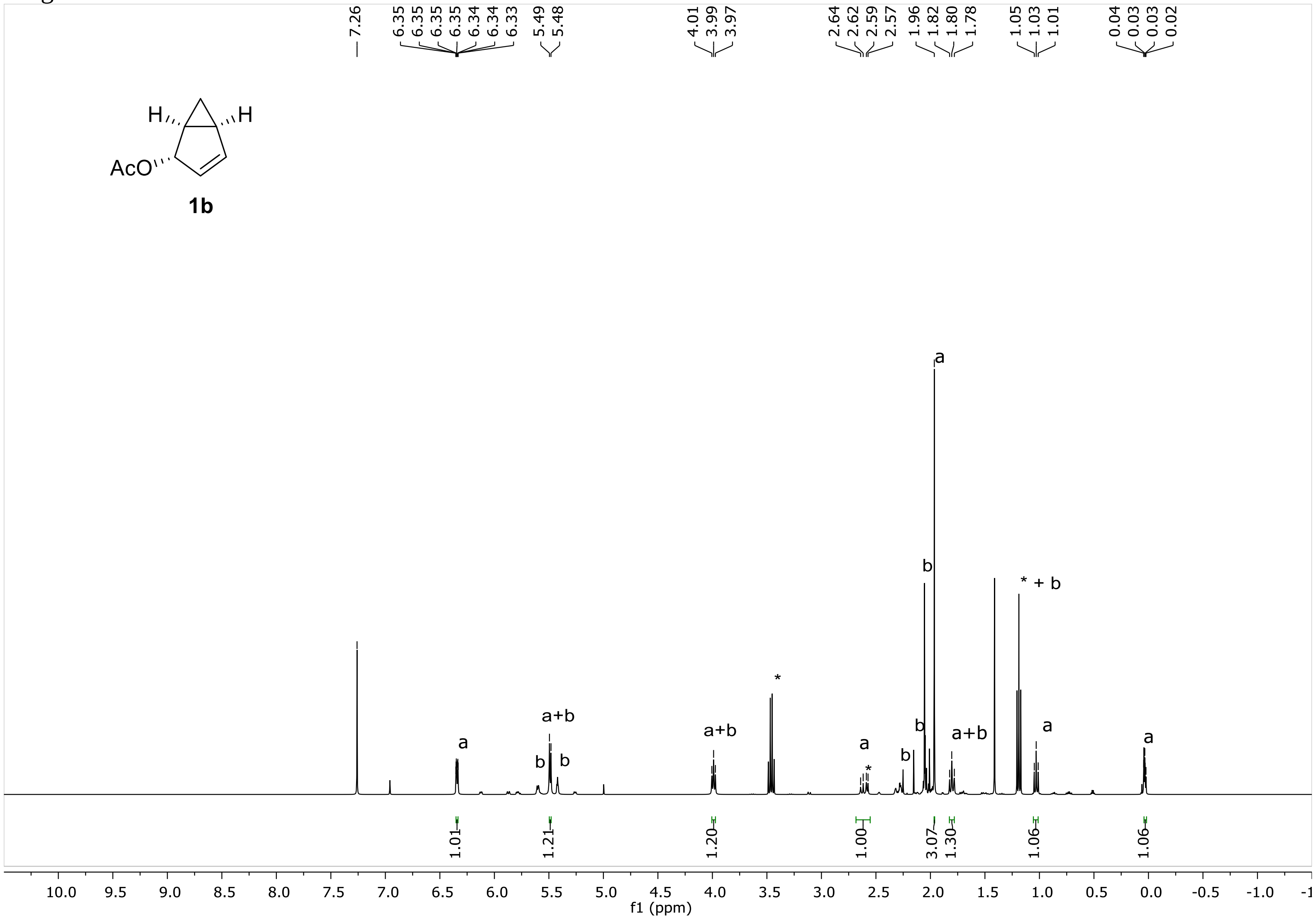

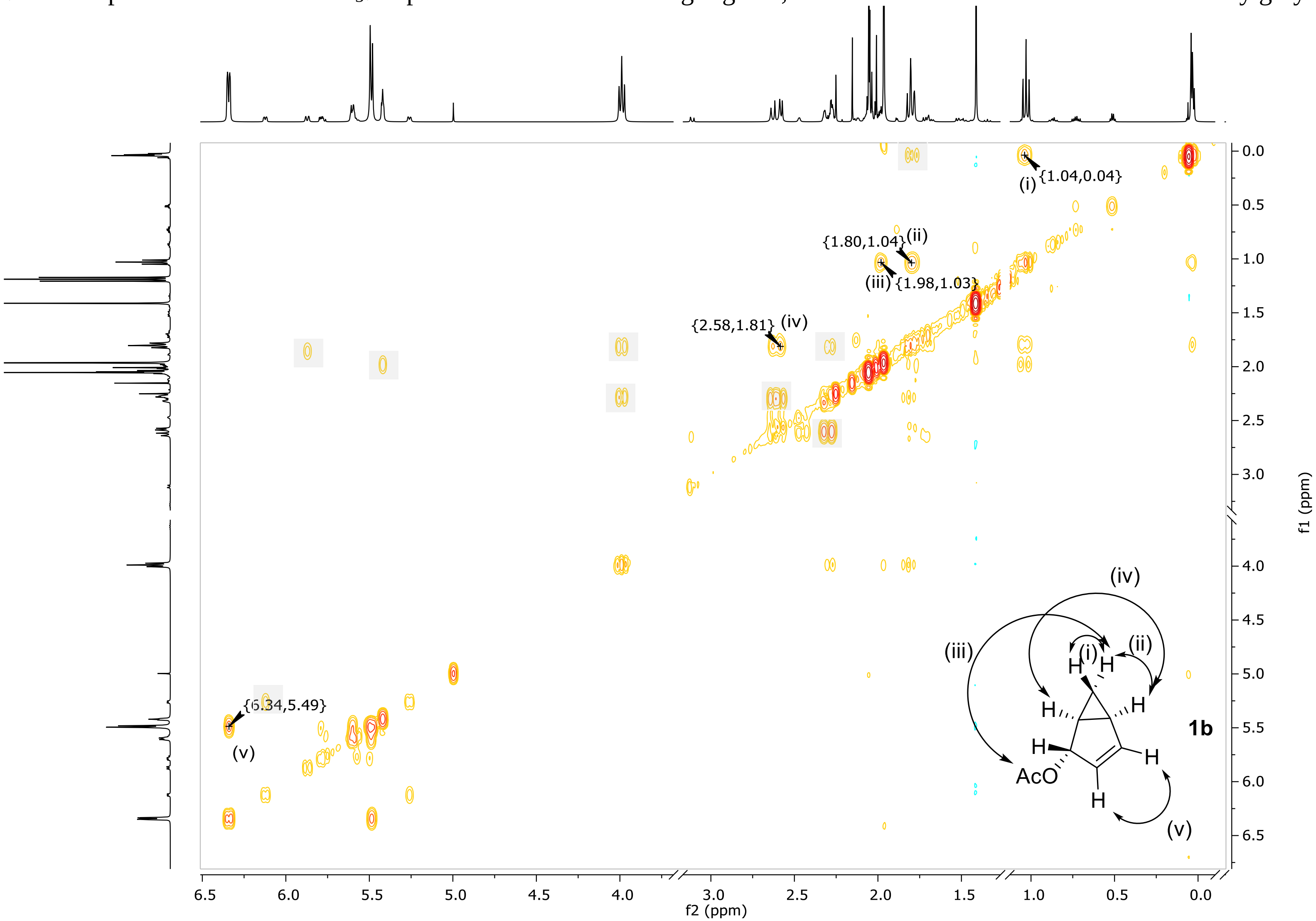

Figure S66: COSY spectrum of **1b** in $CDCl_3$. Important correlations are highlighted, correlations of other isomers are shaded by grey rectangles.

Figure S67: [1]H NMR spectrum of **7** in $CDCl_3$. Mixtures of diastereoisomers.

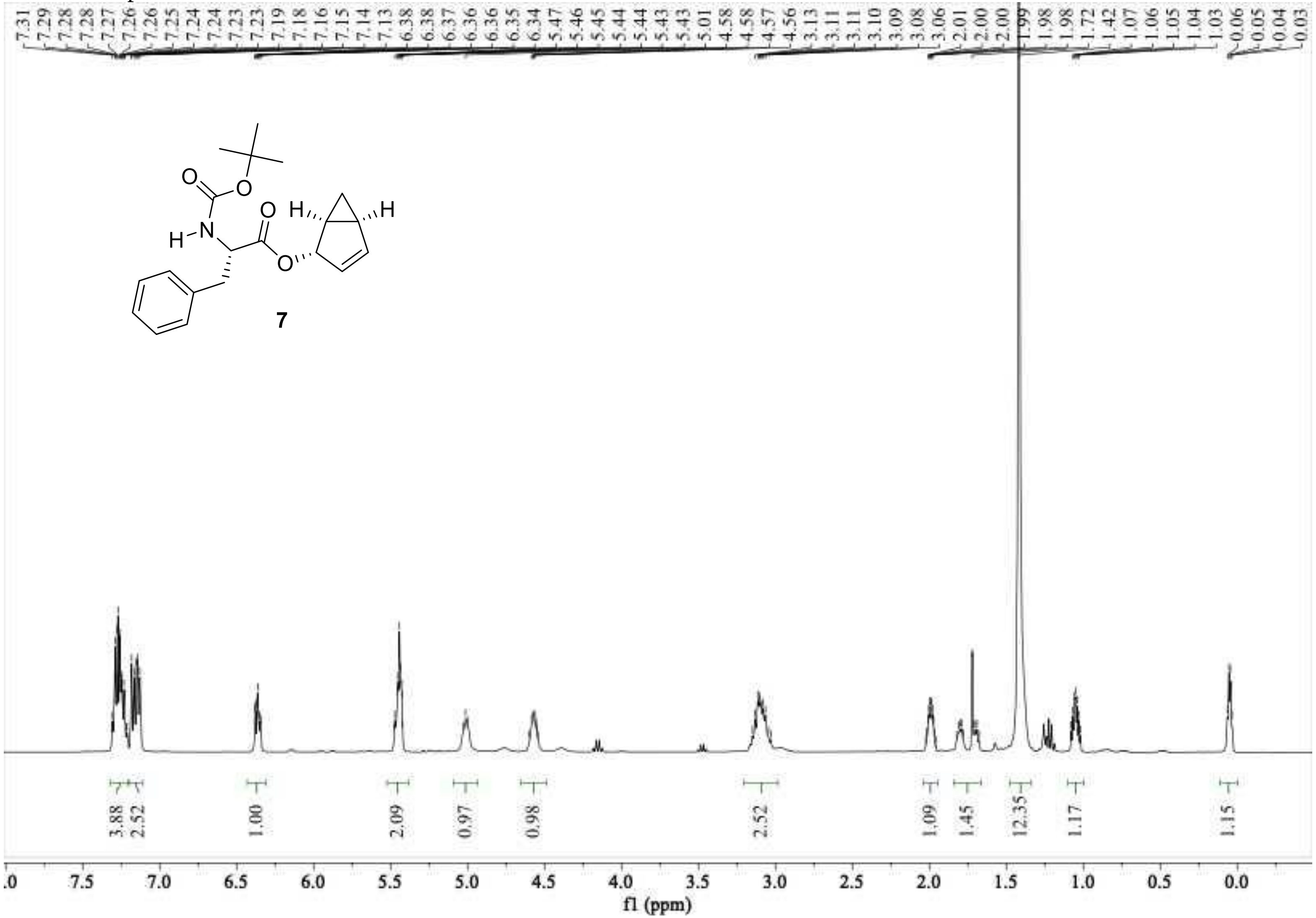

Figure S68: ^{13}C NMR spectrum of **7** in $CDCl_3$. Mixtures of diastereoisomers.

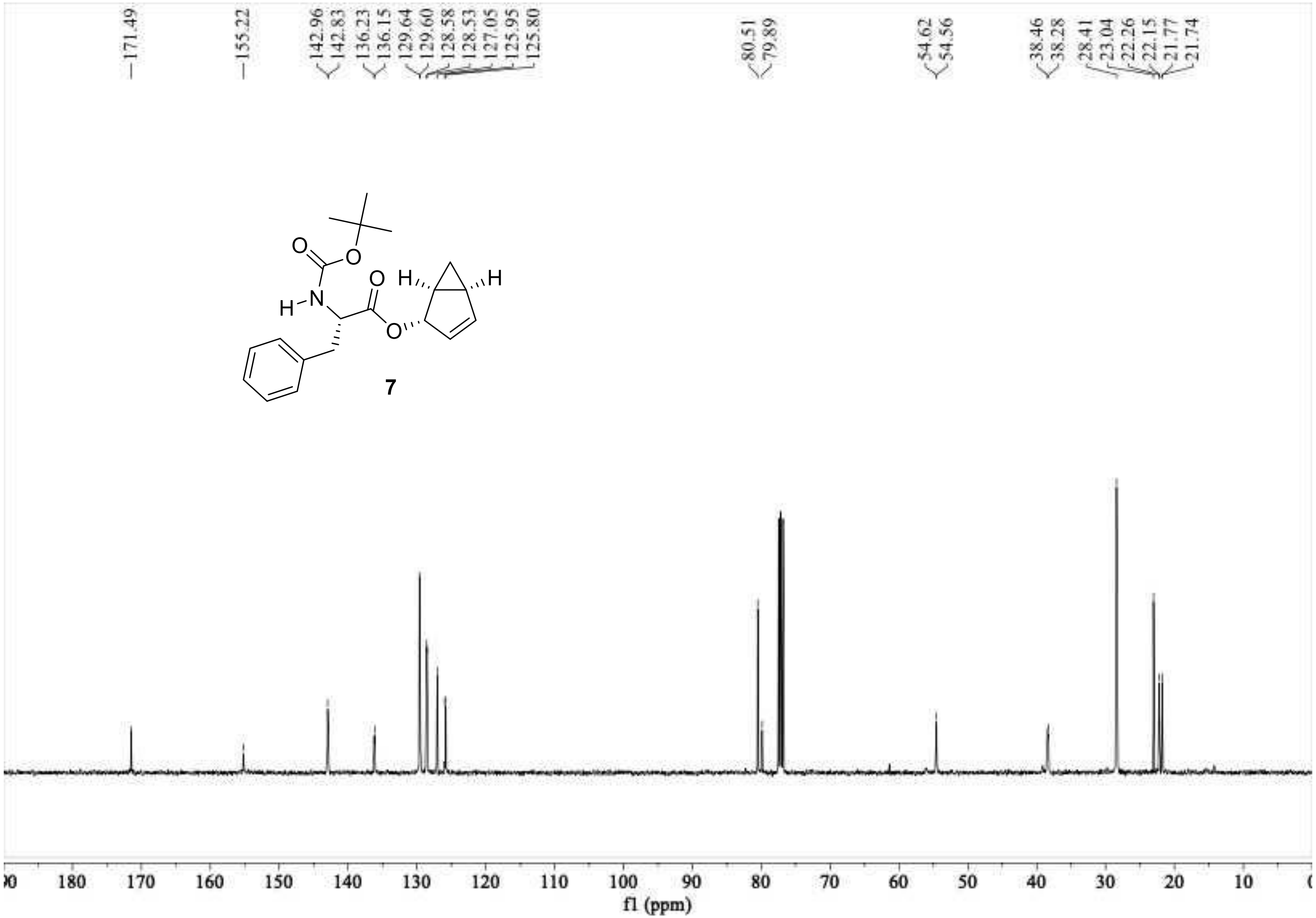

Figure S69: ^{1}H NMR spectrum of **1f** in $CDCl_3$. Signals with asterisk symbol depict residual diethyl ether.

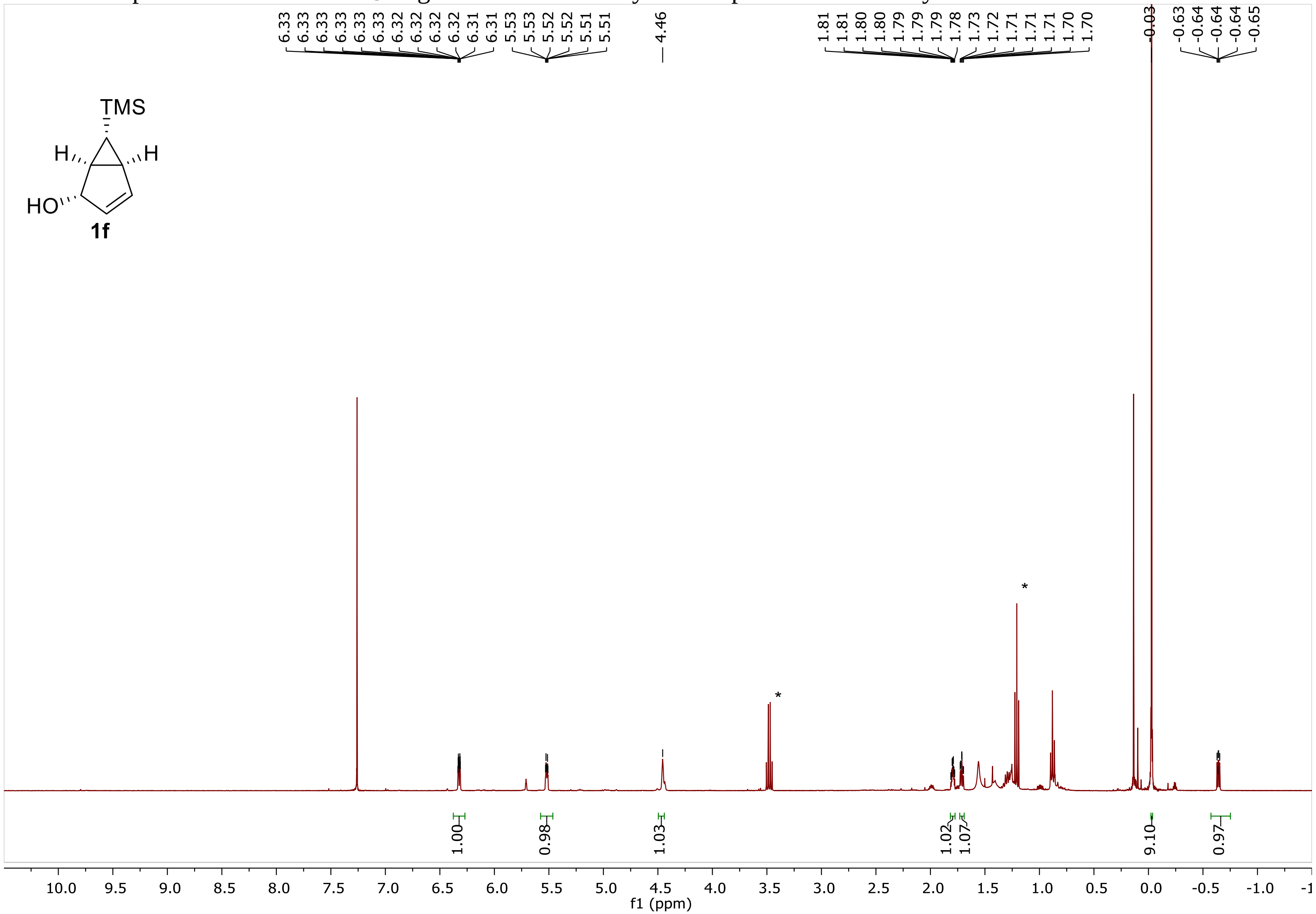

Figure S70: HRMS spectrum of **7**.

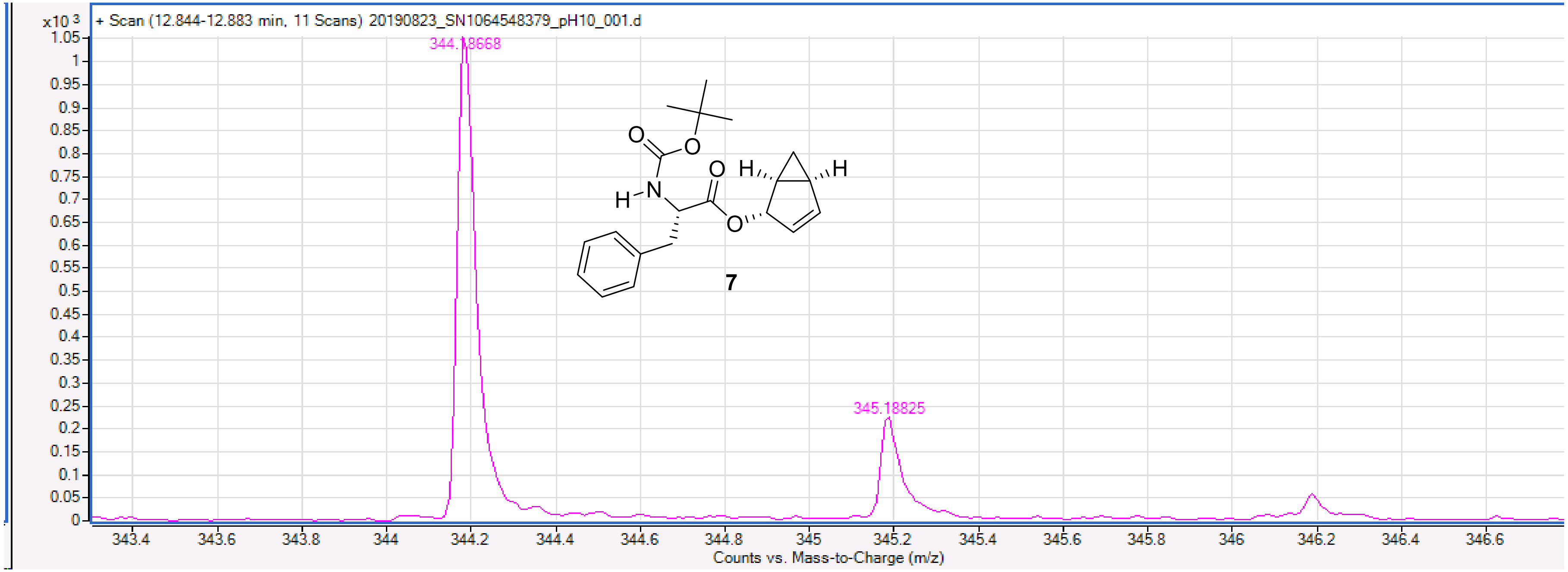

9. References

[1] Hansch, C.; Leo, A.; Taft, R. W. A Survey of Hammett Substituent Constants and Resonance and Field Parameters. *Chem. Rev.* **1991**, *91* (2), 165–195.

[2] Izawa, Y.; Tomioka, H.; Kagami, T.; Sato, T. Photochemical 1,3-Addition of Methanol to t-Butylbenzene. *J. Chem. Soc. Chem. Commun.* **1977**, *0* (21), 780–781.

[3] Farenhorst, E.; Bickel, A. F. Photochemical Reactions of Benzene with Acids. *Tetrahedron Lett.* **1966**, *7* (47), 5911–5913.

[4] Berson, J. A.; Hasty, N. M. Solvolytic Behavior of Bicyclo [3.1.0]Hex-3-En-2-Yl Derivatives. Mechanism of Photolysis of Benzene in Hydroxylic Media. *J. Am. Chem. Soc.* **1971**, *93* (6), 1549–1551.

[5] Gaussian 16, Revision B.01, Frisch, M. J.; Trucks, G. W.; Schlegel, H. B.; Scuseria, G. E.; Robb, M. A.; Cheeseman, J. R.; Scalmani, G.; Barone, V.; Petersson, G. A.; Nakatsuji, H.; Li, X.; Caricato, M.; Marenich, A. V.; Bloino, J.; Janesko, B. G.; Gomperts, R.; Mennucci, B.; Hratchian, H. P.; Ortiz, J. V.; Izmaylov, A. F.; Sonnenberg, J. L.; Williams-Young, D.; Ding, F.; Lipparini, F.; Egidi, F.; Goings, J.; Peng, B.; Petrone, A.; Henderson, T.; Ranasinghe, D.; Zakrzewski, V. G.; Gao, J.; Rega, N.; Zheng, G.; Liang, W.; Hada, M.; Ehara, M.; Toyota, K.; Fukuda, R.; Hasegawa, J.; Ishida, M.; Nakajima, T.; Honda, Y.; Kitao, O.; Nakai, H.; Vreven, T.; Throssell, K.; Montgomery, J. A., Jr.; Peralta, J. E.; Ogliaro, F.; Bearpark, M. J.; Heyd, J. J.; Brothers, E. N.; Kudin, K. N.; Staroverov, V. N.; Keith, T. A.; Kobayashi, R.; Normand, J.; Raghavachari, K.; Rendell, A. P.; Burant, J. C.; Iyengar, S. S.; Tomasi, J.; Cossi, M.; Millam, J. M.; Klene, M.; Adamo, C.; Cammi, R.; Ochterski, J. W.; Martin, R. L.; Morokuma, K.; Farkas, O.; Foresman, J. B.; Fox, D. J. Gaussian, Inc., Wallingford CT, 2016.

[6] Kaplan, L.; Rausch, D. J.; Wilzbach, K. E. Photosolvation of Benzene. Mechanism of Formation of Bicyclo[3.1.0]Hex-3-En-2-Yl and of Bicyclo[3.1.0]Hex-2-En-6-Yl Derivatives. *J. Am. Chem. Soc.* **1972**, *94* (24), 8638–8640.

[7] Montalti, M.; Credi, A.; Prodi, L.; Gandolfi, M. T. *Handbook of Photochemistry, Third Edition*, 3 edition.; CRC Press: Boca Raton, 2006.

[8] Wilzbach, K. E.; Ritscher, J. S.; Kaplan, Louis. Benzvalene, the Tricyclic Valence Isomer of Benzene. *J. Am. Chem. Soc.* **1967**, *89* (4), 1031–1032

[9] Kaplan, L.; Pavlik, J. W.; Wilzbach, K. E. Photohydration of Pyridinium Ions. *J. Am. Chem. Soc.* **1972**, *94* (9), 3283–3284.

[10] Yoon, U. C.; Quillen, S. L.; Mariano, P. S.; Swanson, R.; Stavinoha, J. L.; Bay, E. Exploratory and Mechanistic Aspects of the Electron-Transfer Photochemistry of Olefin-N-Heteroaromatic Cation Systems. *J. Am. Chem. Soc.* **1983**, *105* (5), 1204–1218.

[11] Ling, R.; Yoshida, M.; Mariano, P. S. Exploratory Investigations Probing a Preparatively Versatile, Pyridinium Salt Photoelectrocyclization−Solvolytic Aziridine Ring Opening Sequence. *J. Org. Chem.* **1996**, *61* (13), 4439–4449.

[12] Acar, E. A.; Glarner, F.; Burger, U. Aminocyclopentitols from N-Alkylpyridinium Salts: A Photochemical Approach. *Helvetica Chimica Acta* **1998**, *81* (5–8), 1095–1104.

[13] Li, J.; Lang, F.; Ganem, B. Enantioselective Approaches to Aminocyclopentitols: A Total Synthesis of (+)-6-Epitrehazolin and a Formal Total Synthesis of (+)-Trehazolin. *J. Org. Chem.* **1998**, *63* (10), 3403–3410.

[14] Lu, H.; Mariano, P. S.; Lam, Y. A Concise Synthesis of the (−)-Allosamizoline Aminocyclopentitol Based on Pyridinium Salt Photochemistry. *Tetrahedron Letters* **2001**, *42* (29), 4755–4757.

[15] Feng, X.; Duesler, E. N.; Mariano, P. S. Pyridinium Salt Photochemistry in a Concise Route for Synthesis of the Trehazolin Aminocyclitol, Trehazolamine. *J. Org. Chem.* **2005**, *70* (14), 5618–5623.

[16] Penkett, C. S. New Methods of Preparing Cyclopentenone Ketals: The Photosolvolysis of 3-Alkoxypyridinium Tetrafluoroborates. *Synlett* **1999**, *1999* (01), 93–95.

[17] Ling, R.; Mariano, P. S. A Demonstration of the Synthetic Potential of Pyridinium Salt Photochemistry by Its Application to a Stereocontrolled Synthesis of (+)-Mannostatin A1. *J. Org. Chem.* **1998**, *63* (17), 6072–6076.

[18] Cho, S. J.; Ling, R.; Kim, A.; Mariano, P. S. A Versatile Approach to the Synthesis of (+)-Mannostatin A Analogues. *J. Org. Chem.* **2000**, *65* (5), 1574–1577.

[19] Song, L.; Duesler, E. N.; Mariano, P. S. Stereoselective Synthesis of Polyhydroxylated Indolizidines Based on Pyridinium Salt Photochemistry and Ring Rearrangement Metathesis. *J. Org. Chem.* **2004**, *69* (21), 7284–7293.

[20] Lu, H.; Su, Z.; Song, L.; Mariano, P. S. A Novel Approach to the Synthesis of Amino-Sugars. Routes To Selectively Protected 3-Amino-3-Deoxy-Aldopentoses Based on Pyridinium Salt Photochemistry. *J. Org. Chem.* **2002**, *67* (10), 3525–3528.

[21] Zhou, J.; Gong, M.; Mariano, P. S.; Yoon, U.-C. Observations Made in Exploring a Pyridinium Salt Photochemical Approach to the Synthesis of (+)-Lactacystin. *Bulletin of the Korean Chemical Society* **2008**, *29* (1), 89–93.

[22] Clark, M. A.; Goering, B. K.; Li, J.; Ganem, B. Stereoselective Synthetic Approaches to Highly Substituted Cyclopentanes via Electrophilic Additions to Mono-, Di-, and Trisubstituted Cyclopentenes. *J. Org. Chem.* **2000**, *65* (13), 4058–4069.

[23] Zhao, Z.; Mariano, P. S. Application of the Photocyclization Reaction of 1,2-Cyclopenta-Fused Pyridinium Perchlorate to Formal Total Syntheses of (−)-Cephalotaxine. *Tetrahedron* **2006**, *62* (31), 7266–7273.

[24] Zhao, Z.; Duesler, E.; Wang, C.; Guo, H.; Mariano, P. S. Photocyclization Reactions of Cyclohexa- and Cyclopenta-Fused Pyridinium Salts. Factors Governing Regioselectivity. *J. Org. Chem.* **2005**, *70* (21), 8508–8512.

[25] D. Elliott, L.; P. Knowles, J.; S. Stacey, C.; J. Klauber, D.; I. Booker-Milburn, K. Using Batch Reactor Results to Calculate Optimal Flow Rates for the Scale-up of UV Photochemical Reactions. *Reaction Chemistry & Engineering* **2018**, *3* (1), 86–93.

[26] Siopa, F.; António, J. P. M.; Afonso, C. A. M. Flow-Assisted Synthesis of Bicyclic Aziridines via Photochemical Transformation of Pyridinium Salts. *Org. Process Res. Dev.* **2018**, *22* (4), 551–556.

[27] Cho, D.-W.; Mariano, P. S. Organic Synthesis Based on Ruthenium Carbene Catalyzed Metathesis Reactions and Pyridinium Salt Photochemistry. *Journal of the Korean Chemical Society* **2010**, *54* (3), 261–268.

[28] Glarner, F.; Acar, B.; Etter, I.; Damiano, T.; Acar, E. A.; Bernardinelli, G.; Burger, U. The Photohydration of N-Glycosylpyridinium Salts and of Related Pyridinium N,O-Acetals. *Tetrahedron* **2000**, *56* (25), 4311–4316.

[29] King, R. A.; Lüthi, H. P.; Iii, H. F. S.; Glarner, F.; Burger, U. The Photohydration of N-Alkylpyridinium Salts: Theory and Experiment. *Chemistry – A European Journal* **2001**, *7* (8), 1734–1742.

[30] Sowmiah, S.; S. Esperança, J. M. S.; N. Rebelo, L. P.; M. Afonso, C. A. Pyridinium Salts: From Synthesis to Reactivity and Applications. *Organic Chemistry Frontiers* **2018**, *5* (3), 453–493.

[31] Damiano, T.; Morton, D.; Nelson, A. Photochemical Transformations of Pyridinium Salts: Mechanistic Studies and Applications in Synthesis. *Organic & Biomolecular Chemistry* **2007**, *5* (17), 2735–2752.

[32] Zou, J.; S. Mariano, P. The Synthetic Potential of Pyridinium Salt Photochemistry. *Photochemical & Photobiological Sciences* **2008**, *7* (4), 393–404..

[33] Delgado, A. Recent Advances in the Chemistry of Aminocyclitols. *European Journal of Organic Chemistry* **2008**, *2008* (23), 3893–3906.

[34] Kaur, N. Synthesis of Three-Membered and Four-Membered Heterocycles with the Assistance of Photochemical Reactions. *Journal of Heterocyclic Chemistry* **2019**, *56* (4), 1141–1167.

[35] Clark, M. A.; Schoenfeld, R. C.; Ganem, B. The Photochemistry of Pyrylium Salts: New Photohydrations and Photoamidations of Heterocycles Leading to Bicyclic Oxazolines and Functionalized Cyclopentenes. *J. Am. Chem. Soc.* **2001**, *123* (42), 10425–10426.

[36] Wakita, K.; Tokitoh, N.; Okazaki, R.; Takagi, N.; Nagase, S. Crystal Structure of a Stable Silabenzene and Its Photochemical Valence Isomerization into the Corresponding Silabenzvalene. *J. Am. Chem. Soc.* **2000**, *122* (23), 5648–5649.

[37] Su, M.-D. Mechanistic Study of the Photochemical Isomerization Reactions of Silabenzene. *Organometallics* **2014**, *33* (19), 5231–5237.

[38] (a) Becke, A. D. Density-Functional Thermochemistry. III. The role of exact exchange. *J.Chem. Phys.* **1993**, *98*, 5648-5652. (b) Stephens, P.J.; Devlin, F.J.; Chabalowski, C.F.; Frisch, M.J. Ab initio

Calculation of Vibrational Absorption and Circular Dichroism Spectra Using Density Functional Theory. *J. Phys. Chem.* **1994**, *98*, 11623-11627.

[39] Krishnan, R.; Binkley, J. S.; Seeger, R.; Pople Self-consistent Molecular Orbital Methods. XX. A Basis Set for Correlated Wave Functions. J. A. *J. Chem. Phys.* 1980, *72*, 650–654.

[40] Marenich, A. V.; Cramer, C. J.; Truhlar, D. G. Universal solvation model based on solute electron density and on a continuum model of the solvent defined by the bulk dielectric constant and atomic surface tensions. *J. Phys. Chem. B* **2009**, *113*, 6378-6396.

[41] Fifen, J. J.; Nsangou, M.; Dhaouadi, Z.; Motapon, O.; Jaidane, N.-J. Solvation Energies of the Proton in Methanol, *J. Chem. Theory Comp.* **2013**, *9*, 1173-1181.

[42] Grimme, S.; Antony, J.; Ehrlich, S.; Krieg, H. A Consistent and Accurate *ab initio* Parametrization of Density Functional Dispersion Correction (DFT-D) for the 94 Elements H-Pu. *J. Chem. Phys.* **2010**, ***132***, 154104.

[43] *IUPAC. Compendium of Chemical Terminology, 2nd ed. (the "Gold Book"). Compiled by A. D. McNaught and A. Wilkinson. Blackwell Scientific Publications, Oxford (1997). Online version (2019) created by S. J. Chalk. ISBN 0-9678550-9-8. https://doi.org/10.1351/goldbook.*

[44] Fdez. Galván, I.; Vacher, M.; Alavi, A.; Angeli, C.; Aquilante, F.; Autschbach, J.; Bao, J. J.; Bokarev, S. I.; Bogdanov, N. A.; Carlson, R. K.; Chibotaru, L. F.; Creutzberg, J.; Dattani, N.; Delcey, M. G.; Dong, S.; Dreuw, A.; Freitag, L,; Frutos, L. M.; Gagliardi, L.; Gendron, F.; Giussani, A.; González, L.; Grell, G.; Guo, G.; Hoyer, C. E.; Johansson, M.; Keller, S.; Knecht, S.; Kovačević, G.; Källman, E.; Li Manni, G.; Lundberg, M.; Ma, Y.; Mai, S.; Malhado, J. P.; Malmqvist, P. Å.; Marquetand, P.; Mewes, S. A.; Norell, J.; Olivucci, M.; Oppel, M.; Phung, Q. M.; Pierloot, K.; Plasser, F.; Reiher, M.; Sand, A. M.; Schapiro, I.; Sharma, P.; Stein, C. J.; Sørensen, L. K.; Truhlar, D. G.; Ugandi, M.; Ungur, L.; Valentini, A.; Vancoillie, S.; Veryazov, V.; Weser, O.; Wesołowski, T. A.; Widmark, P.-O.; Wouters, S.; Zech, A.; Zobel, J. P.; Lindh R. OpenMolcas: From Source Code to Insight, *J. Chem. Theory Comput.* **2019**, *15*, 5925-5964.

[45] Malmqvist, P.-Å.; Roos, B. O. The CASSCF state interaction method. *Chem. Phys. Lett*. **1989**, *155*, 189-194.

[46] Widmark, P.-O. ; Malmqvist, P.-Å.; Roos, B. O. Density Matrix Averaged Atomic Natural Orbital(ANO) Basis Sets for Correlated Molecular Functions. *Theor. Chim. Acta*, **1990**, *77*, 291-306.

[47] Finleya, J.; Malmqvista, P.-Å.; Roos, B. O.; Andrés, L. S. The Multi-State CASPT2 Method. *Chem. Phys. Lett.* **1998**, *288*, 299-306.

[48] Ghigo, g.; Roos, B-R. Malmqvist, P.-A. A Modified definition of the zeroth-order Hamiltonian in Multiconfigurtional Perturbation Theory. *Chem. Phys. Lett*., **2004,** *396*, 142.

[49] Malmqvist, P.-Å.; Forsberg, N. Multiconfigurational Perturbation Theory with Imaginary Shift Level. *Chem. Phys. Lett.* **1997**, *274*, 196-204.

[50] Sobolewski, A. L.; Woywod, C.; Domcke, W., Ab initio Investigation of Potential Energy Surfaces Involved in the Photophysics of Benzene and Pyrazine. *Chem. Phys.* **1993,** *98*, 5627-5641.

[51] Wolinski, K.; Hinton, J. F.; Pulay, P. *J. Am. Chem. Soc*.. **1990**, *112*, 8251–8260.

[52] Aidas, K.; Angeli, C.; Bak, K. L.; Bakken, V.; Bast, R.; Boman, L.; Christiansen, O.; Cimiraglia, R.; Coriani, S.; Dahle, P.; Dalskov, E. K.; Ekström, U.; Enevoldsen, T.; Eriksen, J. J.; Ettenhuber, P.; Fernández, B.; Ferrighi, L.; Fliegl, H.; Frediani, L.; Hald, K.; Halkier, A.; Hättig, C.; Heiberg, H.; Helgaker, T.; Hennum, A. C.; Hettema, H.; Hjertenæs, E.; Høst, S.; Høyvik, I.; Iozzi, M. F.; Jansík, B.; Jensen, H. J.; Jonsson, D. ; Jørgensen, P.; Kauczor, J.; Kirpekar, S.; Kjærgaard, T.; Klopper, W.; Knecht, S.; Kobayashi, R.; Koch, H.; Kongsted, J.; Krapp, A.; Kristensen, K.; Ligabue, A.; Lutnæs, O. B.; Melo, J. I.; Mikkelsen, K. V.; Myhre, R. H.; Neiss, C.; Nielsen, C. B.; Norman, P.; Olsen, J.; Olsen, J. M.; Osted, A.; Packer, M. J.; Pawlowski, F.; Pedersen, T. B.; Provasi, P. F.; Reine, S.; Rinkevicius, Z.; Ruden, T. A.; Ruud, K.; Rybkin, V. V.; Sałek, P.; Samson; C. C.; de Merás, A. S.; Saue, T.; Sauer, S. P.; Schimmelpfennig, B.; Sneskov, K.; Steindal, A. H.; Sylvester-Hvid, K. O.; Taylor, P. R.; Teale, A. M.; Tellgren, E. I.; Tew, D. P.; Thorvaldsen, A. J.; Thøgersen, L.; Vahtras, O.; Watson, M. A.; Wilson, D. J.; Ziolkowski, M.; Ågren, H. The Dalton quantum chemistry program system. *WIREs Comput. Mol. Sci.*, **2014**, *4*, 269-284.

[53] Bultinck, P.; Rafat, M.; Ponec, R.; Van Gheluwe, B.; Carbó-Dorca, R.; Popelier, P.Electron Delocalization and Aromaticity in Linear Polyacenes: Atoms in Molecules Multicenter Delocalization Index. *J. Phys. Chem. A*, **2006**, *110*, 7642-7648.

[54] Matito, E.; Duran, M.; Solà, M. The Aromatic Fluctuation Index (FLU): a New Aromaticity Index Based on Electron Delocalization. *J. Chem. Phys*., **2005**, *122*, 014109.

[55] AIMAll (Version 17.11.14 B) TK Gristmill Software (aim.tkgristmill.com), Overland Park KS, USA, **2018.**

[56] Matito, E. ESI-3D: Electron Sharing Indexes Program for 3D Molecular Space Partitioning, Institute of Computational Chemistry and Catalysis, Girona, Catalonia, Spain, **2006**, http://iqc.udg.es/∼eduard/ESI.

[57] Turro, N. J.; Renner, C. A., Katz, T. J.; Wiberg, K. B.; Connon, H. A. Kinetics and Thermochemistry of the Rearrangement of Benzvalene to Benzene. An Energy Sufficient but Non-Chemiluminescent Reaction. *Tetrahedron Lett.* **1976**, *17,* 4133-4136.

[58] Boggio-Pasqua, M.; Groenhof , G. On the Use of Reduced Active Space in CASSCF Calculations. *Comput. Theor. Chem.***, 2014,** *1040-1041***,** 6-13**.**

[59] Dewar, J.S.; Kirschner, S. The Conversion of Benzvalene to Benzene. *J. Am. Chem. Soc.*, **1975**, *97*, 2932.

[60] Freiser, B. S.; Beauchamp, J. L. Acid-base properties of molecules in excited electronic states utilizing ion cyclotron resonance spectroscopy. *J. Am. Chem. Soc*. **1977**, *99*, 3214-3225.

[61] Esteves-López, N.; Dedonder-Lardeux, C.; Jouvet, C. Excited State of Protonated Benzene and Toluene. *J. Chem. Phys*. **2015**, *143*, 074303.

[62] Perkampus, H. H.; Baumgarten, E. Proton-Addition Complexes of Aromatic Hydrocarbons. *Angew. Chem., Int. Ed. Engl*. **1964**, *3*, 776-783.

[63] Childs. R. F.; Sakai, M.; Winstein S. Observation and Behavior of the Pentamethylcyclopentadienylmethyl Cation. *J. Am. Chem. Soc.* **1968**, *90*, 7144–7146.

[64] Olah, G. A.; Liang, G.; Jindal, S. P. Stable Carbocations. CLXXXVIII. Bicyclo[3.1.0]hexenyl Cations. *J. Org. Chem.* **1975**, *40*, 3259–3263.

[65] Matito, E. An Electronic Aromaticity Index for Large Rings. *Phys. Chem. Chem. Phys.*, **2016**, *18*, 11839-11846.

[66] Cyranski, M. K. Energetic Aspects of Cyclic π-Electron Delocalization: Evaluation of the Methods of Estimating Aromatic Stabilization Energies. *Chem. Rev*., **2005**, 105, 3773-3811.

[67] Karadakov, P. B. Aromaticity and Antiaromaticity in the Low-Lying Electronic States of Cyclooctatetraene. *J. Phys. Chem. A* **2008**, *112*, 12707-12713.

[68] Jorner, K.; Jahn, B. O.; Bultinck, P.; Ottosson, H. Triplet State Homoaromaticity: Concept, Computational Validation and Experimental Relevance. *Chem. Sci.* **2018**, *9*, 3165–3176.